UNIVERSIDADE ESTADUAL DE CAMPINAS

Faculdade de Engenharia Mecânica

ISNARDO CADENA RODRIGUEZ

A fuzzy genetic model for estimating forces in link chains from the measurement of the natural frequencies.

Modelo fuzzy genético para a estimação de forças em correntes a partir da medição das frequências naturais.

CAMPINAS
2020

ISNARDO CADENA RODRIGUEZ

A fuzzy genetic model for estimating forces in link chains from the measurement of the natural frequencies.

Modelo fuzzy genético para a estimação de forças em correntes a partir da medição das frequências naturais.

Dissertation presented to the School of Mechanical Engineering of the University of Campinas in partial fulfillment of the requirements for the degree of Master in mechanical engineering, in the area of Solid Mechanics and Mechanical Design.

Dissertação de Mestrado apresentada à Faculdade de Engenharia Mecânica da Universidade Estadual de Campinas como parte dos requisitos exigidos para obtenção do título de Mestre em Engenharia Mecânica, na Área de Mecânica dos Sólidos e Projeto Mecânico.

Orientador: Prof. Dr. Milton Dias Júnior.

ESTE EXEMPLAR CORRESPONDE À VERSÃO FINAL DA DISSERTAÇÃO DEFENDIDA PELO ALUNO ISNARDO CADENA RODRIGUEZ, E ORIENTADA PELO PROF. DR MILTON DIAS JÚNIOR.

CAMPINAS

2020

Ficha catalográfica
Universidade Estadual de Campinas
Biblioteca da Área de Engenharia e Arquitetura
Luciana Pietrosanto Milla - CRB 8/8129

C114f	Cadena Rodríguez, Isnardo, 1996- A fuzzy genetic model for estimating forces in link chains from the measurement of the natural frequencies / Isnardo Cadena Rodríguez. – Campinas, SP : [s.n.], 2020. Orientador: Milton Dias Junior. Dissertação (mestrado) – Universidade Estadual de Campinas, Faculdade de Engenharia Mecânica. 1. Lógica fuzzy. 2. Algoritmos genéticos. 3. Inteligencia artificial. 4. Dinâmica estrutural. 5. Vibração. I. Dias Junior, Milton, 1962-. II. Universidade Estadual de Campinas. Faculdade de Engenharia Mecânica. III. Título.

Informações para Biblioteca Digital

Título em outro idioma: Modelo fuzzy genético para a estimação de forças em correntes a partir da medição das frequências naturais
Palavras-chave em inglês:
Fuzzy logic
Genetic algorithms
Artificial intelligence
Structural dynamics
Vibration
Área de concentração: Mecânica dos Sólidos e Projeto Mecânico
Titulação: Mestre em Engenharia Mecânica
Banca examinadora:
Milton Dias Junior [Orientador]
Robson Pederiva
Rodrigo Nicoletti
Data de defesa: 02-03-2020
Programa de Pós-Graduação: Engenharia Mecânica

Identificação e informações acadêmicas do(a) aluno(a)
- ORCID do autor: https://orcid.org/0000-0001-5706-3318
- Currículo Lattes do autor: http://lattes.cnpq.br/9571402912549268

Agência(s): CAPES

Nº do Proc.: 33003017

UNIVERSIDADE ESTADUAL DE CAMPINAS
FACULDADE DE ENGENHARIA MECÂNICA
COMISSÃO DE PÓS-GRADUAÇÃO EM ENGENHARIA MECÂNICA
DEPARTAMENTO DE PROJETOS INTEGRADOS

DISSERTAÇÃO DE MESTRADO ACADÊMICO

A fuzzy genetic model for estimating forces in link chains from the measurement of the natural frequencies.

Modelo fuzzy genético para a estimação de forças em correntes a partir da medição das frequências naturais.

Autor: Isnardo Cadena Rodríguez

Orientador: Prof. Dr. Milton Dias Júnior

A Banca Examinadora composta pelos membros abaixo aprovou esta Dissertação:

Prof. Dr. Milton Dias Júnior, Presidente.
Instituição: Universidade Estadual de Campinas – UNICAMP/FEM

Prof. Dr. Robson Pederiva
Instituição: Universidade Estadual de Campinas – UNICAMP/FEM

Prof. Dr. Rodrigo Nicoletti
Instituição: Universidade de São Paulo– USP/EESC

A Ata da defesa com as respectivas assinaturas dos membros encontra-se no processo de vida acadêmica do aluno.

Campinas, 02 de março de 2020.

This dissertation is dedicated to my mother Hilda Rodríguez Granados.

Acknowledgements

Firstly, I want to thank my family who always supports me, loves me and be patient with me. My mother Hilda Rodríguez the person who unconditionally believes in my potential and skills, who worked so hard for giving to me the opportunity to accede to high education and encouraged me to follow my dreams. My father Isnardo Cadena who taught me to work to achieve my goals, to be brave to face life and He always provides me security when I need it. My brother Pablo Cadena who is my best friend and my confident, who trusts on me, makes me smile and inspires me to beat myself every day. My boyfriend Thiago Pediani who is my support here in Brazil, helps me to overcome my fears and make me grown as person and professional.

I really thank my advisor Professor Ph.D. Milton Dias who believed in my potential, teaches me to think beyond the obvious, and made possible this work. I also acknowledge to the members of the LDEM (Laboratório de Dinâmica de Estruturas e Máquinas), specially to Hugo Miyasato, Vinícius Simionatto and Fábio Menegatti for solving my doubts as well as the long conversations. I really appreciate the company and friendship of Layse Boere, who appeared to make my days happier and to be my partner in the academic and professional life. I also want to thank the friends that Brazil gave me, Oscar Peña and Victor Saldanha, people who I laughed and cried with, and we created great memories.

I also thanks to Pedro Luiz de Souza Pinto Filho and Leandro Perestrelo for providing their knowledge and experience in the area, for providing their technical support and for enabling the acquisition of the materials for the experiments performed for this work.

I am grateful to the University of Campinas for giving me the opportunity to make the master's degree and develop myself academically and professionally. Finally, I also acknowledge everyone who contributed directly and indirectly for the realization of this work.

This work was carried out with the support of the Coordenação de Aperfeiçoamento de Pessoal de Nível Superior - Brasil (CAPES). Financing code 001.

Resumo

As instalações em alto mar possuem linhas de ancoragem, chamadas de amarras, para proporcionar estabilidade, suporte e sustentação às estruturas. Essas linhas de ancoragem são geralmente compostas por cabos, correntes e cordas de fibra sintética. Quando a solicitação de carga é alta, as linhas de ancoragem devem ser constituídas por corrente. O monitoramento da força atuando nestas correntes é vital para a confiabilidade e segurança da produção de energia. Os métodos atuais para supervisionar as cargas nas amarras são caros e têm muitas incertezas envolvidas. Nesse contexto, propõe-se uma nova metodologia para a estimativa de força em correntes através da medição de suas frequências naturais. Um sistema de inferência difuso e otimizado por um algoritmo genético foi desenvolvido para estimar da carga nas correntes. As entradas dos modelos difusos são as frequências naturais das correntes e a saída é a força estimada. As metodologias Mamdani e Sugeno foram implementadas e comparadas. Funções de pertinência triangular e gaussiana foram usadas para modelar as entradas e a saída. As regras foram definidas de acordo com as relações entre as frequências naturais e a força na corrente. Para otimizar o sistema, o algoritmo genético pode usar como dados de treinamento os resultados fornecidos por um modelo matemático ou por um conjunto de medições. O modelo matemático desenvolvido apresenta boa concordância com os dados experimentais. O modelo genético difuso foi simulado e testado, fornecendo boa precisão na estimativa da força. Finalmente, demonstrou-se que a fuzzificação não singleton pode ser uma ferramenta útil quando as entradas são ruidosas.

Palavras chave: Corrente, frequências naturais, logica difusa, Algoritmo genético.

Abstract

Offshore facilities have mooring lines to provide stability, support and holding to the structures. These mooring lines are commonly made up of synthetic fiber ropes, cables and chains. When the load solicitation is high, the mooring lines must be made up of chain. The monitoring of the strength of these chains is vital for the reliability and security of the production of energy. The current methods for supervising the loads on the chains are expensive and have many uncertainties involved. In this context, it is proposed a new methodology for the force estimation in chains through the measurements of their natural frequencies. The present dissertation arises as an improvement of this approach. A fuzzy inference system optimized by a genetic algorithm is introduced to enhance the estimation of the load on the chains. The inputs of the fuzzy models are the natural frequencies of the chains and the output is the estimated force. The Mamdani and Sugeno methodologies were implemented and compared. Triangular and Gaussian membership functions were used to model the inputs and the output. The rules were set according to the relations between the natural frequencies and the force on the chain. To optimize the system, the genetic algorithm can use the results provided by a mathematical model or by a set of measurements as training data. The mathematical model has good agreement with the experimental data. The fuzzy genetic model was simulated and tested providing good accuracy in estimating the force. In addition, the non-singleton fuzzification demonstrated that can be a helpful tool when the entries are noisy.

Keywords: Chain, Natural frequencies, Fuzzy logic, Genetic algorithm.

List of Figures

Figure 2.1 Variation of the natural frequencies in function of the bead. 24
Figure 2.2 First vibration mode of the spin loaded chain. 25
Figure 2.3 Chain modeled as the joint of cylindrical rods 26
Figure 2.4 Analysis of the critical frequencies as a function of the chain speed. 27
Figure 2.5 Representation of the monochain ropeway. 28
Figure 2.6 Model of the vertical moving chain. 28
Figure 2.7 Lumped mass model of the mooring line. 30
Figure 2.8 Spring model of two elements of the chain. 31
Figure 2.9 Finite elements of the mooring lines 33
Figure 3.1 Representation of the chain. 36
Figure 3.2 Representation of the Angles of Cardan 37
Figure 3.3 Representation of the position of mass center for any link of the chain. 38
Figure 3.4 Free body diagram for the upper link of the chain. 44
Figure 3.5 Free body diagram for a generic link of the chain. 45
Figure 3.6 free body diagram for any link of the chain seen from the second mobile reference frame. 47
Figure 3.7 Representation of the chain. 51
Figure 4.1 Dimensions of the chain. 54
Figure 4.2 Lay out of the experiment. 55
Figure 4.3 Support of the chain and shaker joint to the link. 56
Figure 4.4 Piece for attaching the accelerometers and detail of a strain gauge. 56
Figure 4.5 Running the experiment. 57
Figure 5.1 Representation of a fuzzy set. 62
Figure 5.2 Triangular membership function. 63
Figure 5.3 Trapezoidal membership function. 64
Figure 5.4 Gaussian membership function. 65
Figure 5.5 Generalized bell membership function. 66
Figure 5.6 Sigmoidal membership function. 67
Figure 5.7 Union and Intersection of two fuzzy sets. 68

Figure 5.8 alpha cut of a fuzzy set. 69
Figure 5.9 Concentration and dilatation of linguistic variables. 73
Figure 5.10 Structure of a fuzzy inference system. 75
Figure 5.11 Procedure of inference. 75
Figure 5.12 Representation of an antecedent part of a fuzzy inference system. 76
Figure 5.13 Singleton fuzzification. 77
Figure 5.14 Nonsingleton fuzzification. 78
Figure 5.15 Calculation of the membership degree with singleton fuzzification. 79
Figure 5.16 Calculation of the membership degree with nonsingleton fuzzification. 80
Figure 5.17 Representation the consequent part in a Mamdani fuzzy inference system. 84
Figure 5.18 Mapping of the firing strength of the rules in the consequent part. 85
Figure 5.19 Defuzzification methodologies. 87
Figure 5.20 Representation of constant functions as singletons of a Sugeno fuzzy inference system. 88
Figure 5.21 Surface of a fuzzy inference system. 89
Figure 6.1 Structure of the genetic algorithm. 93
Figure 6.2 Population in the genetic algorithm. 95
Figure 6.3 Crossover in one point. 98
Figure 7.1 Link of the chain modeled in SolidWorks. 100
Figure 7.2 Front and isometric view of the chain. 101
Figure 7.3 Membership functions for the first natural frequency as defined by the author. 102
Figure 7.4 Structure of the fuzzy system for estimating the force on the chain. 103
Figure 7.5 Illustration of the gens of the chromosome in the genetic algorithm for triangular MF. 104
Figure 7.6 Uniform selection process. 106
Figure 7.7 Crossover process. 106
Figure 7.8 Mutation process. 107
Figure 7.9 Structure of the fuzzy genetic system used in this work. 108
Figure 8.1 Natural frequencies of a chain with 6 links. 109
Figure 8.2 Natural frequencies of a chain with 24 links. 110
Figure 8.3 FRF of the acceleration of the link 8. 111
Figure 8.4 FRF of the acceleration of the link 11 112

Figure 8.5 FRF of the acceleration of the link 19. 112
Figure 8.6 Experimental Natural frequencies of the chain. 114
Figure 8.7 Comparison of the natural frequencies. Experimental and Simulated. 115
Figure 8.8 First natural frequency. Experimental and Simulated. 115
Figure 8.9 Simulated frequency Vs Experimental frequency. 116
Figure 8.10 Natural frequencies of the model with elastic supports. 118
Figure 8.11 Natural frequencies calculated with the model with rigid supports and elastic supports. 119
Figure 8.12 Force signal of the strain gauge at 30 kN. 120
Figure 8.13 Force signal of the strain gauge at 50 kN. 120
Figure 8.14 Results of the Mamdani FIS with triangular MF. 122
Figure 8.15 Results of the Mamdani FIS with triangular MF. 122
Figure 8.16 Results of the Mamdani FIS with gaussian MF. 123
Figure 8.17 Results of the Sugeno FIS with triangular MF. 124
Figure 8.18 Results of the Sugeno FIS with gaussian MF. 124
Figure 8.19 Membership functions for the first natural frequency as defined by the author. 126
Figure 8.20 Membership functions for the first natural frequency after the optimization process. 126
Figure 8.21 Results of the optimized FIS with triangular MF. 127
Figure 8.22 Membership functions for the first natural frequency as defined by the author. 128
Figure 8.23 Membership functions for the first natural frequency after the optimization process. 128
Figure 8.24 Results of the optimized FIS. 129
Figure 8.25 Results of the FIS trained with experimental data. 130
Figure 8.26 Performance of the non-singleton fuzzification. 133

List of tables

Table 4-1 Sensors installed on each link of the chain. 57

Table 8-1 Experimental natural frequencies for a loading/unloading cycle of the chain. 113

Table 8-2 Relationship between the experimental natural frequencies of the chain. 117

Table 8-3 Noisy inputs for the Fuzzy inference system. 131

Table 8-4 Comparison of the singleton and non-singleton fuzzification. 132

List of abbreviations and acronyms

Matrices and vectors

$\boldsymbol{S_1}, \boldsymbol{S_2}$	-Transformation matrices
$\boldsymbol{x_a}$	-Vector described in absolute coordinates
$\boldsymbol{x_m}$	-Vector described in mobile coordinates
$\boldsymbol{w}$	-Position vector of the mass center of a link described in absolute coordinates
$\boldsymbol{r}$	-Position vector of the origin of the mobile frame regarding the inertial frame
$\boldsymbol{u}$	-Position vector of the mass center of a link regarding the mobile frame
$\dot{\boldsymbol{w}}$	-Velocity vector of the mass center of a link described in absolute coordinates
$\ddot{\boldsymbol{w}}$	-Acceleration vector of the mass center of a link described in absolute coordinates
$\boldsymbol{\omega}$	-Angular velocity of a link described in absolute coordinates
$\boldsymbol{\alpha}$	-Angular Acceleration of a link described in absolute coordinates
$\boldsymbol{R_x}, \boldsymbol{R_y}, \boldsymbol{R_z}$	-Reaction forces at the link joints
$\boldsymbol{T}$	-Tension force
$\boldsymbol{M}$	-Mass matrix of the chain
$\boldsymbol{K}$	-Rigidity matrix of the chain

Greek letters

$\boldsymbol{\theta}$	-Rotation round y
$\boldsymbol{\beta}$	-Rotation round x
$\boldsymbol{\mu}$	-Degree of membership

Latin letters

$\boldsymbol{L}$	-Length of a link
$\boldsymbol{m}$	-Mass of a link
$\boldsymbol{g}$	-Acceleration of the gravity
$\boldsymbol{I_x}, \boldsymbol{I_y}, \boldsymbol{I_z}$	-Inertias of a link

Summary

1. INTRODUCTION 18
    1.1. Objectives 20
    1.2. Dissertation structure 20
2. DYNAMICS OF CHAINS: A REVIEW 23
    2.1. The hanging chains. 23
    2.2. The moving chain 26
    2.3. The mooring chain 29
        2.3.1. Lumped mass and spring model 29
        2.3.2. Finite elements method 32
        2.3.3. Inextensible links 33
3. MATHEMATICAL MODEL OF A LINK CHAIN 35
    3.1. Assumptions 35
    3.2. Generalized coordinates 36
        3.2.1. Coordinate transformation 37
    3.3. Kinematics 38
        3.3.1. Constraints 42
    3.4. Kinetics 43
    3.5. Linearization 48
    3.6. Equation of Motion of the chain 48
    3.7. Variation of the model 51
4. EXPERIMENTAL PROCEDURE 54
    4.1. Lay out 54
    4.2. Procedure 58
    4.3. Data processing 58

5. FUZZY LOGIC 60
5.1. Basic concepts 60
5.1.1. Fuzzy set theory 60
5.1.2. Fuzzy sets and membership functions 61
5.1.3. Membership function types 63
5.1.4. Operations with Fuzzy sets 67
5.2. Fuzzy Reasoning 69
5.2.1. Extension principle 69
5.2.2. Binary Fuzzy Relation 71
5.2.3. Max-min composition 72
5.3. Linguistic variables 72
5.3.1. Concentration and dilatation of linguistic values 73
5.4. Fuzzy Inference Systems 73
5.4.1. Components of the fuzzy inference system 74
5.4.2. Antecedent parts 76
5.4.3. Fuzzifier 77
5.4.4. Calculation of the degree of membership 79
5.4.5. Inference engine and fuzzy rules 80
5.4.6. Consequent parts 83
5.4.7. Mamdani Fuzzy models 84
5.4.8. Sugeno Fuzzy Models 87
5.4.9. Surface of fuzzy models 89
5.5. Modeling with fuzzy logic 90
5.6. Fuzzy logic and uncertainty 91
6. GENETIC ALGORITHM 92
6.1. Structure of the Genetic Algorithm 93

6.1.1. Initial population 94

6.1.2. Fitness Function 95

6.1.3. Stop criteria 95

6.1.4. Selection 96

6.1.5. Reproduction 97

6.1.6. Crossover 97

6.1.7. Mutation 98

7. PROPOSED METHODOLOGY FOR THIS WORK 100

8. RESULTS 109

8.1. Mathematical model of the chain 109

8.2. Experimental Results 110

8.3. Fuzzy inference system 121

8.4. Optimization of the fuzzy systems with genetic algorithm 125

8.5. The non-singleton fuzzification 130

9. CONCLUSIONS AND FURTHER WORKS. 134

9.1. Further works 135

References 137

APPENDIX. CATALOG CHAINS GRADE 8. 142

1. INTRODUCTION

In the offshore oil and gas industry, the monitoring of the structures is an important and vital work to do in order to ensure the safety of all equipment as well as of the staff that works over there.

As the offshore facilities are not on the ground, it is necessary to have some elements that hold the structure and provide stability. These elements are essential for the correct operation and to ensure the production.

The elements that provide support for the offshore structures are called mooring lines, which are composed by link chains and cables. In some cases, when the load solicitation is high, the mooring lines consist only of a link chain and an anchor.

The knowledge of the mechanical stress in mooring lines allows to work with safety conditions as well as to project the maintenance plan in order to guarantee the reliability of the system.

The measurement of the loads in mooring lines is currently made by techniques like the installation of load cells at the connection of the mooring line with the ship or floating platform, for example, or other types of sensors at the chains (PAPADIMITRIOU, 2016), (DU et al., 2015), (ROBERT et al., 1973), (PRIOUR, 1995) or even through the approximation of the shape of the mooring line to a catenary (JAMIESON, 2013).

The usage of sensors or devices to acquire data of underwater structures makes the maintenance of these equipment to be frequent and, in some cases, requires stopping the monitoring system for a long period of time. In addition, the environment where they work in is hostile, including severe weather conditions, wind, waves and currents, and the contact with salty water. These environmental factors can make these sensors and devices suffer damage and need to be replaced.

Furthermore, the installation of these devices is quite expensive, which is a decisive factor on the selection and implementation of a monitoring system. And finally, once this approach requires a rigorous maintenance program and, in many cases, it is necessary to replace some component, this solution is not viable.

The procedure of approaching the mooring line shape by a catenary in order to estimate the load applied to it is a process that has many uncertainties involved. The process consists on the measurement of the angle of the catenary with the information of the position of the vessel and the anchor, which is obtained with a differential GPS. The estimation of the force on the chain with this method is indirect and it is not accurate since the calculation of the load depends on the approximation of the profile of the mooring chain to a mathematical model of a catenary.

In the context of the mooring line force estimation, it is proposed to analyze the vibrational response of structures subjected exclusively to axial tensile load using vibration sensors and thereby to identify the natural frequencies of such structures and then to estimate the load to which the structure is being subjected. The concept of the technique is largely known, as the classical example of tuning the strings of a fiddle, where the increase in string tension produces a higher pitch and its relaxation results in a lower pitch.

Then, taking advantage of the relationship between the tensile force on the chain and their natural frequencies, it is possible to construct a calibration chart. This chart allows to correlate the measured natural frequencies with the corresponding applied force.

In simple terms, the analysis starts with the measurement of the free vibration of the mooring line. An accelerometer can be used for this purpose. Next, the natural frequencies of the system are calculated. Then, the frequencies are allocated in the calibration chart and the force applied to the mooring line is estimated. Usually, it is necessary an interpolation process to estimate this applied force, since the estimation is made with several entries.

The previous process can have many uncertainties involved. Thus, this work arises as the improvement of this approach aiming to find a methodology to handle the uncertainty and the automation of the process.

This work proposes the implementation of the fuzzy inference systems as a tool to estimate the force applied on a chain through the knowledge of its natural frequencies. Fuzzy logic has demonstrated to be a good tool to handle uncertainty (ZADEH, 1983). Another fact that encourages the use of the fuzzy logic is the high adaptability and the capability of modelling nonlinear systems.

In addition, a linear model of a vertical chain is built to obtain its natural frequencies for a wide loading range. With this information, it was possible to create the fuzzy inference systems. A genetic algorithm is implemented to improve the fuzzy inference systems and obtain an accurate estimate of the load on the chain.

1.1. Objectives

The main goal of this work is to develop a methodology that allows the prediction of the applied force on a link chain axially tensioned through the measurement of its natural frequencies. This approach uses a fuzzy inference system, which has three universes of discourse as antecedent parts representing the first three vibration modes and one universe of discourse as consequent part representing the force of the chain. In addition, a genetic algorithm is implemented in order to improve the estimation of the force of the chain by the fuzzy inference system.

To achieve this main objective, there are some intermediate objectives that also need to be achieved, which are:

1. The construction of a linear mathematical model of the link chain aiming the computation of the natural frequencies as a function of the variation of the applied force. The results produced by this model configure the training data for the fuzzy inference system.
2. The measurement of the natural frequencies of real chains in order to validate the mathematical model as well as to have training data from different sources.

1.2. Dissertation structure

This dissertation was written with the following order: Chapter 3 presents the mathematical model of the chain and chapter 4 the experimental procedure. These chapters configure the dynamic knowledge of the chain, it means, how the natural frequencies vary with the variation of the applied force of the chain. Chapter 5 presents the fuzzy logic, more specifically the fuzzy inference system, which is the tool used to estimate the force of the chain knowing the natural frequencies. Chapter 6 presents the genetic algorithm that is applied to improve the estimation of the fuzzy inference system. Finally, chapter 7 presents the methodology of the work, here it is explained how the mathematical model, the experimental data, the fuzzy inference system and the genetic algorithm work together in order to have an accurate estimation of the force of the chain.

The summarize of each chapter of this dissertation is presented as follows.

Chapter 2: Dynamics of chain: A review

The relevant studies about the dynamics of chains are presented in this chapter. A variety of configurations of chains are analyzed considering from the falling chain until the finite elements of a mooring chain.

Chapter 3: Mathematical model of a chain.

In this chapter, the mooring chain modelling is presented. The chain is modeled as a sequence of rigid elements joined by spherical joints. Applying Newton's Laws and considering small displacement a set of linear equations of motion is obtained. The eigenvalues are calculated in order to identify the natural frequencies.

Chapter 4: Experimental procedure

The experimental setup for the identification of the natural frequencies of the link chain is presented. The lay out as well as the experimental procedure is explained. The data processing techniques are presented.

Chapter 5: Fuzzy logic

The main application of the fuzzy logic is explained in this chapter: the fuzzy inference systems. The common membership functions are presented as well as the difference between the Mamdani and Sugeno fuzzy system. In addition, it is considered two types of fuzzification: singleton and non-singleton. The inference process is explain step by step.

Chapter 6: Genetic algorithm

Each step of the genetic algorithm is shown and an explanation about how it works is presented. The basic structure of a genetic algorithm is highlighted, which consists of: an initial population, the fitness function, the selection, crossover and mutation.

Chapter 7: Methodology for this work

This chapter presents the methodology for modelling the fuzzy inference system for the estimation of the force on the chains. In addition, it is exposed the strategy of optimization of the parameters of the fuzzy system with the genetic algorithm, which uses the training data provided by the mathematical model results and/or the experimental measurements.

Chapter 8: Results

The following results are presented in this work

1 Analysis of the mathematical model of a chain.
2 Results from the experiment and comparison with the mathematical model.
3 Performance of the different fuzzy inference system for estimating the force on the chains.
4 Improvement of the fuzzy inference system with genetic algorithm.
5 Influence of the non-singleton fuzzification.

Chapter 9: Conclusions and final comments.

Synthesis of the main conclusions of the work and relevant results as well as proposals for future works.

Appendix A: Catalog of chains grade 8.

Here is presented the catalog of a manufacturer of chains grade 8 from where the features of the chain were taken as input for the mathematical model.

2. DYNAMICS OF CHAINS: A REVIEW

This chapter has as objective to show the different methodologies to study the dynamics of the chains. A variety of configurations as well as diverse environmental conditions of the chains are considered.

2.1. The hanging chains.

The hanging chain is the simplest configuration of a system formed by link chains. It consists of a vertically positioned chain, with one end fixed while the other is free to move. The study of the dynamic of this type of system can be treated with different approaches.

When the chain is long (the chain length is very long when compared to the link size), and it is restricted to move transversally with small oscillations, the phenomenon can be characterized by the wave equation (PUGSLEY, 1949), that is, the transversal displacement has the shape of a wave that propagates through the chain length. This is the same behavior of a string. Pugsley (1949) related the two equations obtaining a new expression depending on the span, dip and length of the chain that calculates the natural frequencies in a direct way. This approach provides fairly accuracy to predict the first vibration mode.

Whether the chain is taken as a continuous body, the transversal vibration can be described with the wave equation. This type of differential equation can be transformed to Bessel form (VERBIN, 2015). The solution of the system is to find the zeroes of the Bessel equation. The Bessel equation allows adopting different boundary conditions in order to simulate different configurations of the chain. Worth noting that the chain must always be tensioned. Once the zeroes are found, a direct expression of the natural frequencies is obtained. The equation permits to vary physical parameters of the chain, as length and linear density. If a bead is attached to the downiest point with mass greater than chain mass, it is possible to emulate an applied load to the chain. The model is capable to predict a general shape of the vibrate modes and natural frequencies. The figure 2.1 shows the variation of the natural frequencies with the variation of the bead when is fixed at one end (a) and fixed at both ends (b).

Figure 2.1 Variation of the natural frequencies in function of the bead.

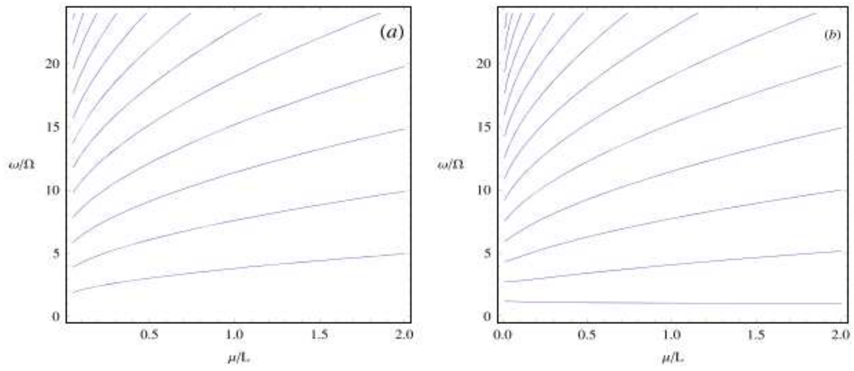

Source: Verbin, 2015

The chain can also be considered as the joint of n rods connected by the ends (Levinson, 1976). The length of each link is L/n and its center of mass lies along the line that connect the two link joints. Each rod has a radius of gyration equal to $k(L/n)^2$, where k is a dimensionless number. Taking the angle between the link position with the vertical direction as generalized coordinate for each link, a linear equation of motion can be written for this system. The determination of the modal parameters is straightforward. This type of modelling is the most general formulation considering the chain as a multibody system. For more accurate results other parameters must be considered.

The chain can be analyzed with both ends fixed, with an applied loaded and subjected to a spin velocity (NOËL et al., 2008) The vibration is assumed to follow the wave shape. The solution of the equation of motion is made through the Bessel equation of zero order. The results of this approach have good accuracy for the first three vibration modes for different applied loads and spin velocities. In addition, it is possible to demonstrate that as the tension increase the resonance frequencies do too. Figure 2.2 shows the first vibration mode of chains made of different materials.

Figure 2.2 First vibration mode of the spin loaded chain.

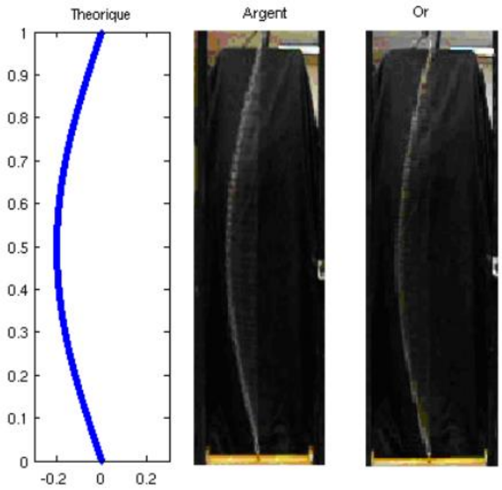

Source: Jean-Marc Noël et al. ,2005

The non-linearized system is studied too (TOMASZEWSKI; PIERANSKI, 2005), (FRITZKOWSKI; KAMINSKI, 2008). Carrying out with the approach of modeling the chain as *n* connected rod and limiting the problem to the plane (Figure 2.3), the Lagrange theory provides the equations of motion of the system. The angles with the vertical are set as the generalized coordinates. The kinetic and potential energy are described for each rod, considering that the mass center is localized in the length center and the joint is spherical. As the obtained equations of motion cannot be linearized, the computational cost is high as well as the time spent for calculating the response. The authors used some techniques in order to facilitate the integration work, as the introduction of dimensionless parameters depending on the sound velocity in the air, so as reducing the mathematical complexity of the system. The dynamic response of the system is a good approximation for the chain profile when is perturbed from the equilibrium position. This modelling also allows incorporating velocity to one end, but internal forces are not studied.

Figure 2.3 Chain modeled as the joint of cylindrical rods.

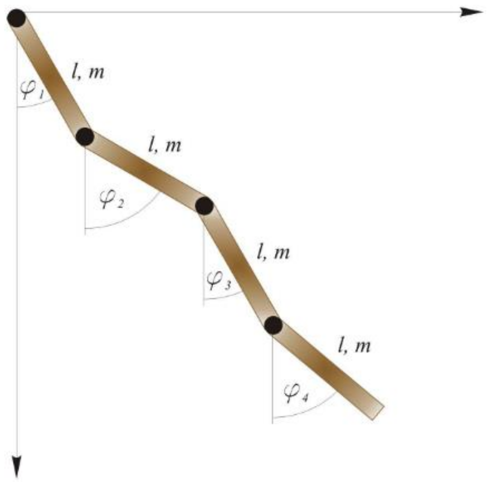

Source: Bertoldi et al., 2007

2.2. The moving chain

The moving chain (link chain) is a special case which is very common in the transportation industry. The chains are capable of transport big loads and objects suspended in the air as a cableway.

The chains used in transportation are normally long, so it is possible to treat them as strings. Considering a particle traveling through its length and taking into account the deflection in an instant of time, a differential equation is proposed to describe the motion of the point (MAHALINGAM , 1957). Centrifugal tension and transversal oscillations are considered. The string presents variations in resonance frequencies with the increase of the chain velocity (figure 2.4). A fact to highlight is that, theoretically, for a constant tension, the natural frequencies decreases until zero as the chain velocity approaches the wave propagation velocity. In practice, this does not happen because the chain tension increases with the chain velocity owing to centrifugal effects.

Figure 2.4 Analysis of the critical frequencies as a function of the chain speed.

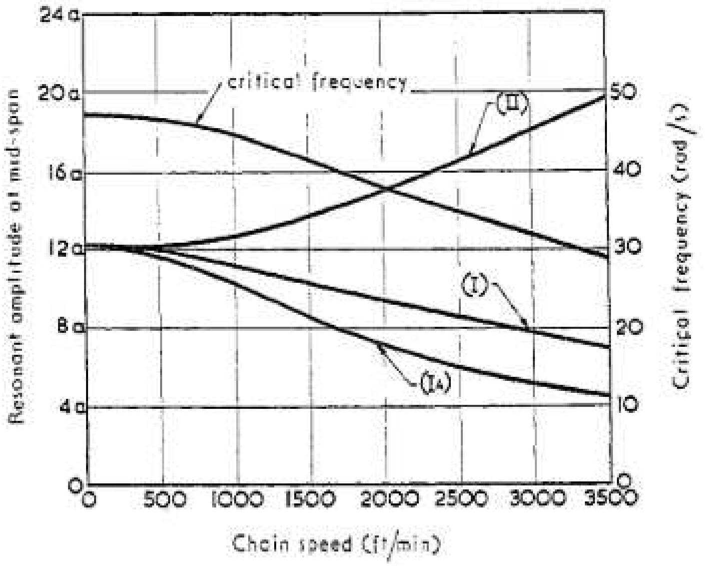

Source: Mahalingam, 1957

Another study was performed by (LI et al., 2014) This study case aims to find how the initial condition of the moving chain affects the resonance frequencies in order to suppress great vibrations. The authors model the chain as a string and formulate the equation of motion in the Laplace domain. The results showed that the amplitude of vibration of axially moving chain increases with the increment of the initial tension. The author proved that the proposed differential equation is valid to predict the effects of operation parameters on vibration frequency.

The characterization of modal parameters and transversal vibration of a monochain ropeway is possible by modelling the chain with uniform mass distribution and concentrated inertia loads (Figure 2.5). (YANG et al. ,2015). The boundary conditions subjected to the polygonal action caused by the chain support engagement, coupling effect, variable tension and time depend speed on transversal vibration is investigated. The results of this approach showed that supporting rollers with small wrap angle increase the vibration because of the polygonal action. The interaction of transportation speed and wave velocity influences the amplitude and frequency of transversal vibration. The amplitude and frequency are proportional to transportation speed. Performed experiments validate the equations. The collected data show good agreement with the calculated results.

Figure 2.5 Representation of the monochain ropeway.

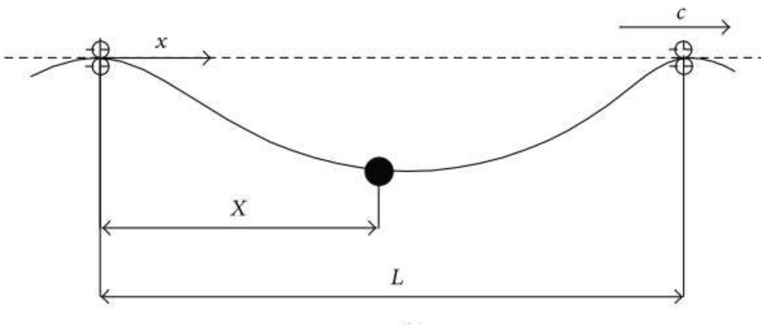

Source: Yang et al. (2015)

The vertically moving chain is studied with non-negligible weight (WANG ,2017). With the appropriate initial value method, the natural frequencies are determined for various axial velocities and string densities. No standing waves are considered as well as bending stiffness. Considering small vibration, the differential equation for a string is posed. The numerical method that the author used to find the natural frequencies is setting an initial value and a value for the frequency, if this frequency accomplishes a proposed constriction, then it is an Eigenvalue. The method shows high efficiency in finding the natural frequencies.

Figure 2.6 Model of the vertical moving chain.

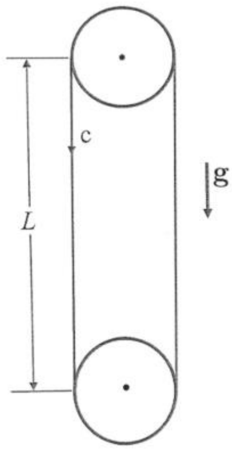

Source: Wang (2017)

2.3. The mooring chain

Mooring chains are largely used in offshore application. Some of them are oil and gas facilities as well as wind energy production. Mooring chains are used to provide sustentation to the structure in several configurations. The mooring lines are usually a combination of cables and link chains.

The analysis of the mooring chains carries out aspects as the contact with the sand, the drag force, the interaction with the water, the induced inertia and others. Some of the methodologies are presented below with different approaches.

2.3.1. Lumped mass and spring model

The lumped mass and spring method (LMM) is largely used to model mooring chains for offshore applications. The method allows studying several configurations of the mooring line such as catenary and taut form. This approach considers the chain links as deformable bodies.

The LMM permits to study tridimensional geometries as well as tridimensional motions. Large displacements are assumed. The inclusion of forces due to the weight of the string, buoyancy, drag and added mass of the fluid is possible. In addition, non-uniform strings can be analyzed, since the method shall have the capacity of include any subsystem. The implementation of several boundary conditions is available (HUANG, 1994).

The method consists in the division of the mooring line in n elements. The mass of each element is concentrated and it is connected to the neighbor mass through an axial spring. Each lumped mass is considered as a node.

The mathematical formulation of the equations of motion is made through the application of the Newton's Laws. A system of non-linear partial differential equations is obtained. The method is versatile and it accepts a variety of boundary conditions, applied to each line end like, for example, the type of drag considered or the vessel floating at the top of the chain. The solution of the system can be obtained applying the finite difference method, which provides stability to the integration.

New assumptions can be introduced to the method. The definition of the boundary conditions reflects directly on the system response. The consideration of the interaction of the line with the seabed and the anchor as a pin configures a new study case (KURIAN et al., 2013). The line is connected to a floating structure, which can be affected by waves, wind and others. The response of the structure and the chain can be separately calculated, since the interference of the line in the dynamics of the structure is negligible. The mooring line rests on a bed of elastic foundation and the touchdown point varies during the oscillation (figure 2.7). The hydrodynamics forces have linear loading variation per element. The line is fully flexible at the bending direction and only the secant stiffness is considered. The frequency of the floating end directly affects the line dynamics tension. When the soil stiffness increases, the line tension decreases. The soil damping dissipates the impact due to mooring dynamics response, resulting in a decrease of the line tension.

Figure 2.7 Lumped mass model of the mooring line.

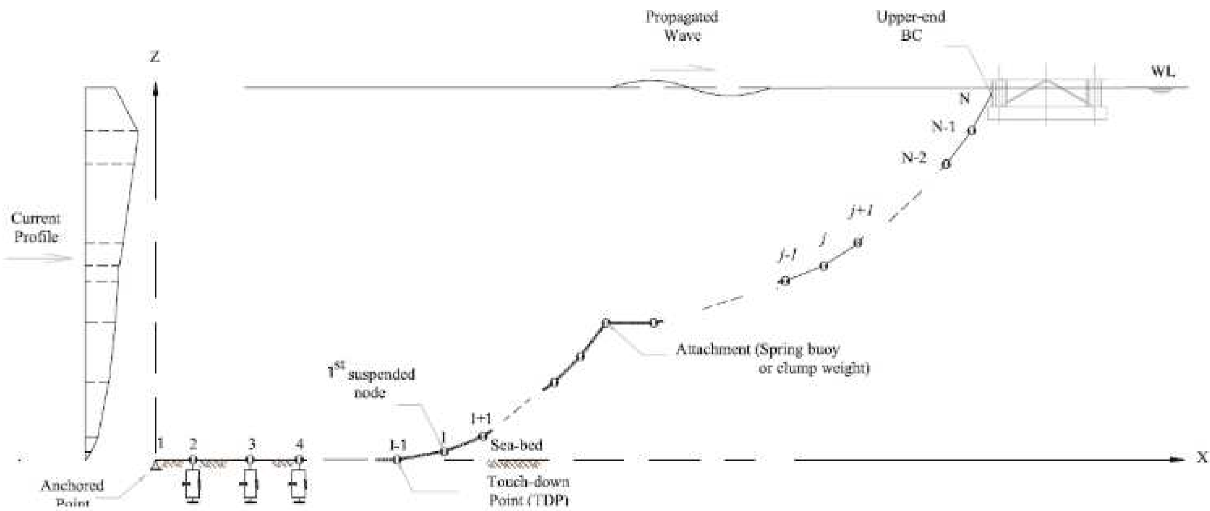

Source: Kurian et al. (2013)

The effects of torsion and bending are included in the method of lumped mass (CHAI et al., 2002). A catenary is considered. Three translational coordinates are set as well as one for torsional direction. The authors declared that this approach provides a simple way to simulate the dynamics of a mooring line, enabling the study of several situations and presenting good outcomes for a great number of cases.

The study of the complete offshore structure comprises the anchor, the mooring line and the floating vessel is a hard work to do. The modeling of the vessel requires the implementation of forces of second order and the handling of non-linearities caused by geometry, drag effects and others (LOW; LANGLEY, 2006). The solution of the system is normally performed in the time domain, but the frequency approach can be accomplished too. This approach is computationally intensive. The vessel is modeled as a rigid body with six degrees of freedom, which experiments forces due to the water waves and the wind. The chain line is modelled applying the LMM with additional rotational springs in order to simulate the bending stiffness (figure 2.8). Large deflections and small strains are assumed. The drag, hydrodynamics, and inertial forces due to added mass are considered to construct the equations of motion. The frequency domain presents improved results when compared to the time domain for vessel motions and line tensions. It is recommended to use frequency domain when the non-linearities are not significant (large mooring lines). In addition, it is advisable to perform time domain coupled analysis to verify special cases.

Figure 2.8 Spring model of two elements of the chain.

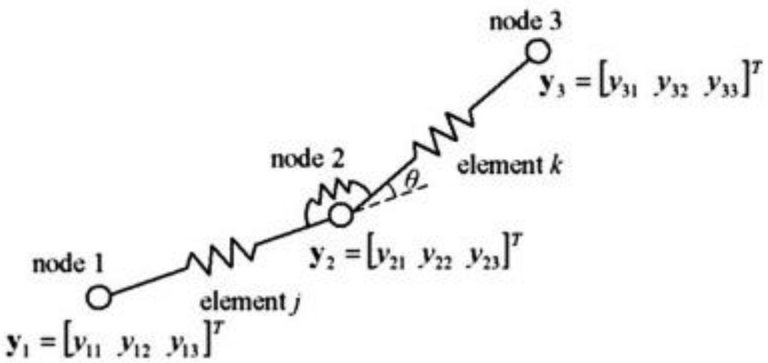

Source: Low and Langley (2006)

The anchor point is commonly considered as a fixed pin. The increase of application of taut configuration (vertical chain) in mooring lines makes the anchor to be embedded several meters beneath the seabed in order to provide enough holding capacity, thus some part of the chain is embedded too, causing interesting interactions between the soil and the line (XIONG et al., 2016). The approach uses a simplified LMM aiming to focus on the analysis of the anchor. Although the embedded part of the line is small, interferes in the dynamics of the chain as well as the load of the line.

2.3.2. Finite elements method

The use of the finite elements method (FEM) is increasing for modelling mooring lines and study their dynamics behavior as well as to be a helpful tool for their project.

A taut mooring line is fully suspended, and the touchdown point is fixed. For modelling this line, a geometrically nonlinear finite element formulation of a spatially distributed cable is presented by the use of an isoparametric cable element (YANG; TENG, 2010). The tangent stiffness and mass matrixes are evaluated and the equilibrium is obtained with the load incremental method and Newton-Raphson iterations. The incremental equations of motion of the cable is derived from the continuous mechanics. Considering the segment between two nodes, the displacements can be interpolated with nodal displacements. Thus, obtaining the interpolate shape functions, it is possible to get the mass and stiffness matrices, which are assembled to form the global matrices. Yang and Teng (2010) declared that the method presents good accuracy to estimate the line tension and the induced damping. The change of the considerations of the line or the boundary conditions, affects the induced damping. In addition, the method presented by the authors is adaptable for a different number of nodes, having the capability to performing many numbers of nodes or conversely only three nodes.

Comparisons between the methods of modelling the mooring line dynamics are made in order to evaluate capability, versatility and numerical efficiency (KIM et al., 2013). The FEM applies the minimum energy principle to formulate the non-linear dynamic of the line with a discrete numerical model. The analysis of the system must be coupled, i.e., the dynamics of the line has to be included in the study of the dynamics of the floating vessel (figure 2.9). The FEM allows the inclusion of damping, a task that is difficult for LMM. In addition, this approach provides direct information about the line tension.

Figure 2.9 Finite elements of the mooring lines

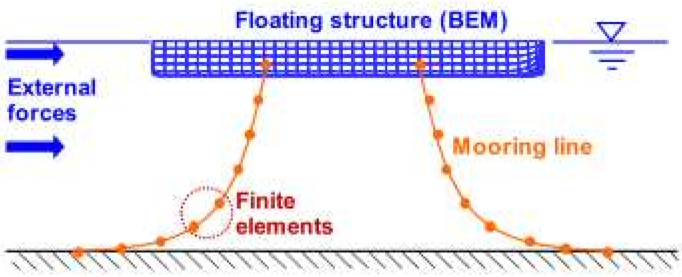

Source: Kim et al. (2013).

The interaction of the embedded chain with the soil is studied by several methods. As shown above, the LMM is one of them but the FEM has been implemented in order to study new conditions since the buried chain length consideration is growing due to holding requirements(LI et al., 2016). The FEM method presents good agreements with tests and theoretical analysis. As the depth increases, the results vary for both methods. This can occur because of the plastic zone of around the chain changes with the location of the attachment point in the soil. In addition, the interaction between the chain and the soil reduces the load at the anchor but can increase the risk of failure.

2.3.3. Inextensible links

The mooring lines are usually taken as the union of several extensible links. A mooring line with enough number of links can establish a chain with inextensible links (FILIPICH; ROSALES, 2007) For each link are defined two nodes, which have three degrees of freedom representing the linear displacements. Applying the Newton´s Laws for every link, the motion equations of motion are obtained, considering the center mass accelerations and the internal forces due to the reactions. The solution of the differential equations is made through the power series method. The results show good agreement with outcomes from the finite elements method.

As conclusion of this chapter, it is possible to observe that it does not exist any mathematical model of a tensioned chain considered as a multibody system with both ends fixed. Thus, in the next chapter, it is proposed a mathematical model of a tensioned link chain as a multibody system, implementing some assumptions from the works of Tomaszewski and Pieranski (2005), Fritzkowski and Kaminski (2008).

3. MATHEMATICAL MODEL OF A LINK CHAIN

This chapter explains the proposed model of a link chain fixed at both ends and tensioned. The chain is treated as a multibody system. The goal of the modeling is to obtain the natural frequencies of vibration of the chain as a function of the applied force at one end. The mathematical model is made implementing some assumptions from the works of Tomaszewski and Pieranski (2005), Fritzkowski and Kaminski (2008) applying a novel methodology for the analysis of the dynamics as well as the consideration of the three-dimensional motion.

3.1. Assumptions

Some assumptions are made aiming to facilitate the modeling of the chain and the understanding of its dynamics. They are cited as follows:

- The links of the chain are inextensible.
- All the links of the chain have the same geometric characteristics, i.e. all of them have the same shape.
- All the links have the same mass per length unit, which is constant.
- The links are considered as cylindrical rods connected by means of spherical joints (TOMASZEWSKI; PIERANSKI, 2005), (FRITZKOWSKI; KAMINSKI, 2008).
- The chain is vertical and constraint at both ends.
- The lowest end is fixed and it does not allow translation movement. The upper end allows little translation at vertical direction because the links do not allow strain.
- The chain is tensioned by a force applied at the upper end.
- Spin motion of the links is neglected.

Figure 3.1 shows a representation of the chain.

Figure 3.1 Representation of the chain.

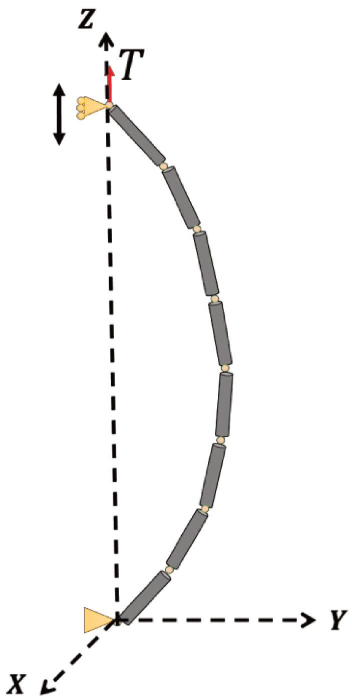

Source: Author.

3.2. Generalized coordinates

Cardan angles allow the orientation of a rigid body in space through the application of sequential elementary rotations around the three axes of the reference system fixed to the body. In this study, this set of angles is used to model the chain links.

The sequence of rotations that each link performs to achieve any position is as follows: firstly, an inertial coordinate system $\Re_0 = \{X, Y, Z\}$ is set at the fixed support of the chain. The length of the link is fixed to the axis Z of the inertial frame. It is performed a rotation θ around the axis Y of $\Re_0$. This rotation configures a new local frame $\Re_1 = \{x_1, y_1, z_1\}$. Then, a new rotation β is performed around the axis x_1, which configures another local coordinate system $\Re_2 = \{x_2, y_2, z_2\}$. See the set of rotations in the figure 3.2. Thus, each link has two generalized coordinates θ and β as well as two local frames $\Re_1$ and $\Re_2$ associated.

Figure 3.2 Representation of the Angles of Cardan

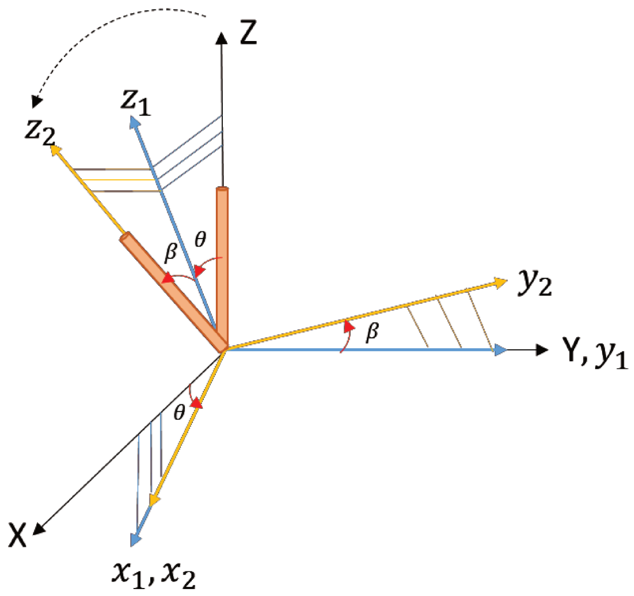

Source: Author

3.2.1. Coordinate transformation

In order to facilitate the analysis, vectors corresponding to the links are described in the local reference frame $\Re_2$. The quantities calculated in this system are relative and they need to be described in the absolute coordinate system. The mean of transforming a vector described in a local reference frame into an inertial coordinate system is through the transformation matrices.

In this case, two transformation matrices are required since for each link two local reference frame are defined, one corresponding to the first rotation and the second one to the second rotation. The transformation matrices are the following:

$$\boldsymbol{S_1} = \begin{bmatrix} \cos(\theta) & 0 & \sin(\theta) \\ 0 & 1 & 0 \\ -\sin(\theta) & 0 & \cos(\theta) \end{bmatrix} \tag{3.1}$$

$$\boldsymbol{S_2} = \begin{bmatrix} 1 & 0 & 0 \\ 0 & \cos(\beta) & -\sin(\beta) \\ 0 & \sin(\beta) & \cos(\beta) \end{bmatrix} \tag{3.2}$$

Let be $\boldsymbol{x_m}$ a vector described in $\Re_2$. Then the vector described in the inertial system is

$$\boldsymbol{x_a} = \boldsymbol{S_1 S_2 x_m} \tag{3.3}$$

where $\boldsymbol{x_a}$ is the vector described in the inertial coordinate system. If a vector described in the inertial system need to be transform into the mobile system, the transformation matrices are the transposed. As the matrices are orthogonal, the transposed is equal to the inverse. The transformation is as follows:

$$\boldsymbol{x_m} = \boldsymbol{S_2^T S_1^T x_a} \tag{3.4}$$

3.3. Kinematics

An inertial coordinate system$\Re_0$ is set at the lower end of the chain. The chain is vertical and lies over the axis Z of the inertial coordinate system. The lower end is fixed. The upper end only may move vertically through the direction Z.

Two local reference frame $\Re_1$ and $\Re_2$ are defined for each link. The length of the link is fixed at the axis z_2 of $\Re_2$ reference frame. The position of the center of mass of each link, considering that it located at the center of the length, is described into $\Re_2$.

Figure 3.3 Representation of the position of mass center for any link of the chain.

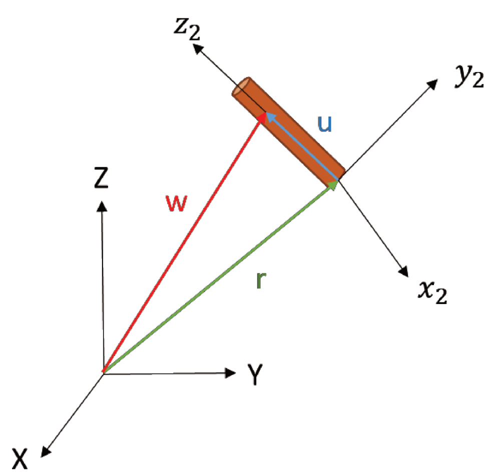

Source: Author

The position of any point of the link described in the inertial coordinates can be calculated with the following equation

$$\boldsymbol{w} = \boldsymbol{r} + \boldsymbol{S_1}\boldsymbol{S_2}\boldsymbol{u}^{\boldsymbol{T}} \tag{3.5}$$

where $\boldsymbol{r}$ is the vector that described the position of the origin of the local reference frame respecting to the inertial system. $\boldsymbol{S_1}$ and $\boldsymbol{S_2}$ are the transformation matrices and $\boldsymbol{u}$ is the position vector of any point of the rod described in the mobile coordinates.

The length of all the links is the same and is denoted by L. The center of mass is considered to be at its midpoint.

In order to develop the equation of motion of the link chain, it is necessary to obtain the position of the center of mass of each link. Starting with the lower link of the chain, one considers that its lower end is located at the origin of the inertial coordinate system. The position of the center of mass of this link is easily described in $\Re_2$ frame as follows:

$$\boldsymbol{u}^{\boldsymbol{T}} = \left\{0, 0, \frac{L}{2}\right\} \tag{3.6}$$

In this case, the vector $\boldsymbol{r}$, described in eq. (3.5), is made up of zeros, because the origin of $\Re_2$ lies at the origin of the inertial coordinate system. Thus, replacing at the equation (3.5) the position of the center of mass in absolute coordinates is

$$\boldsymbol{w_1} = \begin{Bmatrix} \frac{L}{2}\cos(\beta_1)\sin(\theta_1) \\ -\frac{\mathrm{L}}{2}\sin(\beta_1) \\ \frac{L}{2}\cos(\beta_1)\cos(\theta_1) \end{Bmatrix} \tag{3.7}$$

where θ_1 and β_1 are the generalized coordinate for the first link.

In order to obtain the position of the center of mass of the next link, the same procedure is used. The only difference here, and in the case of the next links, is that the vector r is no longer zero. In the case of the second lower link, $\boldsymbol{r}$ is the position of the upper end of the first link. It is worth noting that the vector $\boldsymbol{r}$ must be described in absolute coordinates. Then, the position of the center of mass for the second link is:

$$\boldsymbol{w_2} = \begin{Bmatrix} L\cos(\beta_1)\sin(\theta_1) + \frac{L}{2}\cos(\beta_2)\sin(\theta_2) \\ -\mathrm{L}\sin(\beta_1) - \frac{\mathrm{L}}{2}\sin(\beta_2) \\ L\cos(\beta_1)\cos(\theta_1) + \frac{L}{2}\cos(\beta_2)\cos(\theta_2) \end{Bmatrix} \tag{3.8}$$

Note that if the procedure were applied for the third link, the position would have the same form, but with one additional term corresponding to the position of the center of mass of the third link. As the vector $\boldsymbol{r}$ of any link corresponds to the sum of positions of the end of the previous links and the position of the center of mass is described in the corresponding mobile coordinates, the vector that describes the position of the center of mass of any link of the chain can be generalized as follows:

$$\boldsymbol{w_i} = \begin{Bmatrix} L\sum_{j=1}^{i-1}\cos(\beta_j)\sin(\theta_j) + \frac{L}{2}\cos(\beta_i)\sin(\theta_i) \\ -\mathrm{L}\sum_{j=1}^{i-1}\sin(\beta_j) - \frac{L}{2}\sin(\beta_i) \\ L\sum_{j=1}^{i-1}\cos(\beta_j)\cos(\theta_j) + \frac{L}{2}\cos(\beta_i)\cos(\theta_i) \end{Bmatrix} \tag{3.9}$$

where the integer i represents the number of the link which one the position is being calculated. The link is counted upwards, that is, the first link is the lowest and the last is the highest.

The velocity and acceleration of the center of mass is calculated deriving, with respect to the time, the expression of the position presented in eq. (3.9).

Equations (3.10), (3.11) and (3.12) describe the general expressions of the velocity of the center of mass of any link in the X, Y, and Z directions, respectively:

$$\dot{w}_{i_X} = L\sum_{j=1}^{i-1} -\dot{\beta}_j \sin(\beta_1)\sin(\theta_j) + \dot{\theta}_j \cos(\beta_j)\cos(\theta_j) + \frac{L}{2}\left(-\dot{\beta}_i \sin(\beta_i)\sin(\theta_i) + \dot{\theta}_i \cos(\beta_i)\cos(\theta_i)\right) \tag{3.10}$$

$$\dot{w}_{i_Y} = L\sum_{j=1}^{i-1} -\dot{\beta}_j \cos(\beta_j) - \frac{L}{2}\dot{\beta}_i \cos(\beta_i) \tag{3.11}$$

$$\dot{w}_{i_Z} = L\sum_{j=1}^{i-1} -\dot{\beta}_j \sin(\beta_j)\cos(\theta_j) - \dot{\theta}_j \cos(\beta_j)\sin(\theta_j) + \frac{L}{2}\left(-\dot{\beta}_i \sin(\beta_i)\cos(\theta_i) - \dot{\theta}_i \cos(\beta_i)\sin(\theta_i)\right) \tag{3.12}$$

The general expressions of the acceleration of the center of mass of any link in the X_0, Y_0, and Z_0 directions are presented in equations (3.13), (3.14) and (3.15), respectively:

$$\begin{aligned}\ddot{w}_{\mathrm{i}_X} = L\sum_{j=1}^{i-1} &-\ddot{\beta}_j \sin(\beta_j)\sin(\theta_j) - \dot{\beta}_j^2 \cos(\beta_j)\sin(\theta_j) - \dot{\beta}_j\dot{\theta}_j \sin(\beta_j)\cos(\theta_j) \\ &+ \ddot{\theta}_j \cos(\beta_j)\cos(\theta_j) - \dot{\theta}_j\dot{\beta}_j \sin(\beta_j)\cos(\theta_j) \\ &- \dot{\theta}_j^2 \cos(\beta_j)\sin(\theta_j) \\ &+ \frac{L}{2}\left(-\ddot{\beta}_i \sin(\beta_i)\sin(\theta_i) - \dot{\beta}_i^2 \cos(\beta_i)\sin(\theta_i)\right. \\ &- \dot{\beta}_i\dot{\theta}_i \sin(\beta_i)\cos(\theta_i) + \ddot{\theta}_i \cos(\beta_i)\cos(\theta_i) \\ &\left. - \dot{\theta}_i\dot{\beta}_i \sin(\beta_i)\cos(\theta_i) - \dot{\theta}_i^2 \cos(\beta_i)\sin(\theta_i)\right)\end{aligned} \tag{3.13}$$

$$\ddot{w}_{\mathrm{i}_Y} = L\sum_{j=1}^{i-1} -\ddot{\beta}_j \cos(\beta_j) + \dot{\beta}_j^2 \sin(\beta_j) + \frac{L}{2}\left(-\ddot{\beta}_i \cos(\beta_i) + \dot{\beta}_i^2 \sin(\beta_i)\right) \tag{3.14}$$

$$\ddot{w}_{i_Z} = L\sum_{j=1}^{i-1} -\ddot{\beta}_j \sin(\beta_j)\cos(\theta_j) - \dot{\beta}_j^2 \cos(\beta_j)\cos(\theta_j)$$
$$+ \dot{\beta}_j\dot{\theta}_j \sin(\beta_j)\sin(\theta_j) - \ddot{\theta}_j \cos(\beta_j)\sin(\theta_j)$$
$$+ \dot{\theta}_j\dot{\beta}_j \sin(\beta_j)\sin(\theta_j) - \dot{\theta}_j^2 \cos(\beta_j)\cos(\theta_j)$$
$$+ \frac{L}{2}\big(-\ddot{\beta}_i \sin(\beta_i)\cos(\theta_i) - \dot{\beta}_i^2 \cos(\beta_i)\cos(\theta_i)$$
$$+ \dot{\beta}_i\dot{\theta}_i \sin(\beta_i)\sin(\theta_i) - \ddot{\theta}_i \cos(\beta_i)\sin(\theta_i)$$
$$+ \dot{\theta}_i\dot{\beta}_i \sin(\beta_i)\sin(\theta_i) - \dot{\theta}_i^2 \cos(\beta_i)\cos(\theta_i)\big) \tag{3.15}$$

The angular velocity and acceleration of each link is described, in the inertial reference system, by the equations (3.16) and (3.17), respectively:

$$\boldsymbol{\omega_i} = \begin{bmatrix} \dot{\beta}_i \cos(\theta_i) \\ \dot{\theta} \\ -\dot{\beta}_i \sin(\theta_i) \end{bmatrix} \tag{3.16}$$

$$\boldsymbol{\alpha_i} = \begin{bmatrix} \ddot{\beta}_i \cos(\theta_i) - \dot{\beta}_i\dot{\theta}_i \sin(\theta_i) \\ \ddot{\theta} \\ -\ddot{\beta}_i \sin(\theta_i) - \dot{\beta}_i\dot{\theta}_i \cos(\theta_i) \end{bmatrix} \tag{3.17}$$

3.3.1. Constraints

The links of the chain are considered as inextensible. Aiming to accomplish that condition and knowing that both ends of the chain are fixed in the directions X and Y, the movement in the Z direction of the upper end is allowed.

Another constraint is related to the fact that both ends are fixed in directions X and Y. Then the summation of the positions of all the links in the directions X and Y must be equal to zero. This is because the chain begins and ends at the same point for both directions. This constraint can be expressed in mathematical form by the following equations:

$$\sum_{i=1}^{n} x_{s_i} = 0$$
$$\sum_{i=1}^{n} y_{s_i} = 0 \tag{3.18}$$

Where x_{s_i} and y_{s_i} are the positions of the upper point of each link in the direction X and Y respectively.

3.4. Kinetics

Here the Newton's laws are applied in order to analyze the effects of the forces and moments over the chain.

As all links are connected by spherical joints, three reaction forces are considered for each joint. In order to take the influence of the gravity into account, the weight force of each link is applied at its midpoint. At the upper link, an external force T is applied in order to tension the chain. All the forces are described in directions according to the inertial coordinate system.

For this model, the chain is considered to be always tensioned, i.e., the value of the force T must be equal or greater than the total weight of the chain. The friction between the components is neglected.

The chain is modeled as a multi-body system, and then the links of the chain are analyzed individually. As mentioned previously, the link is fixed on the axis Z_2 of $\Re_2$. For convenience, these axes are taken as the inertia principal axes.

The sum of forces is performed in the inertial coordinate system since all the quantities are described there, and the sum of moments is done in $\Re_2$ because of the facilities for calculating the inertia tensor. It is important to highlight that when choosing $\Re_2$ as inertia principal axes, the inertia tensor does not change with time.

The free body diagram of the upper link of the chain is shown in Figure 3.4.

Figure 3.4 Free body diagram for the upper link of the chain.

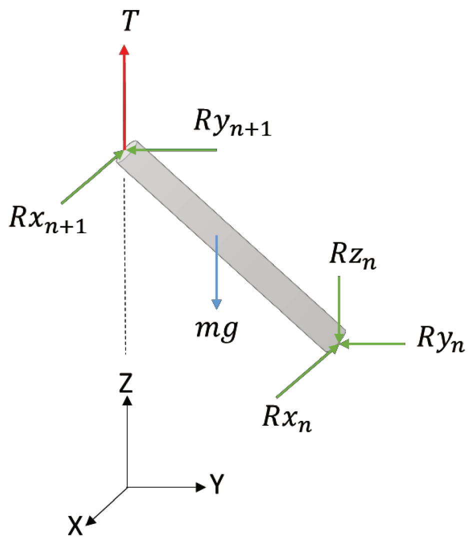

Source: Author.

The forces Rx, Ry and Rz correspond to the reaction forces at the joints along the X, Y, and Z directions, respectively, and the subscript n is the number of the joint, counted upward starting from the bottom end of the lower link. The force mg is the weight of the link.

The sums of forces along the three axes are expressed by equations (3.19) to (3.21):

$$\sum Fx = ma_{x_n} = -Rx_{n+1} - Rx_n \tag{3.19}$$

$$\sum Fy = ma_{y_n} = -Ry_{n+1} - Ry_n \tag{3.20}$$

$$\sum Fz = ma_{z_n} = T - mg - Rz_n \tag{3.21}$$

where m is the mass of the link and a is the acceleration of the center of mass. The reaction forces expressions at joint n can be obtained from the manipulation of equations (3.19) to (3.21), and are given by:

$$Rx_n = -Rx_{n+1} - ma_{x_n} \tag{3.22}$$

$$Ry_n = -Ry_{n+1} - ma_{y_n} \tag{3.23}$$

$$Rz_n = T - mg - ma_{z_n} \tag{3.24}$$

Let the link k be a generic representation of any link in the chain other than the upper link, where the force T is applied. For any link k, the free body diagram is basically the same. Figure 3.4 illustrates the free body diagrams of two consecutive links in the chain.

Figure 3.5 Free body diagram for a generic link of the chain.

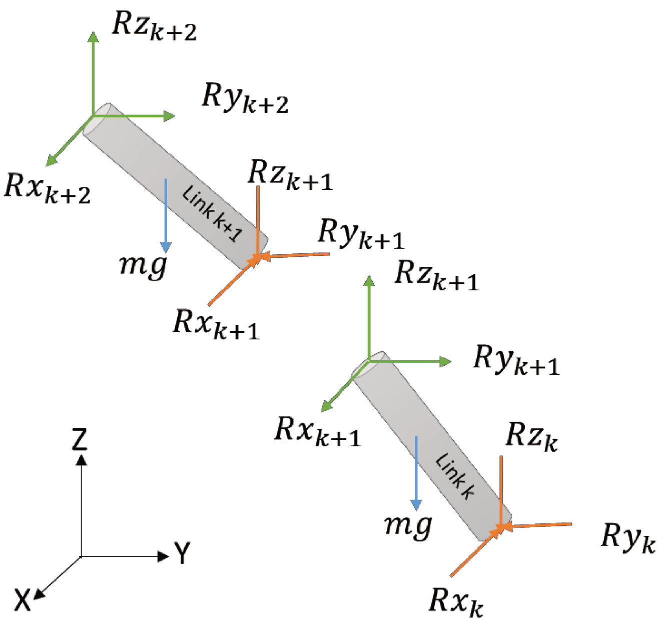

Source: Author.

Based on the fact that all the links are subjected to the same forces, general expressions of the reaction forces at the lowest joint of a link can be written and they are given by:

$$Rx_k = Rx_{k+1} - ma_{x_k} \tag{3.25}$$

$$Ry_k = Ry_{k+1} - ma_{y_k} \tag{3.26}$$

$$Rz_k = Rz_{k+1} - mg - ma_{z_k} \tag{3.27}$$

The reaction force at the lowest end of a link k is calculated because the reaction forces at the upper end are known, since they have been calculated when link $k+1$ is analyzed. Remember that the dynamic equilibrium analysis starts at the upper link n and goes downward until reaches the first link, located at the origin.

As mentioned earlier, in this work, Euler equations are computed in the reference frame fixed to the link. For this reason, it is necessary to write forces and angular accelerations in this reference frame. This can be done using the transformation matrices presented in equations (3.1) and (3.2).

Consider the force vector $R = \left[R_x, R_y, R_z\right]$ written in $\mathfrak{R}_0$. This vector can be written in $\mathfrak{R}_2$ as follows:

$$R_2 = s_2^T s_1^T R \tag{3.28}$$

Substituting the values of s_1 and s_2 given by equations (3.1) and (3.2) in equation (3.28) gives:

$$R_2 = \begin{Bmatrix} R_x \cos(\theta) - R_z \sin(\theta) \\ R_y \cos(\beta) + R_z \cos(\theta)\sin(\beta) + R_x \sin(\theta)\sin(\beta) \\ R_z \cos(\theta)\cos(\beta) - R_y \sin(\beta) + R_x \cos(\beta)\sin(\theta) \end{Bmatrix} \tag{3.29}$$

The transformation given by equation (3.28) is valid for the angular acceleration as well as for any vector fixed in the inertial reference frame.

Consider the link k again. The link has been isolated and its forces have been transformed to the reference frame fixed to the link ($\mathfrak{R}_2$). Figure 3.5 shows the configuration of the forces at the link k. In this figure, the resulting forces applied on the upper and lower end of the link were decomposed on the axis of $\mathfrak{R}_2$.

Figure 3.6 free body diagram for any link of the chain seen from the second mobile reference frame.

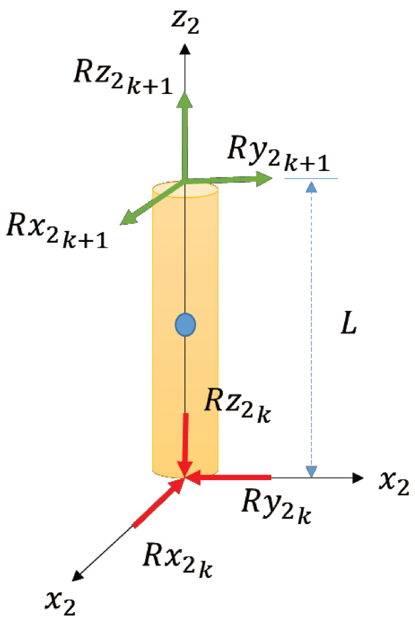

Source: Author.

Applying Euler's equation on link k results in the following components:

1. x_2 direction:

$$\sum M_x = I_x \alpha_{x_2} = -\frac{L}{2} Ry_{2_{k+1}} - \frac{L}{2} Ry_{2_k} \Rightarrow I_x \alpha_{x_2} + \frac{L}{2} Ry_{2_{k+1}} + \frac{L}{2} Ry_{2_k} = 0 \quad (3.30)$$

2. y_2 direction:

$$\sum M_y = I_y \alpha_{y_2} = \frac{L}{2} Rx_{2_{k+1}} + \frac{L}{2} Rx_{2_k} \Rightarrow I_y \alpha_{y_2} - \frac{L}{2} Rx_{2_{k+1}} - \frac{L}{2} Rx_{2_k} = 0 \quad (3.31)$$

3. z_2 direction:

$$\sum M_z = 0 \quad (3.32)$$

Equations (3.30) to (3.32) are valid for all links of the chain since all of them have the same applied forces (the magnitude of the components vary for each link).

3.5. Linearization

As the principal objective of the model of the chain is obtaining the lower frequencies of vibration of the system, it is convenient to consider small angular displacements and linearized the equations of motions, in this case, it is considered that:

$$\sin(\theta) \cong \theta, \quad \cos(\theta) \cong 1 \tag{3.33}$$

and

$$\sin(\beta) \cong \beta, \quad \cos(\beta) \cong 1 \tag{3.34}$$

Substituting the equations (3.25) to (3.27) in the equation (3.29) is obtained the general expressions of the reaction forces at the joints of the links described in $\mathfrak{R}_2$. Then, the forces described in $\mathfrak{R}_2$ are substituted in the equations (3.30) and (3.31). After, the linearization is applied to these expressions.

3.6. Equation of Motion of the chain

The introduction of the constraints shows in the equation (3.18) to the system has as consequent the elimination of two degrees of freedom, which now are described as functions of the others generalized coordinates. Thus, the system that represents the chain has $2(n-1)$ degrees of freedom, where n is the number of links.

The linearized equation of motion of the system is presented as follows:

$$\boldsymbol{M}\{\ddot{\boldsymbol{x}}\} + \boldsymbol{K}\{\boldsymbol{x}\} = \boldsymbol{0} \tag{3.35}$$

where $\boldsymbol{M}$ is the mass matrix, $\boldsymbol{K}$ is the stiffness matrix and $\boldsymbol{x}$ is the vector of generalized coordinates shows in the equation (3.36) and $\ddot{\boldsymbol{x}}$ their derives with respect to time.

$$\boldsymbol{x} = \begin{Bmatrix} \theta_1 \\ \beta_1 \\ \theta_2 \\ \beta_2 \\ \vdots \\ \vdots \\ \theta_{n-1} \\ \beta_{n-1} \end{Bmatrix} \tag{3.36}$$

When analyzing the expression (3.5), it is perceived that as consequent of the linearization the equations are independent for each plane, in other words, for each direction X or Y, the equations of motion of the links are written in function of only one generalized coordinate, β or θ, respectively. The equations for both generalized coordinates are the same.

Considering the previous information, a generic mass matrix $\boldsymbol{M_p}$ is presented in the equations (3.37) to (3.39), where the subscript p is 1 for θ and 2 for β.

$$\boldsymbol{M_p}(i,j) = I_i + \frac{L^2}{4} m_i + L^2 \sum_{k=i+1}^{n-1} m_k + \frac{3}{4} L^2 m_n + I_n, \qquad i = j \tag{3.37}$$

$$\boldsymbol{M_p}(i,j) = \frac{L^2}{2} m_i + L^2 \sum_{k=i+1}^{n-1} m_k + \frac{3}{4} L^2 m_n + I_n, \qquad i > j \tag{3.38}$$

$$\boldsymbol{M_p}(i,j) = \frac{L^2}{2} m_j + L^2 \sum_{k=j+1}^{n-1} m_k + \frac{3}{4} L^2 m_n + I_n, \qquad i < j \tag{3.39}$$

where i and j are the subscript for the rows and columns of the matrix respectively. I_i and m_i are the mass and the inertia of each link, m_n and I_n are the mass and the inertia of the upper link. L is the length of the link.

On the other hand, a generic stiffness matrix $\boldsymbol{K_p}$ is presented in the equations (3.40) and (3.41), where the subscript p is 1 for θ and 2 for β.

$$\boldsymbol{K_p}(i,j) = 2LT - \frac{L}{2}m_i g - Lg\sum_{k=i+1}^{n-1} m_k - \frac{L}{2}m_n g \qquad i = j \tag{3.40}$$

$$\boldsymbol{K_p}(i,j) = LT - \frac{L}{2}m_n g \qquad i \neq j \tag{3.41}$$

where T is the applied force at the upper link and g is the gravity acceleration.

The size of the matrices $\boldsymbol{M_p}$ and $\boldsymbol{K_p}$ is $[n-1 \times n-1]$. It is defined the matrices $\boldsymbol{M_1}$ and $\boldsymbol{K_1}$ for θ and the matrices $\boldsymbol{M_2}$ and $\boldsymbol{K_2}$ for β. The generic matrixes $\boldsymbol{M_1}$ and $\boldsymbol{M_2}$ as well as the generic matrixes $\boldsymbol{K_1}$ and $\boldsymbol{K_2}$, are coupled in the global matrices $\boldsymbol{M}$ and $\boldsymbol{K}$, respectively. The equations (3.42) and (3.43) show the assembly of the global matrixes.

$$\boldsymbol{M} = \begin{bmatrix} M_1(1,1) & 0 & M_1(1,2) & 0 & \cdots & M_1(1,n-1) & 0 \\ 0 & M_2(1,1) & 0 & M_2(2,2) & \cdots & 0 & M_2(1,n-1) \\ M_1(2,1) & 0 & M_1(2,2) & 0 & \cdots & \cdots & \vdots \\ 0 & M_2(2,1) & 0 & M_2(2,2) & \cdots & \cdots & \vdots \\ \vdots & \vdots & \vdots & \vdots & \ddots & \cdots & \vdots \\ M_1(n-1,1) & 0 & \vdots & \vdots & \vdots & M_1(n-1,n-1) & 0 \\ 0 & M_2(n-1,1) & \cdots & \cdots & \cdots & 0 & M_2(n-1,n-1) \end{bmatrix} \tag{3.42}$$

$$\boldsymbol{K} = \begin{bmatrix} K_1(1,1) & 0 & K_1(1,2) & 0 & \cdots & K_1(1,n-1) & 0 \\ 0 & K_2(1,1) & 0 & K_2(2,2) & \cdots & 0 & K_2(1,n-1) \\ K_1(2,1) & 0 & K_1(2,2) & 0 & \cdots & \cdots & \vdots \\ 0 & K_2(2,1) & 0 & K_2(2,2) & \cdots & \cdots & \vdots \\ \vdots & \vdots & \vdots & \vdots & \ddots & \cdots & \vdots \\ K_1(n-1,1) & 0 & \vdots & \vdots & \vdots & K_1(n-1,n-1) & 0 \\ 0 & K_2(n-1,1) & \cdots & \cdots & \cdots & 0 & K_2(n-1,n-1) \end{bmatrix} \tag{3.43}$$

3.7. Variation of the model

The model previously proposed considers the chain pin up at both extremities with rigid supports which do not have any displacement. Here, it is introduced a variation to the model. The supports are no longer considered rigid, on the contrary, they are flexible. The model only considers the motion on the plane.

The calculation of the equations on motion is similar to the model with rigid supports but, in this case, the deformation of them is considered for the kinematics of the model as well as the effects of their flexibility on the dynamics of the system. In addition, as the ends of the chains are no longer fixed, the displacement of these points configures two new degrees of freedom. Then the new system has $n + 1$ degree of freedom, where n is the number of links of the chain.

Figure 3.7 Representation of the chain.

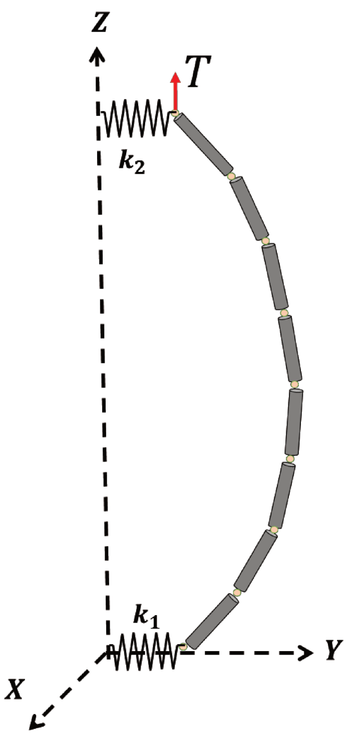

Source: Author.

Applying the Newton's laws and Euler's equation for each link and linearizing, an equation of motion in matrix form as the one described by equation (3.35) is obtained. The elements of mass matrix are presented in equations (3.44) to (3.52):

$$\boldsymbol{M}(i,j) = I_i + \frac{L^2}{2}\sum_{k=i+1}^{n} m_k\,, \qquad i = j = 1 \tag{3.44}$$

$$\boldsymbol{M}(i,j) = I_i + \frac{L^2}{4}m_i + L^2\sum_{k=i+1}^{n} m_k\,, \qquad i = j \neq 1 \neq n+1 \tag{3.45}$$

$$\boldsymbol{M}(i,j) = \sum_{k=1}^{n} m_k\,, \qquad i = n+1 \ \wedge \ j = n+1 \tag{3.46}$$

$$\boldsymbol{M}(i,j) = \frac{L^2}{4}m_j + \frac{L^2}{2}\sum_{k=j+1}^{n} m_k\,, \qquad i = 1 \ \wedge \ j \neq 1 \ \wedge \ j \neq n+1 \tag{3.47}$$

$$\boldsymbol{M}(i,j) = \frac{L}{2}\sum_{k=2}^{n} m_k\,, \qquad i = 1 \ \wedge \ j = n+1 \tag{3.48}$$

$$\boldsymbol{M}(i,j) = \frac{L^2}{2}m_j + L^2\sum_{k=j+1}^{n} m_k\,, \qquad i < j \ \wedge \ i \neq 1 \ \wedge \ j \neq n+1 \tag{3.49}$$

$$\boldsymbol{M}(i,j) = \frac{L^2}{2}m_i + L^2\sum_{k=i+1}^{n} m_k\,, \qquad i < j \ \wedge \ i \neq 1 \ \wedge \ j = n+1 \tag{3.50}$$

$$\boldsymbol{M}(i,j) = \frac{L^2}{2}m_i + L^2\sum_{k=i+1}^{n} m_k\,, \qquad i > j \ \wedge \ i = n+1 \tag{3.51}$$

$$\boldsymbol{M}(i,j) = L^2 m_j + L\sum_{k=j+1}^{n} m_k\,, \qquad i = n+1 \ \wedge \ j \neq n+1 \tag{3.52}$$

The elements of stiffness matrix are given by equations (3.53) to (3.61):

$$\boldsymbol{K}(i,j) = \frac{L^2}{2}k_2 - Lg\sum_{k=i+1}^{n} m_k - \frac{L}{2}gm_i + LT, \qquad i = j = 1 \tag{3.53}$$

$$\boldsymbol{K}(i,j) = L^2k_2 - Lg\sum_{k=i+1}^{n} m_k - \frac{L}{2}gm_i + LT\ , \quad i = j \ \wedge \ i \neq 1 \ \wedge \ i \neq n+1 \tag{3.54}$$

$$\boldsymbol{K}(i,j) = k_1 + k_2 \qquad i = n+1 \ \wedge \ j = n+1 \tag{3.55}$$

$$\boldsymbol{K}(i,j) = \frac{L^2}{2}k_2\ , \qquad i = 1 \ \wedge \ j \neq 1 \ \wedge \ j \neq n+1 \tag{3.56}$$

$$\boldsymbol{K}(i,j) = \frac{L}{2}(k_2 - k_1)\ , \qquad i = 1 \ \wedge \ j = n+1 \tag{3.57}$$

$$\boldsymbol{K}(i,j) = L^2k_2\ , \qquad i < j \ \wedge \ i \neq 1 \ \wedge \ j \neq n+1 \tag{3.58}$$

$$\boldsymbol{K}(i,j) = Lk_2\ , \qquad i < j \ \wedge \ i \neq 1 \ \wedge j = n+1 \tag{3.59}$$

$$\boldsymbol{K}(i,j) = L^2k_2\ , \qquad i > j \ \wedge \ i \neq n+1 \tag{3.60}$$

$$\boldsymbol{K}(i,j) = Lk_2\ , \qquad i = n+1 \ \wedge \ j \neq n+1 \tag{3.61}$$

where k_1 is the stiffness of the lowest support and k_2 is the stiffness of the upper support.

The matrices previously presented are the generic form for any chain with n links.

4. EXPERIMENTAL PROCEDURE

The experimental procedure was carried out with a chain grade 8/CR-16 with 24 links manufactured by Coforja. Each link of the chain had 16 mm of diameter and 48 mm of internal length. The chain was axially loaded by a hydraulic actuator MTS 200 KN, controlled by the controller MTS flex test 60 and excited by a shaker Brüel & Kjær type 4808. The vibration was measured by three accelerometers PCB 353B68. In addition, six strain gauges Excel PA 06 060 BA 120 type S were installed along the chain to measure the specific deformation of some links.

Figure 4.1 Dimensions of the chain.

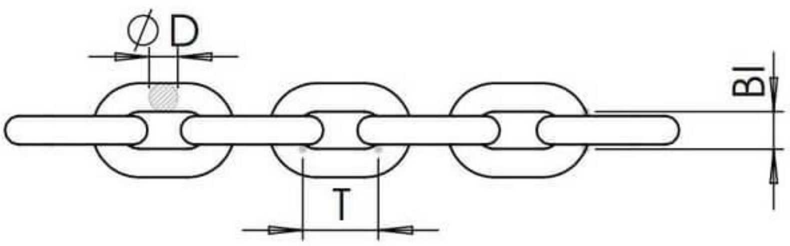

$D = 16\,mm \qquad T = 48\,mm \qquad B = 21\,mm$

Source: Author.

4.1. Lay out

The setup used for the chain measurements is illustrated on Figure 4.2. The hydraulic actuator was fixed at the top of a reaction frame structure. At the front of the piston of the hydraulic actuator a load cell was installed in order to measure directly the force applied to the chain. The chain was fixed to the actuator through an eye bolt and a screw, as shown in Figure 4.3 (a), which allowed the upper link of the chain to oscillate freely around the axis of the screw. The other end of the chain was fixed to the base of the reaction frame using a similar assembly. The hydraulic actuator and the lowest support were aligned in order to keep the chain in the vertical position.

The links of the chain were numbered in ascendant order, being the lowest link the first one and the upper link the twenty-fourth. The shaker was suspended by a giraffe crane and connected to the chain on its eighteenth link by a connecting rod (stringer). To firmly connect the stinger to the link, a piece of aluminum was machined with exactly the same curvature of the link. Then, this piece was screwed to the force transducer PCB 208C03 attached to the end of the stinger and glued to the chain (see Figure 4.3 (b)).

The same type of piece was used to fix the accelerometers to the chain, as can be seen in Figure 4.4 (a). Three uniaxial accelerometers were attached to the chain, at links number 8, 11 and 19. All accelerometers were installed on the side of the link and on the link plane, as illustrated by Figure 4.4 (a). Consequently, the accelerometer installed on link number 8 (even link) measures vibration in one direction, called x direction, while the other two accelerometers, attached to links 11 and 19 (odd links), measure vibration on a perpendicular direction, called y direction.

Figure 4.2 Lay out of the experiment.

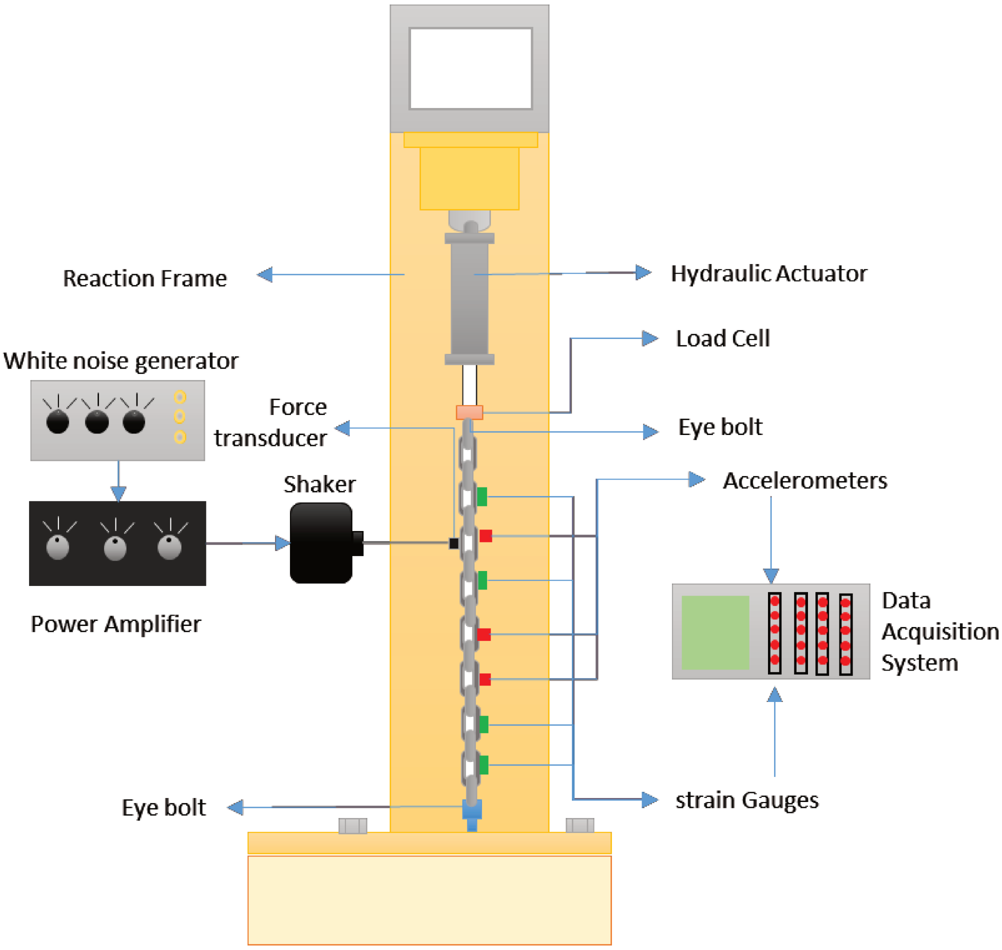

Source: Author.

A total of six uniaxial strain gauges were installed on the chain. These strain gauges were installed as follows: for links number 2 and 16, one strain gauge was to the links; for links number 5 and 12, two strain gauges were installed, on two opposed surfaces. In all cases, the strain gauges measure the axial deformation of the chain. Figure 4.4 (b) shows a strain gauge connected to a chain link.

To excite the system, a white noise signal generated by the GenRad EQ 0331 noise generator was sent to the Brüel & Kjær type 2712 power amplifier and then to the shaker. All signal were collected by the data acquisition system HBM MGCplus. Figure 4.5 shows an overview of the experimental setup while the test is running.

Figure 4.3 Support of the chain and shaker joint to the link.

(a) (b)

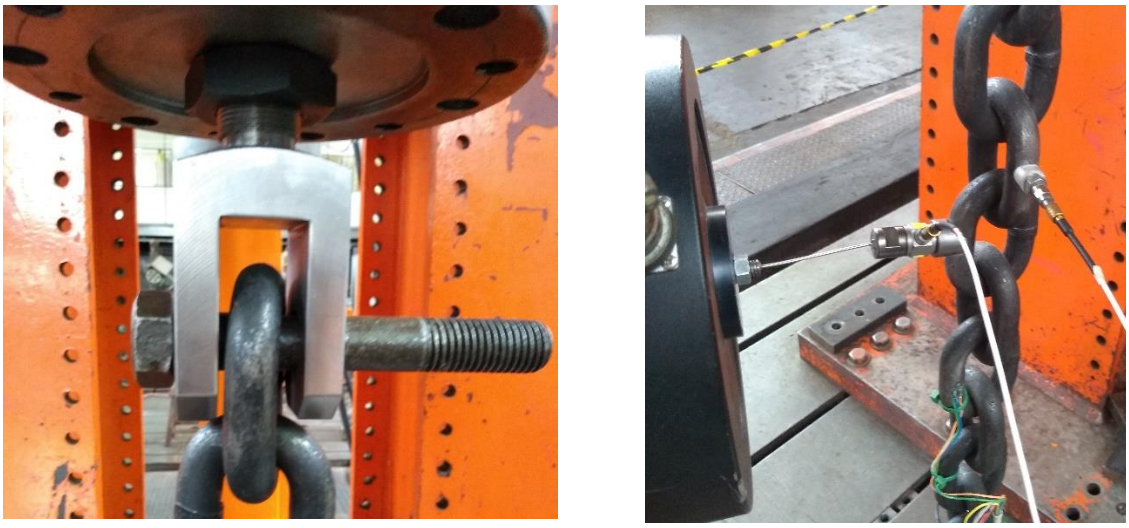

Source: Author.

Figure 4.4 Piece for attaching the accelerometers and detail of a strain gauge.

(a) (b)

Source: Author.

Figure 4.5 Running the experiment.

Source: Author

Table 4.1 summarizes the sensors installed on each link.

Table 4-1 Sensors installed on each link of the chain.

Link number	Sensor
2	External strain gauge
5	External and internal strain gauge
8	Accelerometer-x
11	Accelerometer-y
12	External and internal strain gauge
16	External strain gauge
18	Load cell/Shaker
19	Accelerometer-y

Source: Author.

4.2. Procedure

The first step for the measurements is to set up the data acquisition system. For all the measurements the sample rate was 2400 Hz. As the objective is to analyze the lowest frequencies of the chain, this acquisition rate was more than enough.

As the experiment aims to identify the variation of the natural frequencies depending on the load on the chain, the chain was loaded increasing the force in steps of 5 kN beginning in 5 kN and increasing until 70 kN. Then, the load was released in discrete steps of 5 kN until the minimum of 5 kN. Next, this cycle of loading and unloading was repeated several times. This is done in order to check if the chain presents hysteresis in deformation as well as in the natural frequencies. Before starting a new cycle, the chain is totally unloaded to reset the channels of the data acquisition system aiming to eliminate any residual stress.

4.3. Data processing

The identification of the natural frequencies was performed with the acceleration data and the force collected from the force transducer. The procedure consists of calculating the estimator of the frequency response function (FRF) H_2 with the input signal (Force) and the output signal (Acceleration). The estimator H2 is calculated as follows:

$$H_2 = \frac{G_{yy}}{G_{xy}} \tag{4.1}$$

where Gyy is the auto power spectral density of the output and G_{xy} is the cross power spectral density between the input and output signal. The procedure was made for each loading/unloading cycle.

The extensometry analysis consists of transforming the deformation data into the force applied to the chain. This is easily done through the relation given by equation (4.2):

$$F = \frac{\delta AE}{L} = eAE \tag{4.2}$$

where the strain e is the one measured by the strain gauges, A is the transversal area of the links and E the elasticity modulus of the material of the chain which, in this case, is 200 GPa (Carbon Steel). The transversal area is twice the area given by the diameter of the link wire.

5. FUZZY LOGIC

The way that humanity defines the things is subjective and ambiguous, since each person has different perceptions. The definition of many concepts that usually people use is universal for everyone, as the summation of two numbers, for example, two plus two is four for the entire world no matter where or when the affirmation is done. All those statements are clearly represented by the mathematical world or the Boolean world. The Boolean logic only considers two type of responses for affirmations, true or false.

The real world is expressed with several statements that are relative for each person, depending on the individual experiences and thoughts. The phrase "the lady is beautiful" is a typical situation in which Boolean logic fails, since the perception of beauty is totally influenced by the culture and region in which the statement is made. One can say that the phrase is true (the lady is really beautiful), while others may say that it is false, and there is no parameter to determine who is correct.

As the example previously shown, almost all the concepts of the world are subjective and ambiguous. Zadeh (1965) introduced the concept of fuzzy sets with the need of representing subjective expressions. The author proposes that the elements have degrees of membership with defined sets. For example, the definition of warm or hot is difficult to do by means of Boolean logic, since, for example, the temperature of 40°C can be warm for some people, but for others it can be hot. If the set for "warm" is defined for all temperatures in the range of 20°C to 50°C, and "hot" from 35°C to 70°C, the temperature of 40°C belongs to the sets warm and hot simultaneously, with different degree of membership. Thus, is possible to avoid the ambiguity in the definition of the temperature.

5.1. Basic concepts

5.1.1. Fuzzy set theory

Consider X as a group of elements and x as a generic element that belongs to X. This statement can be mathematically expressed as: $X = \{x\}$. A fuzzy set A in X is characterized by a membership function $f_A(x)$ which assigns a value in the real interval $[0,1]$ with the value of $f_A(x)$ representing the grade of membership of x into A (ZADEH, 1965). Thus, the nearer the value of $f_A(x)$ to the unity, the greater the degree of membership of x in A. it is possible to represent a classical set A by $(x, 0)$ or $(x, 1)$, which indicates that $x \notin A$ or $x \in A$, respectively.

5.1.2. Fuzzy sets and membership functions

The fuzzy sets can be considered as an extension of the classical sets, in which the characteristic function is allowed to assume any value in the interval $[0,1]$. Then, the fuzzy set A can be denoted as:

$$A = \{(x, \mu_A(x)) | x \in X\} \tag{5.1}$$

where X is the universe of discourse, $\mu_A(x)$ is the membership function and x is an element belonging to the universe of discourse. For better understanding, an example is shown next.

Consider the following set B = "Dark colors" and the elements X = {Brown, gray, black}, with the following degree of membership B= {(Brown, 0.7), (gray, 0.8), (Black, 0.99)}. In this case, the discrete universe of discourse X are the colors, and the set are some colors that can be considered as dark depending on the criteria of the writer. Other person can assign different degree of membership according to his or her experience.

A fuzzy set is uniquely defined by its membership function. In order to describe the membership function in a better way, some definitions (ROGER JANG, 2000) are done .

Support: The support of a fuzzy set A is the set of all of points x in X such that $\mu_A(x) > 0$:

$$support(A) = \{ x \mid \mu_A(x) > 0\}. \tag{5.2}$$

Core: The core of a fuzzy set is the set of all points x in X such that $\mu_A(x) = 1$:

$$core(A) = \{ x \mid \mu_A(x) = 1\}. \tag{5.3}$$

Normality: A fuzzy set A is normal if its core is nonempty. In other words, it is possible always to find a point $x \in X$ such that $\mu_A(x) = 1$.

Crossover points: A crossover point of a fuzzy set A is a point $x \in X$ at which $\mu_A(x) = 0.5$:

$$crossover(A) = \{x \mid \mu_A(x) = 0.5\}. \tag{5.4}$$

The figure 5.1 represent a generic fuzzy set defined by the membership function in orange color, which indicates the membership degree defined in the interval [0, 1] of the elements of the supports.

Figure 5.1 Representation of a fuzzy set.

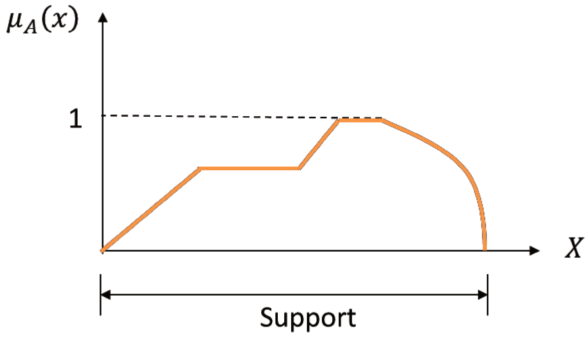

Source: Author.

Fuzzy singleton: A fuzzy set whose support is a single point in X with $\mu_A(x) = 1$ is called a fuzzy singleton.

Containment: The fuzzy set A is contained in fuzzy set B (or equivalently, A is a subset of B) if and only if $\mu_A(x) \leq \mu_B(x)$ for all x. Mathematically:

$$A \subseteq B \Leftrightarrow \mu_A(x) \leq \mu_B(x). \tag{5.5}$$

Complement or negation: The complement of a fuzzy set A, denoted by A $(A, NOT\ A)$ is defined as:

$$\mu_{A_c}(x) = 1 - \mu_A(x). \tag{5.6}$$

As mentioned before, the membership function characterizes the fuzzy set. Therefore, it is not practical to mention all pairs that compose the set, so it is convenient to define the membership function with a mathematical formula. Some types of membership functions are defined below.

5.1.3. Membership function types

The following shapes of membership functions (MF) are the most used to model the fuzzy sets. It is important to highlight that exist other type of MF that are not very common.

Triangular membership function

A triangular MF (Figure 5.2) is specified by three parameters $\{a, b, c\}$ and it is given by:

$$y = triangle(x; a, b, c) = \begin{cases} 0, & x \leq a \\ \dfrac{x-a}{b-a}, & a \leq x \leq b \\ \dfrac{c-x}{c-b}, & b \leq x \leq c \\ 0, & c \leq x. \end{cases} \tag{5.7}$$

Figure 5.2 Triangular membership function.

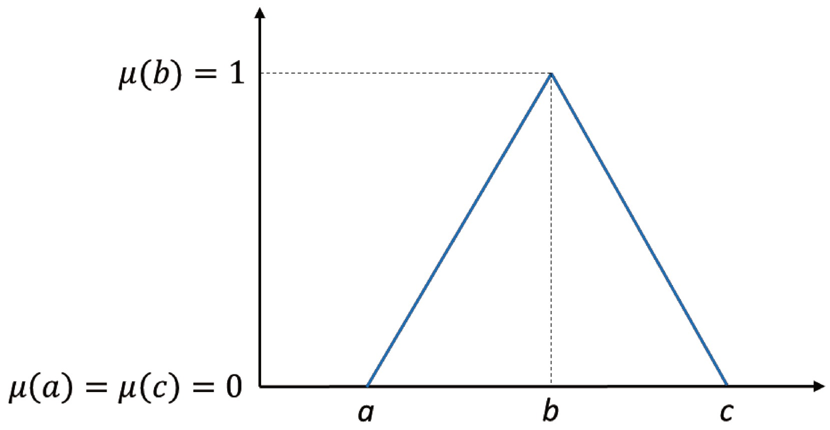

Source: Author.

The parameters $\{a, b, c\}$ (with $a < b < c$) determine the x coordinates of the three corners of the underlying triangular MF.

Trapezoidal membership function

A trapezoidal MF (Figure 5.3) is specified by four parameters $\{a, b, c, d\}$ as follows:

$$trapezoid(x; a, b, c, d) = \begin{cases} 0, & x \leq a \\ \dfrac{x-a}{b-a}, & a \leq x \leq b \\ 1, & b \leq x \leq c \\ \dfrac{d-x}{d-c}, & c \leq x \leq d \\ 0, & d \leq x \end{cases} \tag{5.8}$$

Figure 5.3 Trapezoidal membership function.

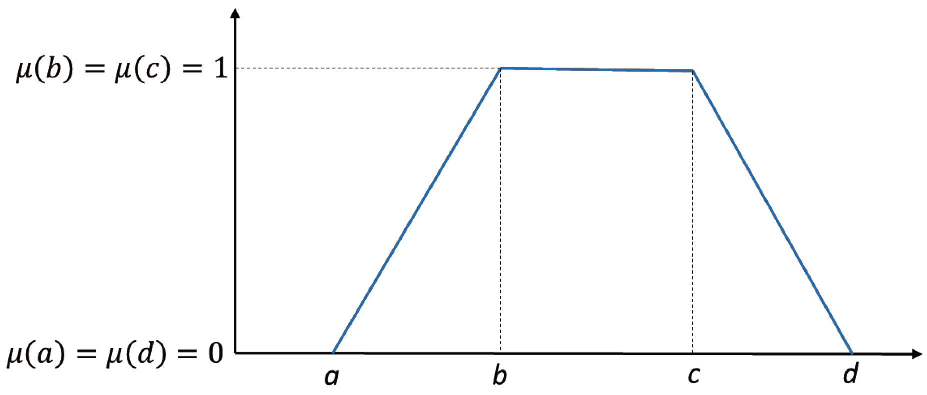

Source: Author.

The parameters $\{a, b, c, d\}$ (with $a < b < c < d$) determine the x coordinate of the four corners of the underlying trapezoidal MF.

Due to its simplicity and easy understanding, the triangular and trapezoidal MF has been extensively used, especially in real-time applications. However, since the triangular and trapezoidal MF are composed by straight lines, the points of joint are not smooth. Then, other types of MF are shown, defined by smooth and nonlinear functions.

Gaussian membership functions

A Gaussian membership function (Figure 5.4) is specified by two parameters $\{c, \sigma\}$ and it is expressed by:

$$gaussian(x; c, \sigma) = e^{-\frac{1}{2}\left(\frac{x-c}{\sigma}\right)^2} \tag{5.9}$$

A Gaussian MF is completely determined by c and σ; c represents the center (mean) and σ determines the MF width. Figure 4.4 illustrates a Gaussian MF.

Figure 5.4 Gaussian membership function.

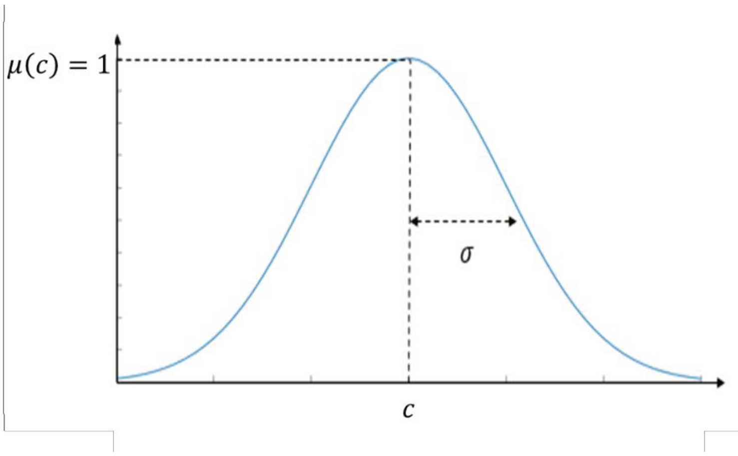

Source: Author.

Generalized bell membership function

A generalized bell membership function (Figure 5.5) is specified by three parameters, $\{a, b, c\}$, and it is given by:

$$bell(x; a, b, c) = \frac{1}{1 + \left|\frac{x-c}{a}\right|^{2b}} \tag{5.10}$$

Figure 5.5 Generalized bell membership function.

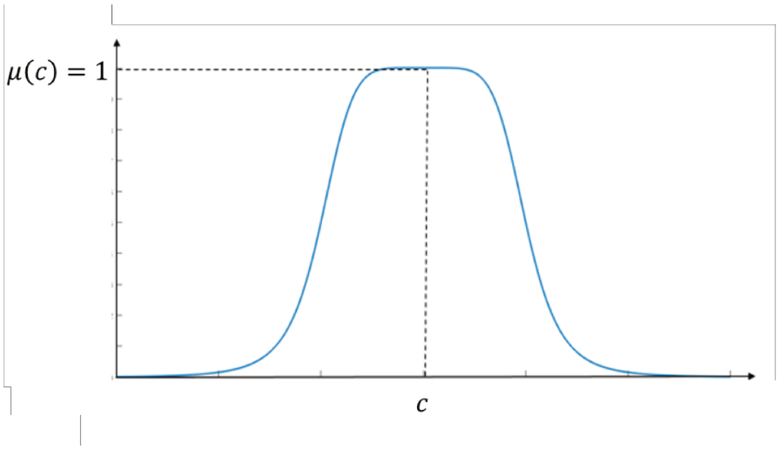

Source: Author.

where the parameter b is usually positive. This MF is a direct generalization of the Cauchy distribution used in probability theory and, for this reason, it is also called as Cauchy MF. Although the Gaussian MF and bell MF are smooth, they are not able to represent asymmetric MF, which are important in some applications.

Sigmoidal membership function

A sigmoidal membership function (Figure 5.6) is defined by the following equation:

$$sig(x; a, c) = \frac{1}{1 + \exp\big(-a(x - c)\big)} \tag{5.11}$$

where a controls the slope at the crossover point $x = c$. Depending on sign of the parameter a, a sigmoidal MF is inherently open right or left and thus is appropriate for representing concepts with the adverb "very".

Figure 5.6 Sigmoidal membership function.

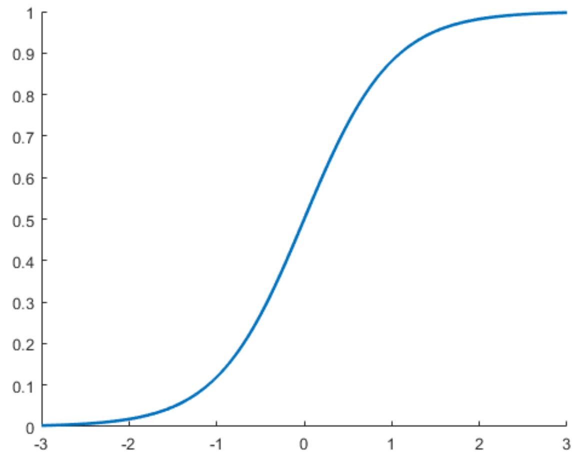

Source: Author.

5.1.4. Operations with Fuzzy sets

Most of the applications of fuzzy sets requires the interactions between different fuzzy sets. Thus, some of the operation with fuzzy set commonly used are shown next (MIZUMOTO; TANAKA, 1981).

Union

The union of two fuzzy sets A and B is a fuzzy set C, written as $C = A \cup B$ or $C = A\ or\ B$, whose MF is related to those of A and B by:

$$\mu_C(x) = \max\big(\mu_A(x), \mu_B(x)\big) = \mu_A(x) \vee \mu_B(x). \tag{5.12}$$

Figure 5.7 (a) illustrates a union of two triangular sets.

Intersection

The intersection of two fuzzy sets A and B s a fuzzy set C, written as $C = A \cap B$ or $C = A\ and\ B$, whose MF is related to those of A and B by

$$\mu_C(x) = \min\big(\mu_A(x), \mu_B(x)\big) = \mu_A(x) \wedge \mu_B(x). \tag{5.13}$$

Figure 5.7 (b) illustrates the intersection of two triangular sets.

Figure 5.7 Union and Intersection of two fuzzy sets.

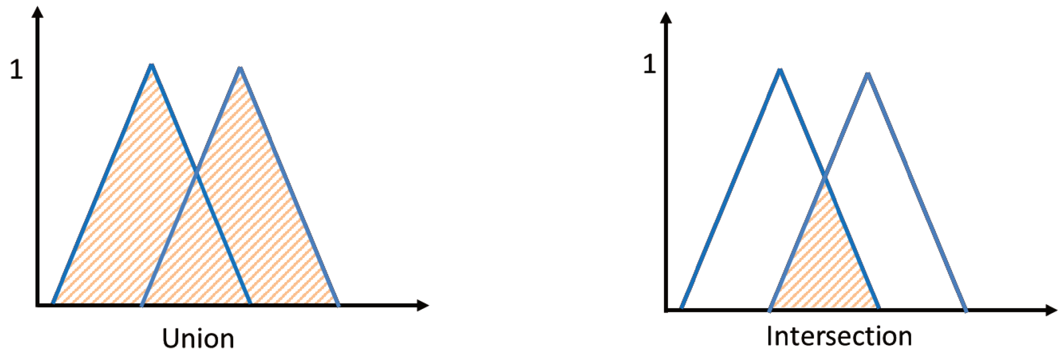

(a) (b)

Source: Author.

α – cut and strong α- cut

The α-cut or α-level set of a fuzzy set A (see Figure 5.8) is a crisp set defined by:

$$A_\alpha = \{\, x \mid \mu_A(x) \geq \alpha \}. \tag{5.14}$$

Strong α-cut or strong α-level set is defined similarly by:

$$A'_\alpha = \{\, x \mid \mu_A(x) > \alpha \}. \tag{5.15}$$

Using the notation for a level set, it is possible to express the support and core of a fuzzy set as:

$$support(A) = A'_0 \quad \text{and} \quad core(A) = A_1. \tag{5.16}$$

Figure 5.8 alpha cut of a fuzzy set.

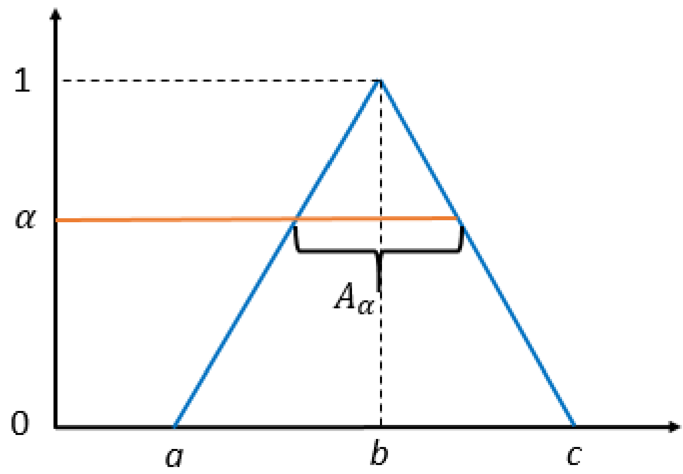

Source: Author.

5.2. Fuzzy Reasoning

In this section, the concepts of extension principle for fuzzy sets, linguistic variables and fuzzy rules are presented. The objective of this section is to explain how to make relations between fuzzy sets and prepare the exposition of fuzzy inference system, which is the most important modeling tool on the fuzzy set theory.

5.2.1. Extension principle

The extension principle was proposed by Zadeh (1975) and resumed by Nguyen (1978) and Gerla (1994). The extension principle provides a general procedure to apply mathematical relations used in crisp domain into fuzzy domain. The procedure generalizes the mapping between fuzzy sets.

Consider that f is a function from X to Y and A is a fuzzy set in X defined as:

$$A = \mu_A(x_1)/x_1 + \mu_A(x_2)/x_2 + \cdots + \mu_A(x_n)/x_n \tag{5.17}$$

The extension principle establishes that the image of the fuzzy set A under the mapping f is the fuzzy set B given by:

$$B = \mu_A(x_1)/y_1 + \mu_A(x_2)/y_2 + \cdots + \mu_A(x_n)/y_n \tag{5.18}$$

where $y_i = f(x_i), i = 1,2, \dots, n$. In other words, the fuzzy set B can be defined by the mapping of the values x in f. Once the mapping is carried out, if there are two or more repeated value for y, the degree of membership for this value will be the maximum degree of membership. Mathematically,

$$x_1, x_2 \in X\,, \quad x_1 \neq x_2 \tag{5.19}$$

and

$$f(x_1) = f(x_2) = y\,*, \qquad y * \in Y \tag{5.20}$$

Then, the membership degree of B at $y = y\,*$ is the maximum of the membership degrees at A, that is,

$$\mu_B(y) = \max(\mu_A(x_1)\,, \mu_A(x_2)) \tag{5.21}$$

Then,

$$x = f^{-1}(y) \tag{5.22}$$

The theory previously explained is embodied in an example:

Consider the following discrete universe of discourse with the respective degree of membership:

$$A = 0.1/{-2} + 0.3/{-1} + 0.5/0 + 0.2/1 + 0.4/2 \tag{5.23}$$

And the mapping function f from x to y

$$y = x^2 + 2 \tag{5.24}$$

Applying the extension principle, the following result is obtained:

$$B = 0.1/6 + 0.3/3 + 0.5/2 + 0.2/3 + 0.4/6 \tag{5.25}$$

$$B = 0.5/2 + (0.3 \vee 0.2)/3 + (0.1 \vee 0.4)/6 \tag{5.26}$$

$$B = 0.5/2 + 0.3/3 + 0.4/6 \tag{5.27}$$

Where $\vee$ means union, that is, the maximum value.

5.2.2. Binary Fuzzy Relation

Castillo and Melin (2008) explain in an easy way the binary fuzzy relation between fuzzy sets. "Binary fuzzy relations are fuzzy sets in $X \times Y$ which map each element in $X \times Y$ to a membership grade between 0 and 1".

Let X and Y be two universes of discourse. Then,

$$\mathfrak{R} = \{ \left((x,y), \mu_{\mathfrak{R}}(x,y)\right) \big| \, (x,y) \in X \times Y\} \tag{5.28}$$

Equation (5.28) presents a binary relation in $X \times Y$.

Consider the following example from Castillo and Melin (2008):

Let $X = \{1,2,3\}$ and $Y = \{1,2,3,4,5\}$ and $\mathfrak{R}$="$y \textit{ is slightly greater than } x$". The MF of the fuzzy relation can be defined (subjectively) as:

$$\mu_{\mathfrak{R}}(x,y) = \begin{cases} \dfrac{y-x}{y+x}, & if\ y > x, \\ 0, & if\ y \leq x. \end{cases} \tag{5.29}$$

This fuzzy relation can be expressed as a matrix in the following form:

$$\mathfrak{R} = \begin{bmatrix} 0 & 0.333 & 0.500 & 0.600 & 0.666 \\ 0 & 0 & 0.200 & 0.333 & 0.428 \\ 0 & 0 & 0 & 0.142 & 0.250 \end{bmatrix} \tag{5.30}$$

where the element at row i and column j is equal to the membership grade between the ith element of X and jth element of Y. In the literature, other common examples of binary relations are found, as "$x \textit{ is similar to } y$", "$x \textit{ depends on } y$" , "$\textit{if } x \textit{ is small then } y \textit{ is small}$" and others.

5.2.3. Max-min composition

The max-min composition proposed by Zadeh (1965) states that: "Let $\Re_1$ and $\Re_2$ be two relations defined on $X \times Y$ and $Y \times Z$, respectively. The max-min composition is a fuzzy set (CASTILLO; MELIN, 2008) defined by:

$$\Re_1 \circ \Re_2 = \{[(x,z), \max\min(\mu_{\Re_1}(x,y), \mu_{\Re_2}(y,z))] \mid x \in X, y \in Y, z \in Z\} \quad (5.31)$$

The calculation of the composition is almost the same as matrix multiplication, except that $\times$ and $+$ are replaced by the min and max operations, respectively.

5.3. Linguistic variables

The concept of linguistic variables was introduced by Zadeh (1975). The linguistic variables represent crisp information that can carry some degree of ambiguity, which is independent of a measure device or a mathematical expression. For example, the conception of age is linguistic, if rather that number as 21, 22, etc., is represented with young, not young, old, very old and others.

Usually, when a universe of discourse is a linguistic variable, the sets are linguistic variables too. Linguistic variables allow a better communication and notion of some procedure and it is easy to understand since they are used daily (Banks, 2002). Most of the instructions are given in linguistic variables, such as open *a little*, cook over *medium* heat, hold *strongly* and others.

Zadeh (1965) defined that a linguistic variable is characterized by a quintuple $(x, T(x), X, G, M)$ in which x is the name of the variable, $T(x)$ is the term set of x that is, the set of its linguistic values or linguistic terms, X is the universe of discourse, G is a syntactic rule which generates the terms in $T(x)$, and M is semantic rule which associates with each linguistic value A its meaning $M(A)$, where $M(A)$ denotes a fuzzy set in X.

5.3.1. Concentration and dilatation of linguistic values

Let A be a linguistic variable. A modified version of A can be obtained applying the concepts of concentration and dilatation. In the literature, usually these operations are expressed by:

$$CON(A) = A^2 \tag{5.32}$$

$$DIL(A) = A^{0.5} \tag{5.33}$$

where A is a fuzzy set, and $CON\ (A)$ and $DIL\ (A)$ are the concentration and dilatation of the set, respectively. Conventionally, $CON()$ and $DIL()$ are taken to be the results of applying the edges "*very*" and "*more or less*", respectively. The addition of the edges is a good approach for some applications. Figure 5.9 presents a concentration and dilation of a sigmoidal membership function.

Figure 5.9 Concentration and dilatation of linguistic variables.

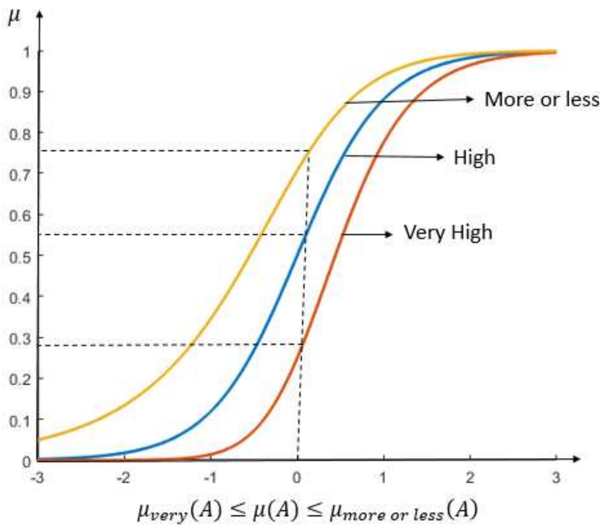

Source: Author.

5.4. Fuzzy Inference Systems

The fuzzy inference systems (FIS) are a powerful tool for modelling and handling data, and it is vastly used in applications of artificial intelligence. The fuzzy world is more common than it is thought. Fuzzy allows expressing complex concepts in compressible expressions. The fuzzy inference system simulates how the brain works, since most of the decision that human beings make are based on statements and rules that are constructed through the life.

The fuzzy inference systems can be an optimal tool to transmit information. Usually, the intelligent systems use terms as p-values, eigenvalues, frequencies, derives and others, which only the experts understand and are able to handle the information. The society requires information understandable for everybody. Fuzzy logic is capable to communicate information with expressions used daily and by everyone.

Facts that encourage the use of fuzzy logic are, for example, the nature of the environment. The nature and all the environment are not organized as expected, and the interactions that there occur have grades of imprecise and uncertainty and a touch of complexity.

Then, a review of the fuzzy inference systems is presented and the operation of the inference machine is explained.

5.4.1. Components of the fuzzy inference system

The fuzzy inference systems are composed by three parts, which are the Antecedents, the rules, and the Consequences. Figure 5.10 presents the structure of a fuzzy inference system. At the same time, there exist three procedures associated with each of those parts (Figure 5.11), which are: the fuzzification, the inference, and the defuzzification. Thus, it is possible to say that the fuzzification is associated with the antecedents, the inferences with the rules, and the defuzzification is associated with the consequences.

Figure 5.10 Structure of a fuzzy inference system.

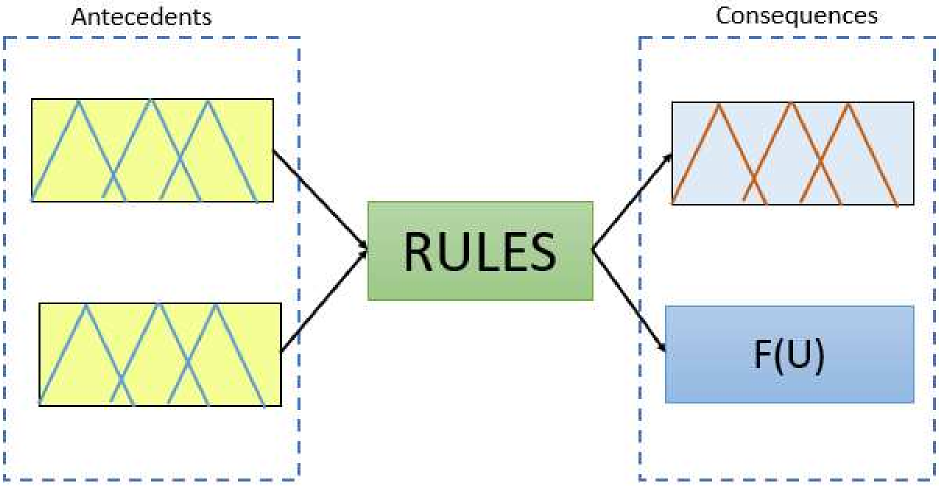

Source: Author.

The antecedents correspond to the input variables and they are always represented by fuzzy sets. The rules are the relations between antecedents and consequences. The consequences correspond to the output variables, which can be fuzzy sets or not, depending on the type of fuzzy inference system.

Figure 5.11 Procedure of inference.

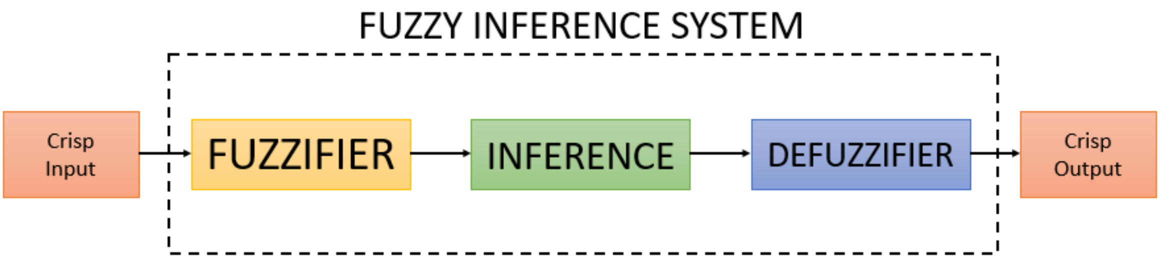

Source: Author.

The fuzzy inference system can be considered as a machine that transform the crisp information (real numbers) into the fuzzy domain, and handle the information with the inference engine, which is fueled with the rules. The outcome of the inference engine is a fuzzy set, so the defuzzifier transforms the result from fuzzy domain into the crisp domain.

The procedure of defuzzification is not always needed depending on the type of fuzzy inference system. This difference is explained deeper later.

Each part of the fuzzy inference system is explained in the next sections.

5.4.2. Antecedent parts

The antecedent parts in the fuzzy inference systems represent the input variables of the systems. Each variable configures a universe of discourse. Each universe of discourse is divided into fuzzy sets and each fuzzy set may be described by any membership function. Figure 5.12 presents a typical antecedent part in a fuzzy inference system.

The form of the membership functions and the number of fuzzy sets for each universe of discourse depend on the type of system that is been modelled. Each universe of discourse is independent of the others, that is, the number and shape of the fuzzy sets of one variable do not depend on the other variables. Each fuzzy set of the universe of discourse is associated with a linguistic variable that can be perceived as the name of the set.

Figure 5.12 Representation of an antecedent part of a fuzzy inference system.

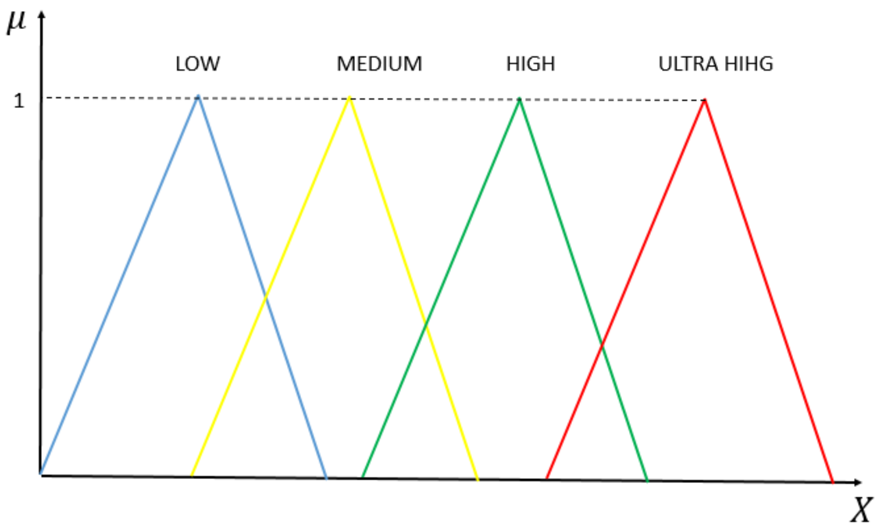

Source: Author.

The process of definition of the universes of discourses and the respective fuzzy sets requires enough expert knowledge, since it influences the performance of the fuzzy inference system. For example, when the system presents a linear behavior, the triangular membership function is a suitable shape for the set, or, if the system has nonlinearities, a Gaussian membership function can provide a good performance.

Besides the type of membership function for each set, it is important to define how the sets interact, that is, clearly define the boundaries of the fuzzy sets, knowing that a crisp number can belong to different fuzzy sets.

5.4.3. Fuzzifier

The fuzzifier is the first procedure of the fuzzy inference system. The fuzzifier maps a crisp point $x \in X$ into a fuzzy set $A \in X$ (MOUZOURIS; MENDEL, 1997). The fuzzification can be understood as the transformation of a crisp value (real number) into a fuzzy set.

There exist two type of fuzzifiers: the singleton and the nonsingleton. Each of them is explain as follows.

5.4.3.1. Singleton fuzzifier

The singleton fuzzifier (Figure 5.13) maps the crisp point $x \in X$, into a fuzzy set $A \in X$ with support x_i, where $\mu_A(x_i) = 1$ for $x = x_i$ and $\mu_A(x_i) = 0$ for $x \neq x_i$, i.e. the single point in the support of A with nonzero membership function value is $x_i = x$. The singleton fuzzifier is defined as:

$$\mu(x) = \begin{cases} 1, & x = x_i \\ 0, & x \neq x_i \end{cases} \tag{5.34}$$

Figure 5.13 Singleton fuzzification.

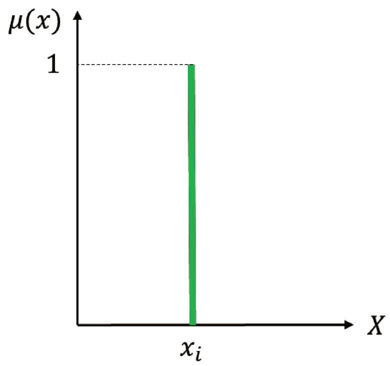

Source: Author.

5.4.3.2. Nonsingleton fuzzifier

The nonsingleton fuzzifier maps the point $x_i \in X$ into a fuzzy set $A \in X$, with support x_i, where μ_A achieves maximum value at $x_i = x$ and decreases while moving away from $x = x_i$. In other words, the crisp value is transformed into a fuzzy set. Usually, the Gaussian function is used for fuzzification, since the standard deviation has a sense of uncertainty. Figure 5.14 shows a non-singleton fuzzification with a Gaussian function. Its mathematical expression is given by equation (5.35):

$$\mu(x) = e^{-\frac{1}{2}\left(\frac{x-x_i}{\sigma}\right)^2} \tag{5.35}$$

Nonsingleton fuzzification can be very useful when the training data or the input data is contaminated with noise. Conceptually, the nonsingleton fuzzifier implies that the value x_i is likely the most correct value from all the values in its immediately neighborhood, and once the input is corrupted with noise, the points round x_i can be the correct value but this is less likely. It is important to highlight that most of the applications of fuzzy inference system use singleton fuzzifier, due to the ease of its application and understanding.

Figure 5.14 Nonsingleton fuzzification.

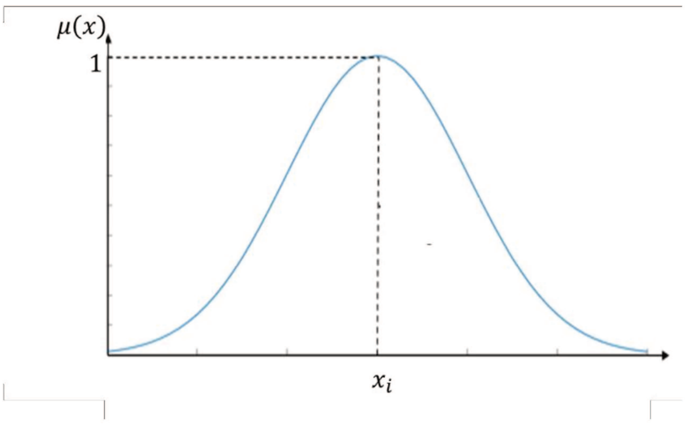

Source: Author.

5.4.4. Calculation of the degree of membership

Once the fuzzification is done, the input is transformed into the fuzzy domain. The next step is to calculate the membership grade of the fuzzy input according to the membership functions of the antecedent parts.

The degree of membership of a crisp value into a fuzzy set is how much that value belongs to the set. For a crisp set, the possible degrees of membership are 0 or 1. In fuzzy sets, the possible membership degrees are infinite, since they can be any real number in the interval [0, 1].

Usually, the singleton fuzzification method is adopted because of its simplicity and easy perception of the process. When the fuzzifier is nonsingleton, the calculation of the membership degree implies more complexity, but the theory is the same.

Now, the calculation of the membership degree is explained. The degree of membership of a fuzzy input is the point of intersection of the membership function and the line that represents the singleton. Figure 5.15 shows the process of calculation of the membership degree for singleton fuzzification.

Figure 5.15 Calculation of the membership degree with singleton fuzzification.

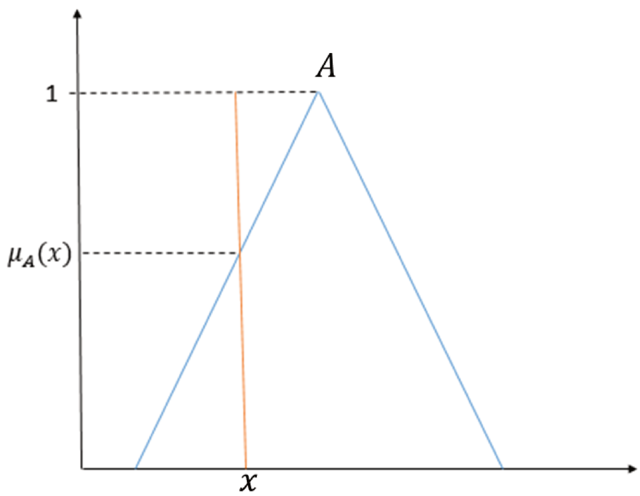

Source: Author.

For the case in which the nonsingleton fuzzifier is used, the calculation of the degree of membership has the same logic. As the fuzzy input is no more singleton, instead is a set of values described by a fuzzy set, the degree of membership function is the maximum value of the intersection of both fuzzy sets.

Figure 5.16 represents the calculation of the degree of membership with non-singleton fuzzification. The set A is the fuzzy set of the universe of discourse, and the set Ax is the fuzzy set of x, and the green line represent the intersection of both functions.

Figure 5.16 Calculation of the membership degree with nonsingleton fuzzification.

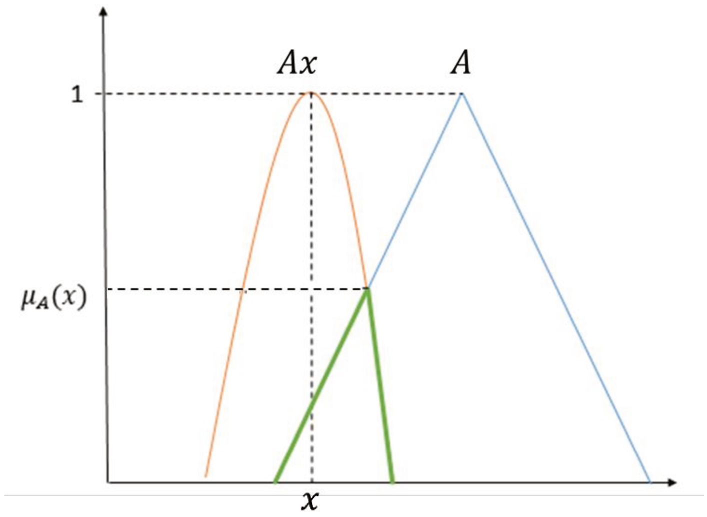

Source: Author.

5.4.5. Inference engine and fuzzy rules

The rules are the second part of the fuzzy inference system. The process associated with the rules is the inference. The structure of the fuzzy rules and the inference process is explained next.

Fuzzy rules

As previously mentioned, the fuzzy sets configure linguistic variables. The linguistic variables represent how the universe of discourse is or, in other words, they provide a sense of how the universe of discourse can be “measured” or appreciated. As an example, when the universe of discourse is temperature, the possible linguistic values are cold, warm or hot. On the other hand, if the universe of discourse is, for example, velocity of a car, the possible linguistic values are slow, medium, or high.

Once the antecedent and consequent parts are defined, it is necessary to create connections between the antecedent parts and the consequent parts that describe the relations between the fuzzy sets of the universes of discourse. The relations are called fuzzy rules.

Zadeh (1996) explains the type of relationships that can be created between linguistic values and how the word calculation procedure works. The author explains a variety of possibilities for making correspondences between diffuse sets and their implications. In this work, the *if-then* fuzzy rules are explained, since these are the most common and applied to fuzzy inference systems.

The *if-then* fuzzy rules are conditional rules and have the following form:

$$\boldsymbol{if}\ x\ is\ A\ \boldsymbol{then}\ \ y\ is\ B$$

where A and B are linguistic variables define by fuzzy sets of the universe of discourse X and Y, respectively. In this case, x is the antecedent part and y is the consequent part. Some classical examples of fuzzy rules are:

- If pressure is low, then volume is big.
- If the risk is low, then the business is profitable.
- If the water flow is high, then close the valve a lot.

The fuzzy rules dictate how the output is if a certain condition in the antecedent part is accomplished. The fuzzy rules describe the behavior of the system. For example, if a machine is being modeled by a fuzzy inference system, the fuzzy rules describes how the machine works.

Inference engine

The inference engine, that is, the inference procedure, is fueled by the rules which module and order the relationships for the inference. The inference engine calculates the firing strength of the fuzzy rule; it means that the inference engine calculates a value in the crisp interval [0, 1] that represents how the antecedent part is mapped into the consequent part.

For the case when the antecedent part is composed by only one element, the firing strength of the rule is the degree of membership of the cited fuzzy set. Consider the fuzzy rule

$$if\ x\ is\ A\ then\ y\ is\ B$$

The firing strength of the rule is the membership degree of x in A, that is $\mu_A(x)$.

Generally, fuzzy rules have more than one antecedent that are related by two types of connectors: $\boldsymbol{and/or}$.

When the connector $\boldsymbol{and}$ is used, the inference is performed applying the T-norm, and when the connector is $\boldsymbol{or}$, the inference is performed by the T-conorm (GARCÍA-CERDAÑA; ARMENGOL; ESTEVA, 2010). The T-norm has two methods for its application: the first one is the minimum and the other one is the product. The T-conorm has also two methods: the first one is the maximum and the other one is the probabilistic or.

Consider the next fuzzy rule:

$$if\ x\ is\ A\ \boldsymbol{and/or}\ \ y\ is\ B\ \boldsymbol{then}\ z\ is\ C$$

where A and B are fuzzy sets of the universes of discourse of the antecedent parts and C is a fuzzy set of the universe of discourse of the consequent part.

The previous fuzzy rule has two antecedent parts, and then it is necessary to infer a value from them. For the connector $\boldsymbol{and}$ the inference can be:

$$\mu_A(x)\ \boldsymbol{and}\ \mu_B(y) = \min\big(\mu_A(x)\,, \mu_B(y)\big) \tag{5.36}$$

or

$$\mu_A(x)\ \boldsymbol{and}\ \mu_B(y) = \mathrm{prod}\big(\mu_A(x)\,, \mu_B(y)\big) \tag{5.37}$$

And for the connector $\boldsymbol{or}$ the inference can be:

$$\mu_A(x)\ \boldsymbol{or}\ \mu_B(y) = \max\big(\mu_A(x)\,, \mu_B(y)\big) \tag{5.38}$$

or

$$\mu_A(x)\ \boldsymbol{or}\ \mu_B(y) = \mathrm{probor}\big(\mu_A(x)\,, \mu_B(y)\big) \tag{5.39}$$

where the min or max is the calculation of the minimum or maximum of the degree of membership, respectively. The prod is the product of the degree of membership and the probor is the or probabilistic that is defined as:

$$\text{Probor} = \mu_{A(x)} + \mu_{B(y)} - \left(\mu_{A(x)} * \mu_{B(y)}\right). \tag{5.40}$$

The outcome of the inference process is a degree of membership called rule firing strength $\boldsymbol{W}$ which is how the antecedent part is mapped into the consequent part. Thus, the relationships between the antecedent parts are represented by the firing strength of the rules.

Each rule has a firing strength for a specific crisp input, that is, if the crisp input changes, the firing strength does too. That is because the firing strength depends on the inference, which depends on the degree of membership, which depends on the crisp inputs.

Weight of the fuzzy rules

The fuzzy inference system allows assigning weights to fuzzy rules. Weights can be perceived as the importance of the rule in the system and can assume values in the crisp interval [0, 1].

Usually, all rules have weight of 1, i.e., all rules have the same importance for the system. When the weight is different than 1, the firing strength of the rules is multiplied by the weight of the rule and a new firing strength is calculated as follows:

$$\boldsymbol{Wn} = W_t * \boldsymbol{W} \tag{5.41}$$

where $\boldsymbol{W}$ is the firing strength calculated in the inference, W_t is the weight of the rule and $\boldsymbol{W_n}$ is the new firing strength modified by the weight of the rule.

5.4.6. Consequent parts

In fuzzy logic applications, two fuzzy inference systems are widely used: Mamdani and Sugeno. The difference between them lies in the consequent part of the system. Consequently, the process of associating with the consequent parts also has differences.

5.4.7. Mamdani Fuzzy models

The Mamdani fuzzy inference system (MAMDANI; ASSILIAN, 1975) was proposed as the first attempt to control a steam engine and boiler combination, by a set of linguistic rules obtained from experimental human operators.

In Mamdani fuzzy systems, the consequent parts are composed by fuzzy sets as the antecedent ones (see Figure 5.17). The process applied to discretize the antecedent parts is applied again to the consequent parts.

Figure 5.17 Representation the consequent part in a Mamdani fuzzy inference system.

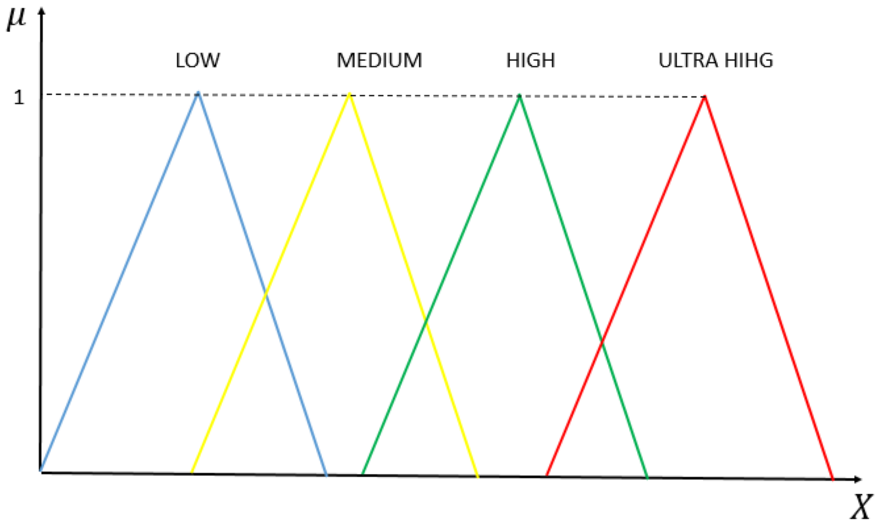

Source: Author.

The mapping of the firing strength of the rules on the consequent part consists in the location of the firing strength of the rule that is a membership degree, and cutting the corresponding fuzzy set described in the rule, with a horizontal line corresponding to the firing strength. The set under the cutting line is taken as the outcome of the mapping.

As each crisp input can fire several rules, it is necessary to apply the aggregation procedure that is the union of all the consequent parts fired. The union of the consequent parts forms a new fuzzy set.

Figure 5.18 presents the inference procedure for two rules with firing strength $\boldsymbol{W1}$ and $\boldsymbol{W2}$, respectively. The consequent part is formed by two triangular membership functions. The firing strength $\boldsymbol{W1}$ cuts the fuzzy set A and $\boldsymbol{W2}$ cuts the fuzzy set B. The union of the fuzzy sets configures a new fuzzy set.

Figure 5.18 Mapping of the firing strength of the rules in the consequent part.

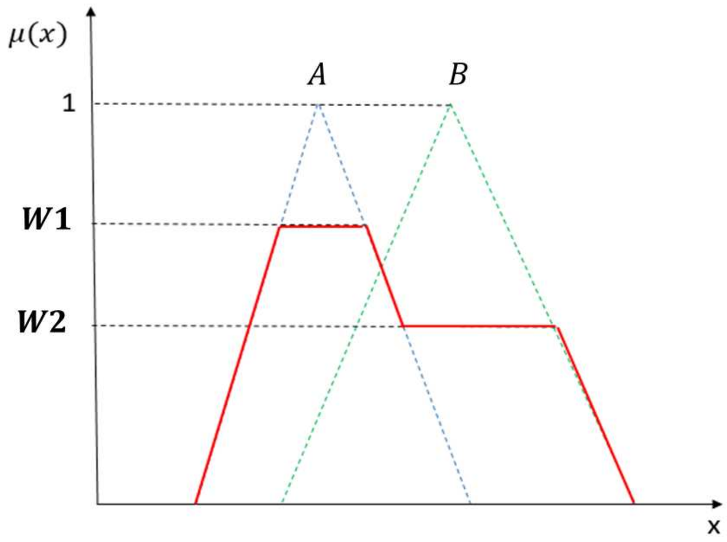

Source: Author.

As the output of the inference engine is a fuzzy set for Mamdani fuzzy systems, it is necessary to convert the output into the crisp domain in order to obtain a crisp number (real number).

5.4.7.1. Defuzzification

The defuzzification refers to the way that a numeric value is extracted from a fuzzy set as representative value. In the literature, five methods of defuzzification are commonly found. These methods are presented next:

- Centroid of area

$$Z_{COA} = \frac{\int_z \mu_A(z)zdz}{\int_z \mu_A(z)dz} \tag{5.42}$$

where $\mu_A(z)$ is the aggregated output membership function. This procedure consists of calculating the centroid of the area under the fuzzy set formed after the aggregation process.

- Bisector of area

The bisector of area satisfies

$$\int_{\alpha}^{Z_B} \mu_A(z)dz = \int_{Z_B}^{\beta} \mu_A(z)dz \tag{5.43}$$

where $\alpha = \min\{z \mid z \in Z\}$ and $\beta = \max\{z \mid z \in Z\}$. It can be understood as the point that divides the area in two equal parts.

- Mean of maximum

The mean of maximum is the average of the maximizing z at which the membership function reaches a maximum μ^*. Mathematically:

$$Z_{MOM} = \frac{\int_{z'} z dz}{\int_{z'} dz} \tag{5.44}$$

where $z' = \{z \mid \mu_A(z) = \mu^*\}$. If $\mu_A(z)$ has a single maximum at $z = z^*$, then $Z_{MOM} = z^*$. Moreover, if $\mu_A(z)$ reaches its maximum whenever $z \in [z_{left}, z_{right}]$ the $Z_{MOM} = \frac{z_{left}+z_{right}}{2}$.

- Smallest of the maximum

The smallest of the maximum is the minimum of maximizing Z.

- Largest of the maximum

The largest of the maximum is the maximum of maximizing Z

Figure 5.19 shows the value Z for the different defuzzification methods represented by the blue points. The method frequently used is the centroid defuzzification and this is the method used in this work.

Figure 5.19 Defuzzification methodologies.

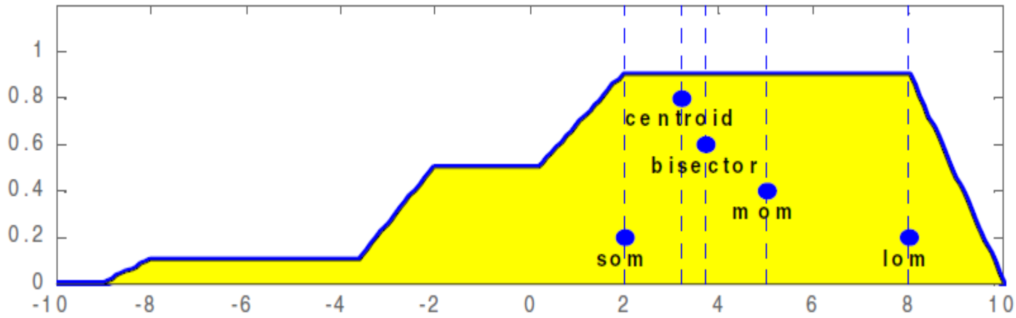

Source: Castillo & Melin (2008)

5.4.8. Sugeno Fuzzy Models

The Sugeno fuzzy models emerged from the attempt to develop an approach to generate fuzzy rules from input-output data set (TAKAGI; SUGENO, 1985), (SUGENO; KANG, 1988). The Sugeno models differ from Mamdani model in the consequent part of the fuzzy rules. While Mamdani models have fuzzy sets as consequents, the Sugeno models have mathematical functions as consequents. Sugeno fuzzy rules have the following form:

$$if\ x\ is\ A\ and\ y\ is\ B\ then\ z = f(x,y)$$

where A and B are the fuzzy antecedent sets and $f(x,y)$ is a traditional function as consequent. Usually, this function is a polynomial in the input variables x and y, but it does not mean that it cannot take other forms. When the consequent function is of zero order, in other words, constants, the system can be considered as a special case of Mamdani fuzzy model, with consequents as singleton fuzzy sets.

The functions that describe the consequent parts depend on the inputs of the system. When the functions are evaluated with the input values, they provide an output level that is the value of the function for the crisp inputs.

Then, for each input the rules provide a firing strength and the functions, an output level. As the firing strength and the output level both are crisp number, the process of defuzzification is not needed anymore; instead the crisp output is calculated as an average of the firing strengths and the output levels.

When the consequent part of the fuzzy rules is a function, the average process is made as follows. Consider the functions presented in equations (5.45) and (5.46).

$$z_1 = p_1 x + q_1 y + r_1 \tag{5.45}$$

$$z_2 = p_2 x + q_2 y + r_2 \tag{5.46}$$

where z_1 and z_2 are the consequent parts of two fuzzy rules. The output of the fuzzy system is:

$$Z = \frac{z_1 w_1 + z_2 w_2}{w_1 + w_2} \tag{5.47}$$

where w_1 and w_2 are the firing strength of the fuzzy rules.

Most of the Sugeno fuzzy systems take as consequent part constant functions because of its interpretability and easy association with the average process. As previously mentioned, this type of Sugeno systems can be perceived as a Mamdani system with consequent part as singleton sets. Thus, the average process provides more sense. Figure 5.20 represents a consequent Sugeno fuzzy part with constant functions. Here, the average process can be represented. Once w_1 and w_2 have values in the crisp interval [0, 1], when multiplied by the respective consequents, z_1 and z_2, the value is truncated, and the outcome is the average, since the set is singleton. It is important to note that the process shown in Figure 5.20 is a mere representation.

Figure 5.20 Representation of constant functions as singletons of a Sugeno fuzzy inference system.

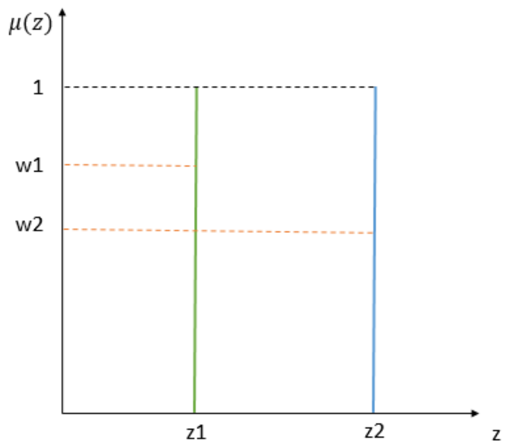

Source: Author.

5.4.9. Surface of fuzzy models

The fuzzy systems can be represented by a surface generated from the inputs and the fuzzy rules, in order to map the output when combining two inputs. Figure 5.21 shows a surface of a fuzzy inference system with two inputs. For the system which has just one input, the surface has no sense, instead, a curve or line is a suitable representation.

The fuzzy surface is useful for the case when the system has two input and one output, since the surface maps all possible matches for the inputs; thus, the surface predicts the crisp output for any pair of inputs.

On the other hand, if the system has more than two inputs or outputs, the surface will be the representation of the combination of two inputs and any output. In this case, the surface is useful for analyzing the influence of specific inputs on any output.

Figure 5.21 Surface of a fuzzy inference system.

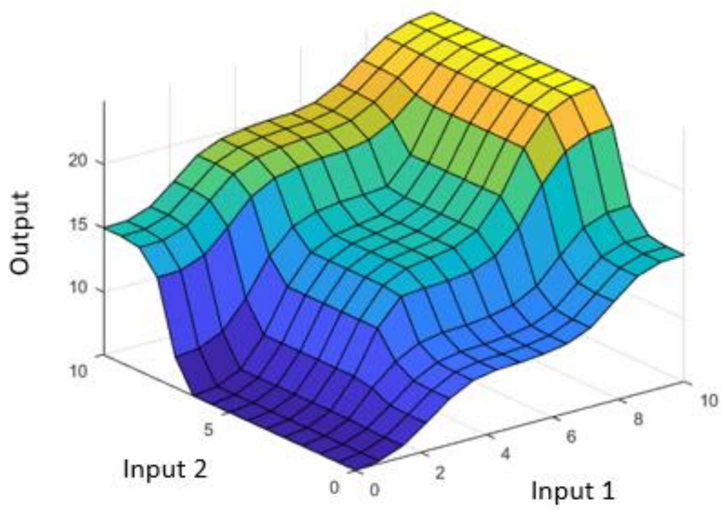

Source: MathWorks, 2019 (Adapted)

5.5. Modeling with fuzzy logic

The process of modeling a system with fuzzy logic requires prior knowledge of the functioning of the system. Wherever the system knowledge is taken from, the fuzzy system must be able to represent all situations in an approximate manner and with good precision. In general, all the fuzzy system has the same features for modeling the system.

There are some basic steps that help to create a new system. The first and most important step is to have the knowledge of the system to be modeled. Generally, the fuzzy system is modeled based on the knowledge of human specialists, that is, people who have worked with the system for long periods and have experienced various operating situations can provide the necessary information about the performance of the system.

Another alternative is to obtain sufficient data on the operation of the system in order to be able to identify relationships and thus generate knowledge of the system. The availability of these data can be useful for later design stages aiming the optimization of the system. The best of the cases is when human knowledge and performance data are available and combined.

Once the system is identified, the next step is to choose the type of fuzzy inference system. The choice of the type of fuzzy system is closely associated with the application. Then, the inputs and outputs of the fuzzy system are identified. Each input has to be divided into fuzzy sets with respective membership functions. For each membership function, a linguistic variable is associated. The outputs depending on the type of inference system can be divided into fuzzy sets or represented by functions.

The next step is to create the relationship between the linguistic variables, that is, the fuzzy rules and its respective weights. The number of fuzzy rules to fully define the system is the multiplication of the number of membership functions for all inputs. It is necessary to highlight that not all the possible fuzzy rules are required for the functioning of the system. Depending on the application, only some rules are essential, in other words, not all the fuzzy rules are fired, then the unused fuzzy rules can be deleted.

The last step is to choose the defuzzification method, if needed, depending on the type of fuzzy system applied. The previous steps are general for the construction of the fuzzy system, independent on the type of application.

For some applications, the construction of the fuzzy system is more complex and requires other techniques, as the creation of fuzzy trees or adaptive systems.

5.6. Fuzzy logic and uncertainty

Fuzzy logic is a powerful tool for modeling data and systems. As mentioned previously, fuzzy logic is able to represent things that make sense for human brain but mathematically is somewhat blurry or not clear.

All the processes that occur in the world have uncertainty embedded. The uncertainty appears from different sources and it is important to learn how to deal with it. Mathematical equations and crisp data have no capacity to deal with uncertainty, since their construction assume that all the information is certain.

Fuzzy logic allows working with values or quantities that are not rigidly bounded. This characteristic is helpful to handle data and systems, which have uncertainty involved. The definition of linguistic variables is a feature that simulates how the human brain thinks.

Depending on the type and definition of the fuzzy systems, the uncertainty can be treated in different ways. For example, the nonsingleton fuzzification allows considering uncertainty in the input data. The grade of consideration of uncertainty depends on the application and the designer.

The introduction of uncertainties in the system can improve the results, but the greater the uncertainties, the greater the computational time required. The fuzzy logic system designer must be aware of how the consideration of uncertainty will influence the outcome and whether it is worth doing.

In general, the fuzzy logic systems have proved to be a powerful tool to handle uncertainty (ZADEH, 1983), (MENDEL, 2000), (VULLINGS et al., 2013). The fuzziness approach can provide a solution for problems where the mathematical description is difficult to do and have degrees of subjectivity.

6. GENETIC ALGORITHM

Many engineering problems seek to find the optimal solution, requiring that the solution be the cheapest, easy to apply and quick to implement. Finding the right solution is not an easy job to do. Usually, the knowledge of the designers and the experience of the engineers and technicians are not enough, and it is necessary to use some methods to find the profitable solution.

In engineering, the process of finding a suitable solution is usually based on the search of a variable or a set of variables that minimize or maximize some quantity. For example, for the project of a shaft, it is necessary to find the material that is flexible, but with enough hardness. In this case, the searching targets are flexibility and hardness, which need to be optimal for the same solicitation.

When the problem requires finding only one variable, the procedure of searching is not generally complex and can be performed by using methodologies as try and failure, or a more sophisticated one, as least square. Unfortunately, most of the problems in engineering are not that simple and involve the searching of many variables to optimize a defined condition.

Depending on the definition of the problem and the quantity of information available to solve it, several techniques can be applied, as the case of Newton-Raphson method, which aims to find the values of the target variables that zero a function or a set of functions. This method is widely used when the number of variables matches the number of equations. Otherwise, it is not possible to use it, as its procedure is based on the definition of the Jacobian matrix, which is square.

In many optimization situations, the number of variables overcome the number of equations, making it difficult applying traditional methods to solve them. New optimization methods have been developed in order to face cases when traditional methods do not fit. Evolutionary algorithms are a large family of techniques that seek to solve complex optimization problems that can involve a large number of target variables, based on the theory of natural evolution.

One of the most famous evolutionary algorithms is the Genetic Algorithm, called in the literature as GA and introduced by John Henry Holland in 1960. Holland, (1960) proposed the

Genetic Algorithm based on Darwin's natural evolutionary theory. His student David Edward Goldberg in 1989 extended the definition of the genetic algorithm.

This chapter aims to explain the Genetic Algorithm functionality, as well as its application in the optimization of functions and systems.

6.1. Structure of the Genetic Algorithm

A basic Genetic Algorithm is composed of five essential parts or steps that simulates the process of natural evolution (Goldberg, 1989). Figure 6.1 presents the five steps and the structure of a genetic algorithm.

Figure 6.1 Structure of the genetic algorithm.

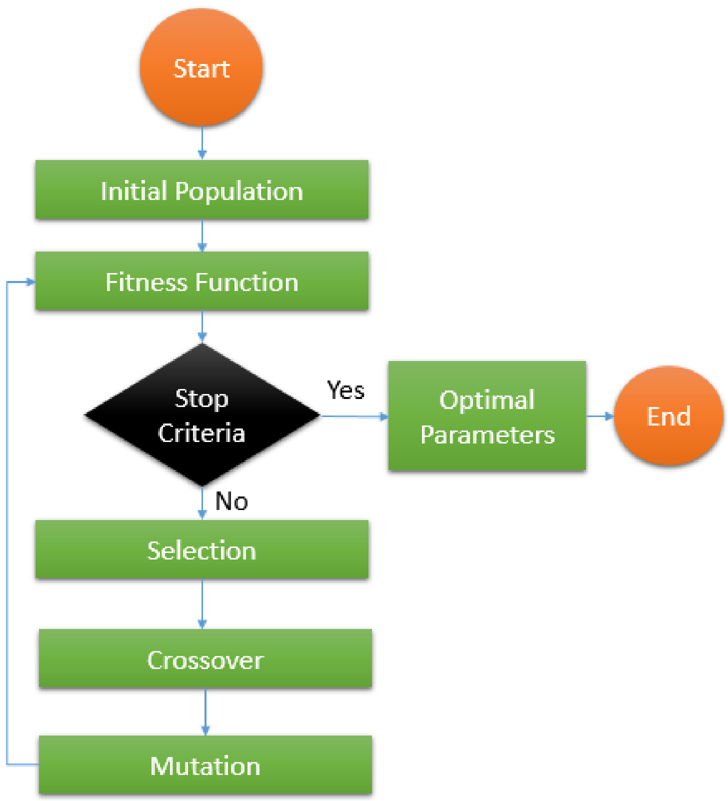

Source: Author.

A genetic algorithm starts by creating an initial population that contains the possible optimal values for the optimization. These values are evaluated by the fitness function. The result of the fitness function is compared with the stop criteria. If the comparison satisfies the condition, the procedure ends, but if it does not, three stages are performed: selection, crossover and mutation, which creates new populations that are candidates for possible solution. These stages are defined and explained in the next sections.

6.1.1. Initial population

A population is composed of chromosomes that are composed by genes. A gene is the possible value for a specific variable. The set of all genes form a chromosome. The number of genes in each chromosome is equal to number of variables to optimize. A population can be composed of many chromosomes, as needed, in order to find the solution. Figure 6.2 shows an example of gene, chromosome, and population in genetic algorithm.

A population can be seen as a matrix, in which the rows are the chromosomes and the columns are the genes. The genes do not change position during iteration.

There are generally two ways to generate the initial population: the heuristic initialization and the random initialization. Heuristic initialization has a problem finding the ideal solution to a large scale problem due to the lack of diversity, being the random initialization a better option (Gen M. and Lin L, 2008).

The generation of the initial population must respect the system the boundary conditions. The number of chromosomes is defined by the designer of the algorithm. Roeva, Fidanova, and Paprzycki (2013) proposed that there is an adequate number of chromosomes in the population and, in their case, this value was 200, for a problem with three target variables, that is, approximately 66 times the number of variables. Many applications of the genetic algorithm use, by default, 10 times the variable number for the population size.

On the other hand, Gotshall and Rylander (2000) concluded that a great population size has more chances to contain the optimal solution, but it has a price: a large number of generations will be needed since the genes are more mutated. Thus, the designer must find the equilibrium between convergence possibility and computational time.

Some strategies are proposed in order to set the adequate population size, as the case of Eiben, Marchiori, and Valkó (2004), who proposed dynamic population size, then the population can increase or decrease as the iterations run. Their studies show promising results in consuming time, fitness evaluation and required memory.

Figure 6.2 Population in the genetic algorithm.

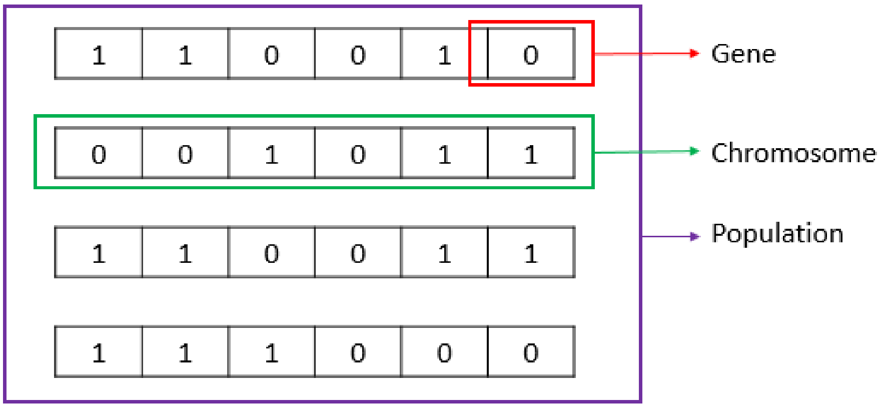

Source: Author.

6.1.2. Fitness Function

The fitness function determines how fit an individual (chromosome) is. The fitness function defines if an individual has the capacity of compete with other individuals. The capability is expressed by the fitness score that is the result of the evaluation of the fitness function.

The choice of the fitness function is an important task to do. The fitness function influences on the capacity of the genetic algorithm to optimize the system (YANG et al., 2014). Many studies have analyzed the effect of the definition of the fitness function on the performance of the optimization, as is the case of Lima et al (1996).

The shape of the fitness function depends on the type of problem being optimized. Many studies define the error based on the comparison of an optimal value with the obtained value. Several engineering problems have specific quality estimators that can be used as a fitness function in the optimization procedure.

6.1.3. Stop criteria

The stop criteria are the conditions that must be accomplished for the genetic algorithm for its stopping. The stop criteria are usually three:

1. the fit condition is achieved,

2. the number of generations (iterations) is overcome or
3. the number of stall generations is reached.

A stall generation is a generation in which the minimum does not change compared to the previous generation. Once one of the conditions is reached, the algorithm stops. When the algorithm reaches the fit conditions, which is the best case, the results are the suitable values of the optimization.

On the other hand, when the algorithm stopped because it has reached the maximum number of iterations, this does not mean that the results obtained are the appropriate values and it is necessary to modify the structure of the algorithm to ensure convergence. If the algorithm stops because of the number of stall generations, it means that the algorithm has possibly converged to a local minimum.

6.1.4. Selection

When the initial population does not accomplish the fit conditions, other stages of the algorithm are activated in order to find the best individual. The first step to create a new generation is the selection. As all individual are evaluated by the fitness function and consequently, they have assigned a fitness score, the selection process chooses the best chromosomes to be the "parents" of the next generation.

The selection method that currently exist can be grouped into two sets: the first group is composed by the methods that use the probability of being chosen and the second group is composed by the methods that use the best fitness value as choice criterion (Jebari and Madiafi, 2014).

One characteristic of the first group is that it keeps the genetic variety, a feature that helps the algorithm to achieve the global optima, but that requires a large number of generations. On the other hand, the elitist methods (second group) usually require few iterations, but can tent to lie in local optima (Jebari and Madiafi, 2014). Razali and Geraghty, (2011) analyzed the methods of selection and proposed the tournament method, which randomly chooses some fitness values where the best is selected to be the parent.

To improve the selection methods, Jadaan, Rajamani, and Rao, (2008) proposed a combination of probabilistic methods with the elitist method, showing promising results and overcoming questions about computing time and lack of diversity. One of these methods is the rank selection, which provides good performance and achieves the convergence to the global optimal. In general, depending on the application of the genetic algorithm, the selection method must be adjusted.

6.1.5. Reproduction

The reproduction in genetic algorithm refers to the procedures that are performed in order to create a new generation with the selected parents. The two main procedures are crossover and mutation.

Compared with the Darwin's theory, crossover is associated with the sexual reproduction and mutation with the asexual reproduction, since the first procedure requires two parents and the second one requires only one.

In addition to the previous process, some parents are considered as elite. This means that they survive for the next generation and generate new children. They do not suffer any alteration on their genes.

The elite children are important for a new generation because they ensure that the fittest value of one generation will be at least the same as the previous one, or better.

6.1.6. Crossover

The crossover is the most significant phase of the genetic algorithm and it is where the offspring is created. Once the parents are selected, the children are generated from the combination of the parents. Each chosen chromosome is a potential parent that will combine its genes with the genes from other parents. The combination of the genes becomes a new child as occurs in the nature.

The way that the combination of the genes occurs can be different depending on the strategy applied to generate offspring. The most useful types of crossover are explain as follows (KORA; YADLAPALLI, 2017):

a. Single point crossover: Two possible parents are selected and matched. A random point that represents the position of the genes is chosen and the chromosomes are divided in two parts. One part of the first chromosome is exchanged with one part of the second chromosome, thus creating two new children. Figure 6.3 presents an example of crossover in one point.

Figure 6.3 Crossover in one point.

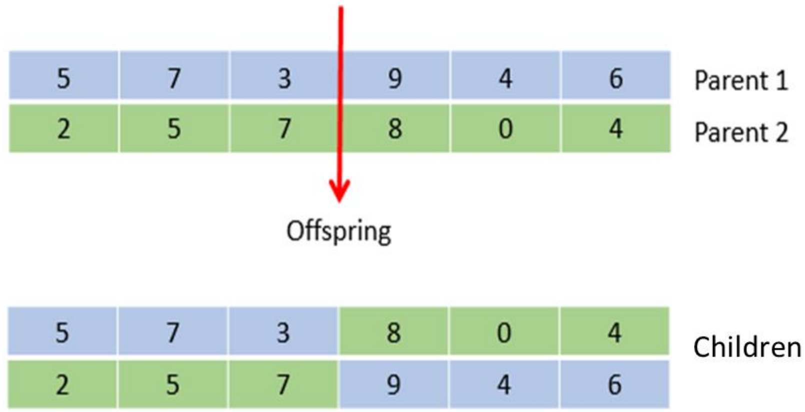

Source: Author.

b. N point crossover: instead of using only one point to divide the chromosomes, the parents are divided into N parts and combined.
c. Flat crossover: a linear combination is made with the genes of the parents.

It is important to highlight that there exist other crossover operators and the designer of the genetic algorithm can introduce new methodologies in order to improve the performance of the algorithm.

6.1.7. Mutation

The mutation procedure consists in the creation of new children from only one parent. As the name indicates, the chromosome is mutated, it means that the genes of the individual (parent) are altered.

There exist several methods for mutating the genes of a chromosome. Some of them are based on the change of position within the chromosome (ABDOUN; ABOUCHABAKA; TAJANI, 2012) that is, the values of the genes are not altered but the position, then the gene receives a new value for the next generation. Other methods modify the value of the gens multiplying of addition a random number.

7. PROPOSED METHODOLOGY FOR THIS WORK

The main objective of this work is to create a fuzzy inference system capable of predicting the force applied on a chain from the measurements of its natural frequencies.

The mathematical model explained in the chapter 3 and the experiment explained in the chapter 4 provides the variation of the natural frequencies as a function of the variation of the applied force. This variation configures the training data and the expert knowledge for the fuzzy inference system.

The input data of the mathematical model is the geometric and mass characteristics of the chain. The chain features are obtained from the Coforja catalog (see appendix A). Of course, the links of the chain were measured to check the dimensions. A link of the chain was modelled in SolidWorks[1], as illustrates Figure 7.1, in order to get the inertias. The mass of the links was obtained weighting the chain.

Figure 7.1 Link of the chain modeled in SolidWorks.

Source: Author.

As the links of the chain are not equally oriented, that is, a link is perpendicular to the previous and to next one, the inertias with respect to each axis change, and that change is considered in the model. Figure 7.2 presents a frontal view of the chain showing the perpendicularity of the links.

[1] Dassault Systèmes SolidWorks Corporation.

Figure 7.2 Front and isometric view of the chain.

Source: Author.

The chain was loaded with a vertical force ranging from 5 kN to 70 kN. The natural frequencies were calculated for each applied force. The results of the mathematical model were compared with the results of the experimental procedure in order to validate the mathematical model.

As mentioned before, the output of the mathematical model and the experiment configures the expert knowledge for the construction of the fuzzy inference systems (FIS). For the modeling of the FIS, the natural frequencies are taken as the inputs of the model and the force on the chain is the output. For this study case, the first three natural frequencies of the chains were the inputs of the model.

The fuzzy inference system for estimating the force applied on the chain is modeled using the two methodologies: Mamdani and Sugeno. For both methodologies, the inputs are discretized in fuzzy sets with membership functions of type triangular and Gaussian.

For the Mamdani type, the output was discretized in fuzzy sets with membership functions of the same type than the inputs. This means that, if the inputs were described in triangular fuzzy sets the output did too. This also applies for the Gaussian membership functions.

The inference system of type Sugeno has mathematical function as consequent parts of type constant. They were the same for both type of membership functions.

The fuzzy inference systems, regardless of the type, had the same number of fuzzy sets in each universe of discourse. In this study case, all the universes of discourse had fuzzy sets. For the construction of the fuzzy sets of the universe of discourse, it was selected the centers of the fuzzy sets, it means a core, the point where the membership degree is 1. For the triangular membership functions, the range starts at the center of the previous MF and it ends at the center of the next MF. For the Gaussian MF the standard deviation was a constant value for all the MF. The figure 7.3 presents the triangular MF of the universe of discourse corresponding to the first natural frequency.

Figure 7.3 Membership functions for the first natural frequency as defined by the author.

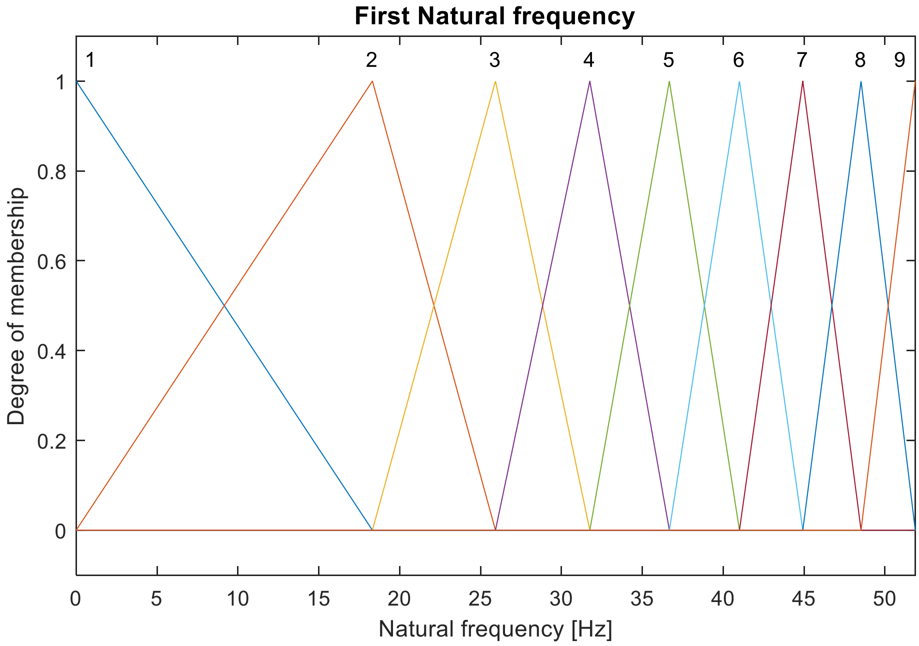

Source: Author

The rules for both types of inference systems used the connector and. The connector or was not considered for this work. For the Mamdani type, the t-norm was applied using the maximum, and for the Sugeno type, the t-norm was applied using the product of the membership degrees. Some examples of the rules used in this work are presented as follows:

$$If\ (f1\ is\ 2)\ and\ (f2\ is\ 2)\ and\ (f3\ is\ 1)\ then\ (T\ is\ 2)$$

$$If\ (f1\ is\ 5)\ and\ (f2\ is\ 4)\ and\ (f3\ is\ 4)\ then\ (T\ is\ 4)$$

$$If\ (f1\ is\ 6)\ and\ (f2\ is\ 5)\ and\ (f3\ is)\ then\ (T\ is\ 5)$$

where $f1, f2, f3$ are the universe of discourse corresponding to the first three natural frequencies and T the universe of discourse corresponding to the force of the chain. All the rules of the fuzzy inference systems were constructed with the premise that higher the natural frequencies, the greater the force of the chain is. the systems are defined by 69 rules.

The Mamdani fuzzy inference system adopted the centroid defuzzification method for the calculation of the crisp output, while the Sugeno fuzzy inference system used the average between the firing strength and the corresponding output levels.

Figure 7.3 shows the structure of FIS for estimating the force, remembering that the frequencies always were described in fuzzy sets and the force can be described in fuzzy sets or constant functions.

Figure 7.4 Structure of the fuzzy system for estimating the force on the chain.

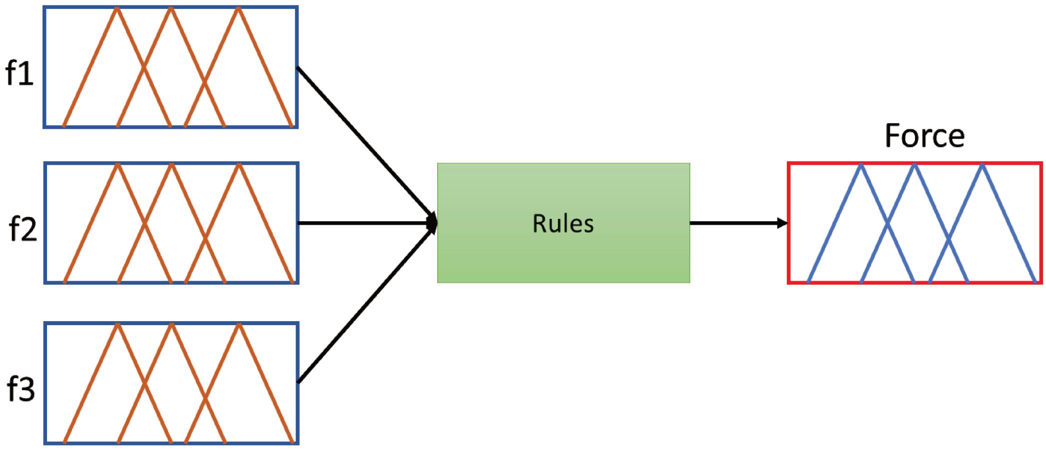

Source: Author.

Sometimes, the expert knowledge is not enough to get good accuracy of the results, and that is why an optimization process may be a powerful tool to improve the fuzzy system. In this study case, the genetic algorithm was implemented in order to enhance the results of the prediction.

The genetic algorithm had the structure presented in the chapter 6. The definition of the genes (variables to optimize) was as follows: for triangular membership functions, the parameters to be improved were the vertices of the triangle; and for the case of using Gaussian membership functions, the parameters were the mean and the standard deviation. Figure 7.4 shows how the chromosomes in the genetic algorithm are composed with the parameters of the membership functions of the antecedent parts.

Equation (7.1) correspond to the mathematical expression of the triangular membership functions:

$$y = triangle(x; a, b, c) = \begin{cases} 0, & x \leq a \\ \dfrac{x-a}{b-a}, & a \leq x \leq b \\ \dfrac{c-x}{c-b}, & b \leq x \leq c \\ 0, & c \leq x. \end{cases} \quad (7.1)$$

where the tunable parameters are a, b and c.

Equation (7.2) represents Gaussian membership function:

$$y = gaussian(x; c, \sigma) = e^{-\frac{1}{2}\left(\frac{x-c}{\sigma}\right)^2} \quad (7.2)$$

where the tunable parameters are c and σ.

Figure 7.5 Illustration of the gens of the chromosome in the genetic algorithm for triangular MF.

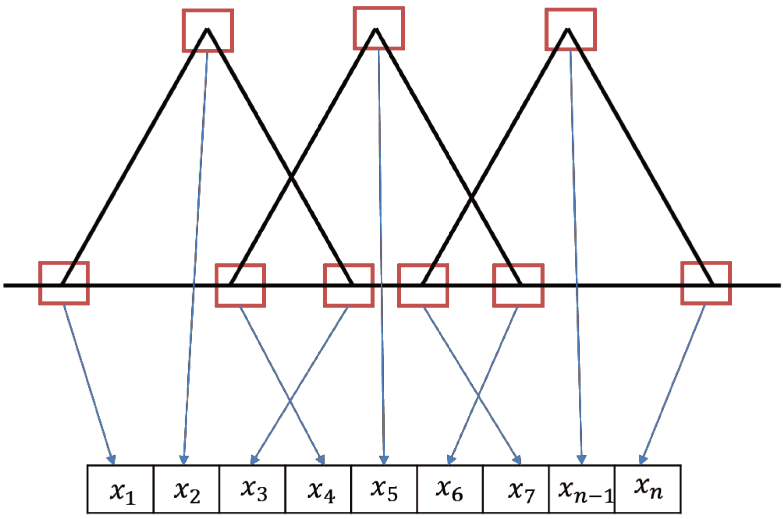

Source: Author.

The chosen size of the population (number of chromosomes) was 200. The maximum number of generations (iterations) was set to 1000. The fitness function (function to minimize), for this study case, was the root of mean squared error (RMSE). It is defined as:

$$RMSE = \sqrt{\frac{\sum(y_i - \hat{y}_i)^2}{n}} \quad (7.3)$$

where y_i is the real value, $\hat{y_i}$ is the estimated value and n is the number of samples. For this case, the samples are the training data obtained with the mathematical model of the link chain or the experimental data.

As mentioned in the chapter 6, the stop criteria for the genetic algorithm are three: the fitness value is achieved, i.e., the algorithm converged successfully; the number of maximum generations is reached; the number of stall generations is reached.

The selection procedure was made in two steps. The first was the scaling of the scores of the chromosomes and the next was the selection of the parents. The scaling of the scores was made as follows: the scores were ordered in ascending order, where the best score was the minimum one, since the function was been minimized. Once the scores were ordered, they were scaled by a function dependent on the position on the rank, which is given by:

$$r = k\left(\frac{1}{\sqrt{n_r}}\right) \tag{7.4}$$

where n_r is the position on the ranking, k is a proportional constant and r is the scaled value. The constant k can be calculated with the premise that the summation of the scaled values must be equal to the number of parents required to create a new generation. The process of scaling is performed because the raw scores can have much dispersion, then the scaling function eliminates this issue.

The selection method for this study case was the uniform stochastic selection, shown in Figure 7.4. The method consists of creating a line by joining lengths equivalent to the scaled values of the scores. After the line is created, the selection of the parents is performed by simulating a pointer that moves along the length of the line with the same step size. The algorithm allocates a parent of the section on which the pointer lands. The step size depends on the number of parents.

Figure 7.6 Uniform selection process.

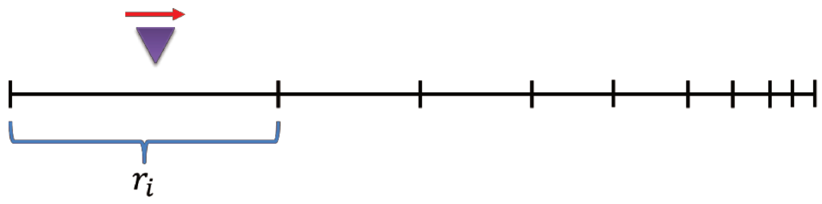

Source: Author.

The offspring was created with three procedures of reproduction. The elite children, the crossover and the mutation. Elite children are parents who must survive until the next generation because their genes were considered the best of the current generation and must be present in the next. Elite children were chosen according to the scaled value, where the first ones in the ranking were selected. The fraction of elite children corresponded to 0.05 of the population size, that is, 5% of the total number of children are elite children.

The crossover process was made with N points as described in the chapter 6. The algorithm created a random binary vector of length equal to the number of gens. At the positions where the vector was equal to 1, the algorithm allocated the genes of the first parent, and at the positions where it was 0, the algorithm took the genes from the second parent. These chosen genes configured a new chromosome. The crossover fraction was 0.08, that is, 80% of the children left to generate after the elite process were created by crossover. This means 76% of the total number of children.

Figure 7.5 shows the process of crossover, where the first vector provided the positions where the genes were extracted from the parents (second and third vector) in order to create a new child.

Figure 7.7 Crossover process.

1	0	0	1	1	0

5	7	3	9	4	6
2	5	7	8	0	4

5	**5**	**7**	**9**	**4**	**4**

Source: Author.

The mutation process was performed by adding up to each gen a random number (normal distribution) k_i, where i is the number of genes, with zero mean and standard deviation depending on the optimization boundaries. It important to note that each value k_i is different for each gene. Figure 7.6 shows an example of the process of mutation.

Figure 7.8 Mutation process.

4	6	8	2	4	9
		+			
k_i	k_i	k_i	k_i	k_i	k_i

Source: Author.

Since the random numbers of the normal distribution is close to zero, the genes undergo only small mutations, which prevents the process of falling into a random search.

Figure 7.8 shows the structure of the fuzzy genetic system proposed for this work. The system consists of a fuzzy inference system created with the expert knowledge of the author. The entries for the inference system are the three first natural frequencies of the chain taken from the training data (variation of the natural frequencies regarding the applied force in the chain), which can be from the mathematical model or the experimental measurements. The output of the inference system is the estimated force in the chain. The estimated force is compared with the force of the training data (simulated or experimental) by the genetic algorithm. If the genetic algorithm perceives that the estimation error is great, then it modifies the parameters of the membership functions of the antecedent parts in order to estimate a new force. The process is repeated until the fuzzy inference system is able to estimate the applied force in the chain with minimal error.

Figure 7.9 Structure of the fuzzy genetic system used in this work.

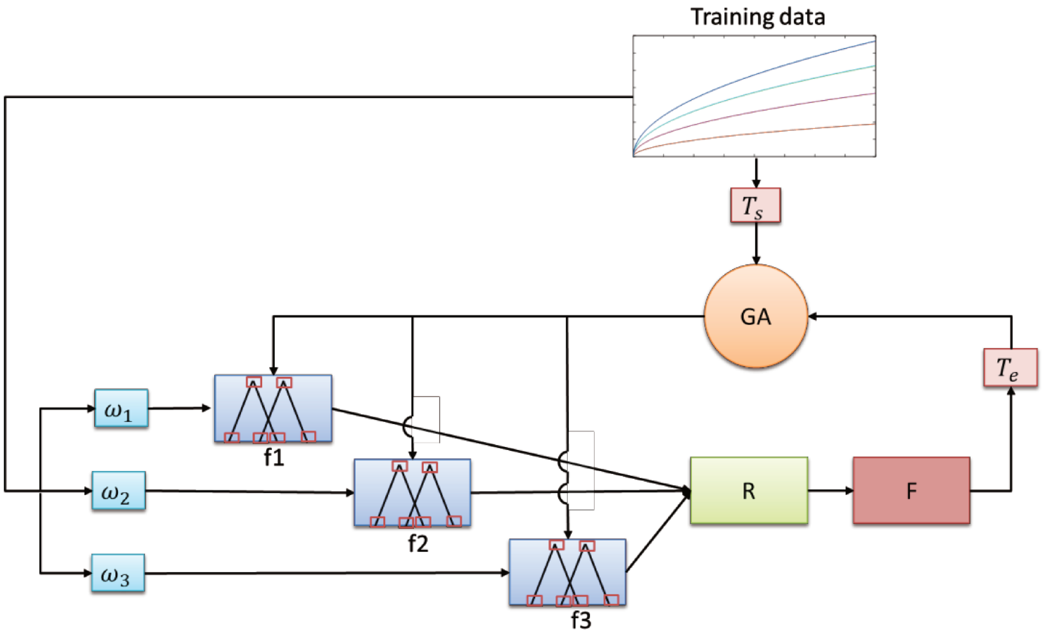

Source: Author.

All fuzzy systems with singleton fuzzification were simulated in MATLAB[2], with the help of the fuzzy logic designer toolbox. The optimization with genetic algorithm of these fuzzy system was performed with the support of the optimization toolbox of MATLAB.

The fuzzy system with non-singleton fuzzification was tested with the help of the toolbox for fuzzy logic (WAGNER; PIERFITT; MCCULLOCH, 2014) created by Christian Wagner[3]. This toolbox was developed in Java[4]. It was used this toolbox since the fuzzy logic designer of MATLAB does not support non-singleton fuzzification. The Java toolbox only supports fuzzy system of type Mamdani.

The fuzzy inference systems were evaluated looking for finding which of them had the best performance.

---

[2] The MathWorks, Inc.
[3] School of Computer Science. University of Nottingham.
[4] Oracle.

8. RESULTS

8.1. Mathematical model of the chain

When analyzing the matrices of the mathematical model of the chain, it is expected to calculate pairs of equal frequencies corresponding to each plane. The unique difference in the matrixes is given by the introduction of the inertias because of the perpendicularity of the links. Some simulations are done and presented below.

Figure 8.1 shows the lowest natural frequencies as a function of the applied force for a chain with only 6 links. Observe that the natural frequencies are not equal pairs. They have the same behavior but differ in value. A new simulation is done increasing the number of links. Figure 8.2 shows the natural frequencies for a chain with 24 links. Observe that, in this case, the natural frequencies are equal pairs for each plane.

Figure 8.1 Natural frequencies of a chain with 6 links.

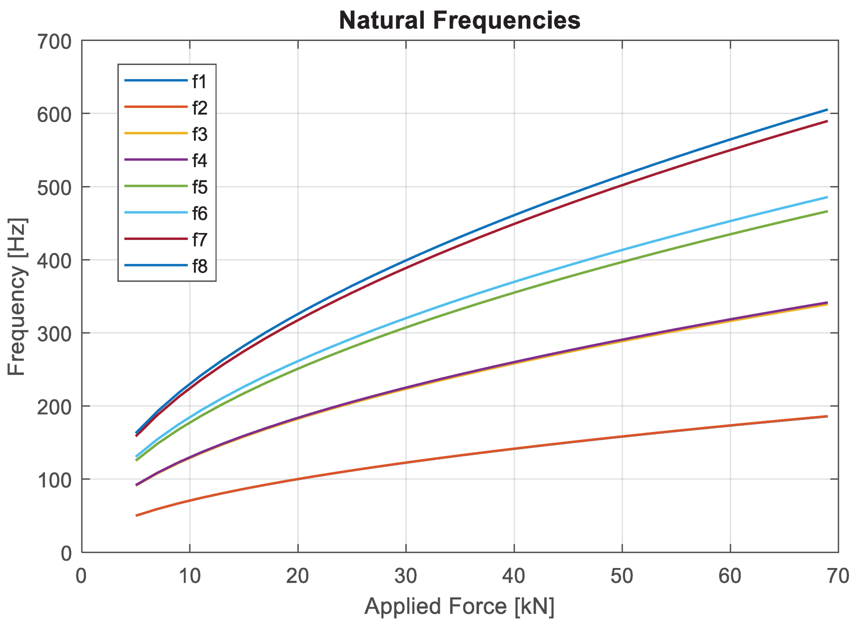

Source: Author.

When the chain has a small number of links, the effect of the variation of the moments of inertia of the links greatly influences the dynamics of the chain, making the natural frequencies have different values for each plane. This is due to the position of each link along the chain. Thus, as the number of links increases and the chain becomes long (the length of the chain is large compared to the dimension of the link), the variation in the moments of inertia of the links starts to influence little or almost nothing in the vibrational behavior of the chain and, as a consequence, the natural frequencies on each plane become equal.

Figure 8.2 Natural frequencies of a chain with 24 links.

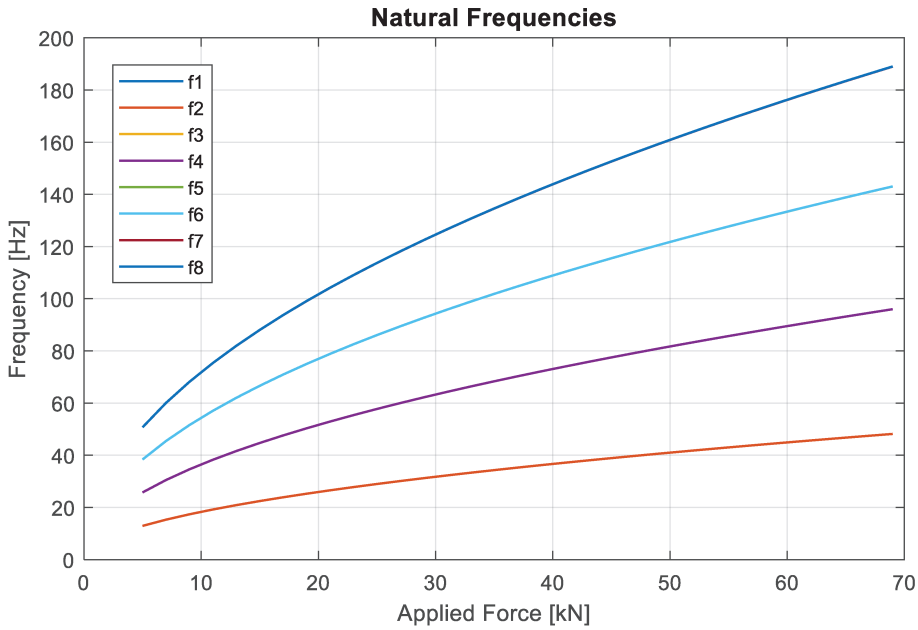

Source: Author.

Another important fact to highlight is that the dynamic behavior of the chain depends on the axial load. For low axial force, the weight of the links influences the stiffness of the system, but for high loads, the stiffness of the systems practically depends only on the axial external force applied to the chain.

8.2. Experimental Results

The analysis of the experimental data was performed as explained in the Chapter 4, calculating the Frequency Response Function (FRF) with the signal of the force provided by the force transducer and the vibration signal from the accelerometers. It was identified the first four natural frequencies for each applied force.

Remembering that the shaker was installed at the link number 18, and the three accelerometers were installed as follows: at link number 8 in X direction, at link number 11 in Y direction, and at link 19 also in Y direction. The links were numbered upwards.

The first analysis was performed evaluating the frequencies measured in the three accelerometers for a specific applied force, in this case, 30 kN. Figures 8.3, 8.4 and 8.5 show the FRF estimated with accelerations measured at links 8, 11 and 19, respectively.

Figure 8.3 FRF of the acceleration of the link 8.

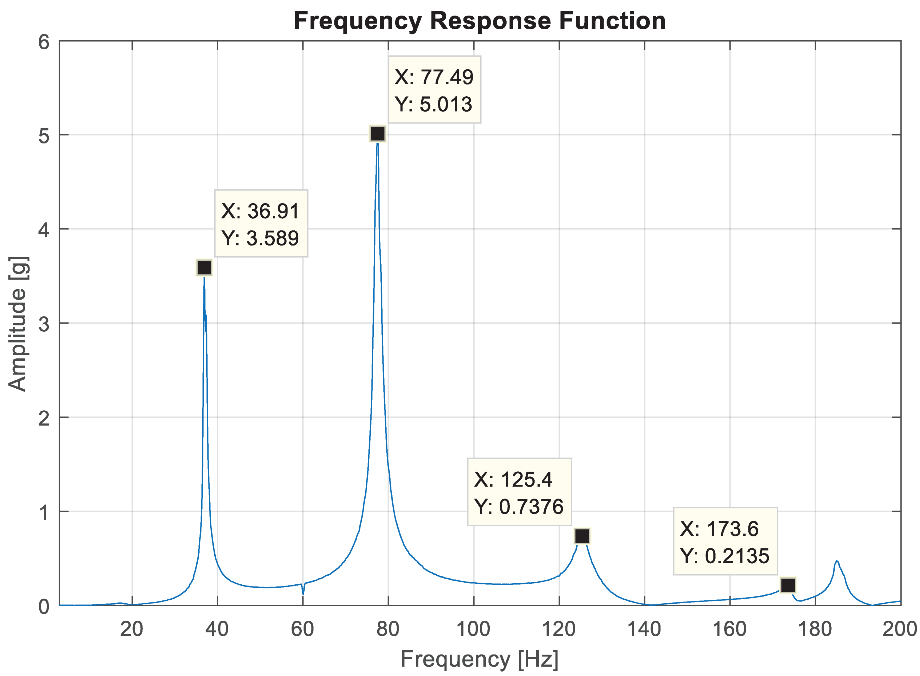

Source: Author.

When comparing the values of the first four natural frequencies measured on the three links, it is noted that these values are equal. Knowing that the accelerometers were installed in perpendicular directions, it is possible to infer that the natural frequencies are the same for both planes.

Figure 8.4 FRF of the acceleration of the link 11.

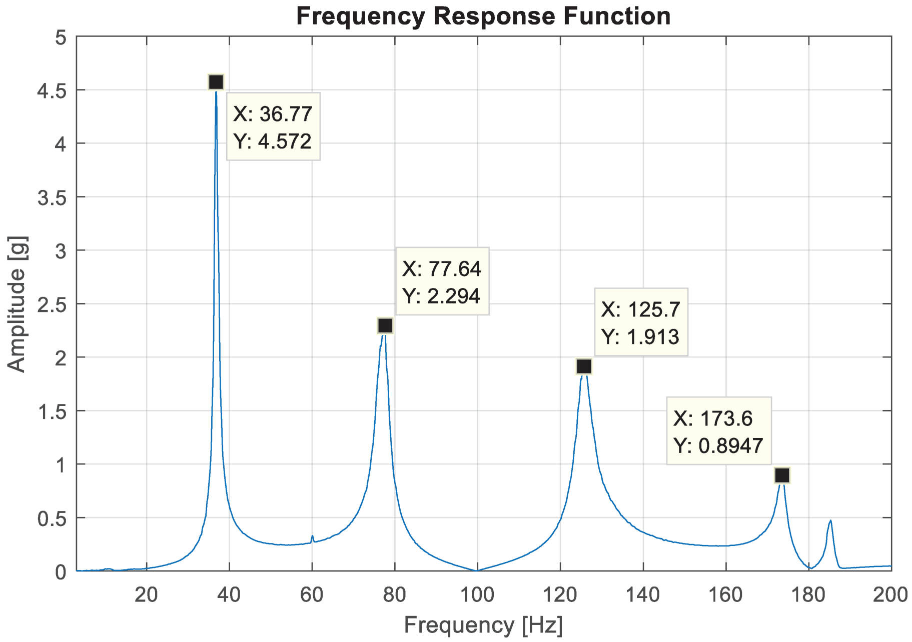

Source: Author.

Figure 8.5 FRF of the acceleration of the link 19.

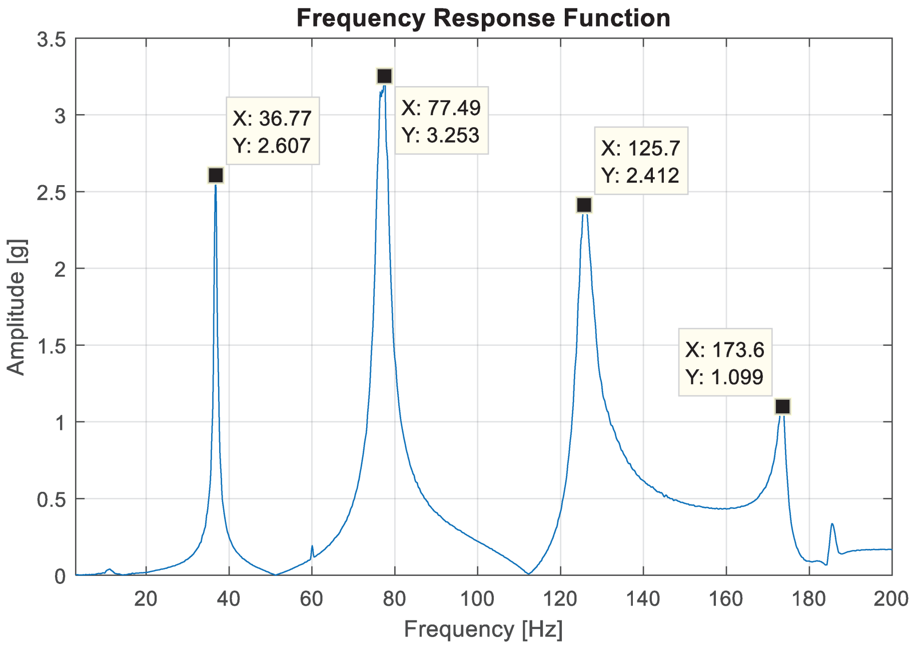

Source: Author.

The first four natural frequencies of the chain were identified for a cycle of loading/unloading. The values of the frequencies are presented in Table 8-1. The symbol ↑ means loading and ↓ means unloading.

Table 8-1 Experimental natural frequencies for a loading/unloading cycle of the chain.

Force [kN]	ω_1[Hz] ↑	ω_1[Hz] ↓	ω_2[Hz] ↑	ω_2[Hz] ↓	ω_3[Hz] ↑	ω_3[Hz] ↓	ω_4[Hz] ↑	ω_4[Hz] ↓
5	16.7	16.1	36.5	36.18	59	58.59	81.9	80.86
10	22.9	22.27	49.5	49.22	79.4	79.25	119.5	118.9
15	27.4	27.1	58.6	58.45	96.9	93.16	143.3	143
20	30.9	30.62	65.6	65.63	105.6	107.8	156.6	155
25	34.3	33.8	72.1	71.9	116.5	116.5	166.3	165.1
30	36.6	36.8	77.6	77.5	125.7	125.5	173.9	172.4
35	39.4	39.2	82	82.2	134.3	134.3	180.2	179.2
40	41.8	41.5	86.1	85.6	142.5	142.1	185.2	184.9
45	44.1	44	92.4	92.1	149.1	149	191.2	190.1
50	45.9	45.9	99.2	98.9	155.4	155.1	195.7	195.1
55	47.9	47.8	104.6	104.2	161.1	161.3	200.1	199.5
60	49.5	49.5	108.1	108.1	166.8	166.7	203.6	203.2
65	51.6	51.1	111.8	111.6	172.1	172.1	207	206.8
70	52.9	52.9	114.7	114.7	177.1	177.1	209.5	209.5

Source: Author.

Observing the values of the first four natural frequencies calculated for a cycle of loading/unloading is possible to note that the values of the natural frequencies practically are equal for the loading and the unloading process. Then, the chain presents low hysteresis in relation to natural frequencies, which can be neglected. These results were the same for experiments carried out in several days.

Figure 8.6 shows the first four natural frequencies of the chain estimated with the experimental data. The natural frequencies have the expected behavior, they increase with the increasing of the applied force.

Figure 8.6 Experimental Natural frequencies of the chain.

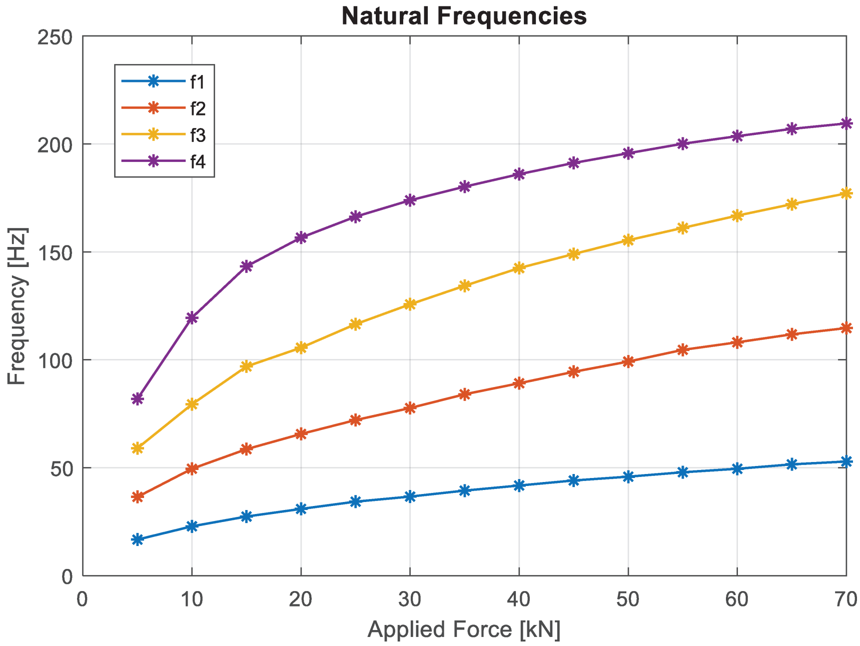

Source: Author.

Figure 8.7 presents a comparison between the experimental and the numerical natural frequencies. Comparing the results of the mathematical model with the experimental data, it can be noted that the model provides good qualitative outcomes, once the behavior of the curves that represent the natural frequencies is similar. Regarding quantitative results, the mathematical model differs from the experimental data.

Figure 8.8 shows the comparison of the first natural frequency calculated with the model and the one calculated experimentally, and Figure 8.9 shows the first natural frequency calculated experimentally as a function of the first natural frequency obtained from the mathematical model.

Figure 8.7 Comparison of the natural frequencies. Experimental and Simulated.

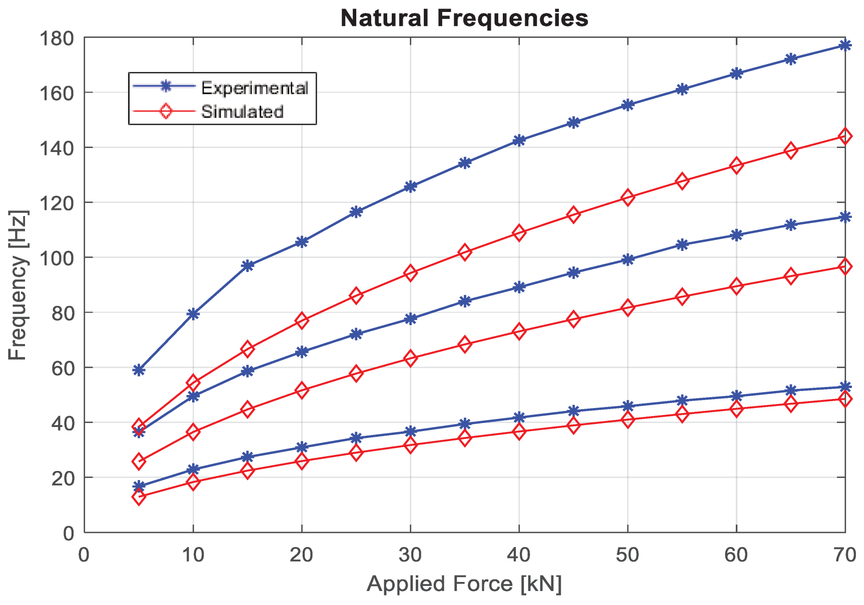

Source: Author.

Figure 8.8 First natural frequency. Experimental and Simulated.

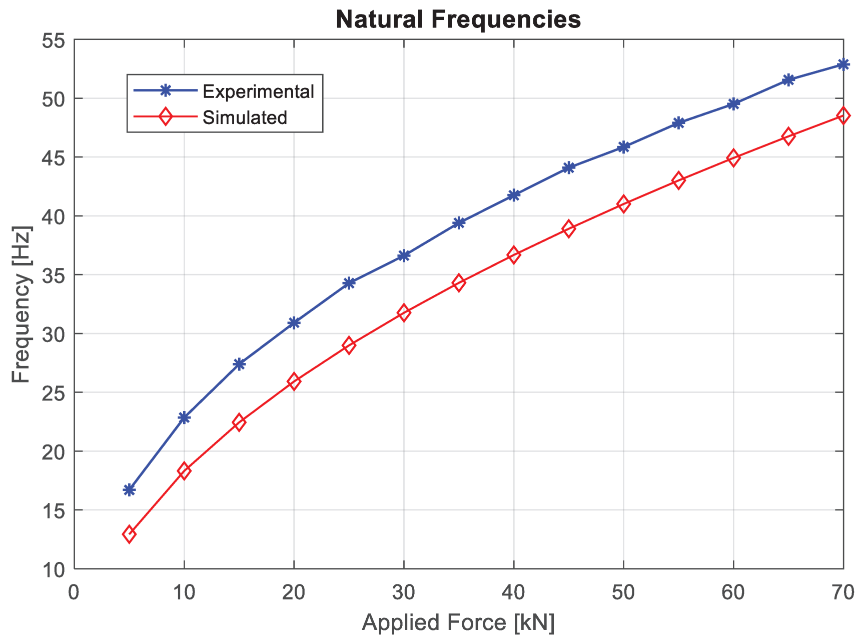

Source: Author.

Figure 8.9 Simulated frequency Vs Experimental frequency.

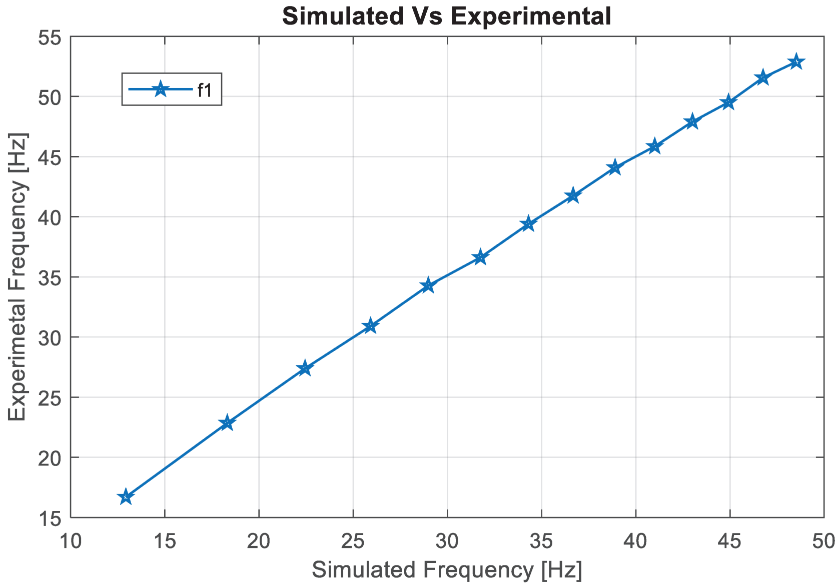

Source: Author.

These figures make it clear that the two results, experimental and numerical, have the same behavior, but their values are slightly different. The graphic of the simulated natural frequencies versus the experimental ones presented in Figure 8.9 shows that the two results are related by function pretty close to a straight line whose equation is $\omega_E = 1{,}004 * \omega_S + 4.946$, where ω_E is the experimental frequency and ω_S is the simulated on. From the equation, the slope of the line is 45^{o} and all the values have a difference of approximately 4.9 Hz. This graphic indicates that the mathematical model does not present any discrepancy regarding the material properties.

The 4.9 Hz difference between the experimental and numerical values of the first natural frequencies is the same for any value of the applied force. The difference in the first natural frequencies affects all other natural frequencies of the chain, since the other natural frequencies depend on the value of the first.

Several works about the estimation of the natural frequencies in chains or cables, as the case of Verbin, (2015), show that the natural frequencies of these system are related with the first frequency as follows:

$$\omega_n = n * \omega_1 \tag{8.1}$$

where ω_1 is the value of the first natural frequency, n is the number of the natural frequency, that is, 1, 2, 3, etc., and ω_n is the value of the nth frequency. The results of the mathematical model of the chain present the relation described in equation (8.1). The experimental results also show a relationship between the frequencies, which can be seen in Table 8-2.

Table 8-2 Relationship between the experimental natural frequencies of the chain.

Force [kN]	ω_2/ω_1	ω_3/ω_1	ω_4/ω_1
5	2.18	3.53	4.90
10	2.17	3.47	5.19
15	2.14	3.54	5.23
20	2.12	3.42	5.07
25	2.10	3.40	4.85
30	2.12	3.43	4.75
35	2.08	3.41	4.57
40	2.06	3.41	4.46
45	2.10	3.38	4.34
50	2.16	3.39	4.27
55	2.18	3.36	4.18
60	2.18	3.37	4.11
65	2.17	3.34	4.01
70	2.17	3.35	3.96
Mean	2.15	3.40	4.51

Source: Author.

According to Table 8-2, the second natural frequency is approximately 2.1 times the first, the third is 3.4 times the first, while the value of the fourth natural frequency is 4.5 times the value of the first. Then, the 4.9 Hz difference is amplified depending on the relationship for each natural frequency, making the higher the natural frequency, the greater the discrepancy of the model and the experimental data.

Aiming to investigate the differences between the results of the model and the experimental data, a variation of the model was developed and explained in section 3.7 of this work. In this case, the supports of the chain were considered elastic, with stiffness k_1 for the upper support and k_2 for the lower one. Some simulations were run, and the results are explained next.

Figure 8.10 shows the first four natural frequencies calculated with the following combination of stiffness: $k_1 = 1 \times 10^7$ kN/m and $k_2 = 1 \times 10^7$ kN/m. The natural frequencies present the same behavior than the ones of the model with rigid supports. Running other simulations, it was found that this behavior is obtained for any combination of stiffness of the supports in the interval $[1 \times 10^4, 1 \times 10^{14}]$ kN/m. When the combination of stiffness is lower than the lower limit of this interval, the natural frequencies of the chain present a different dynamic behavior and its study is out of consideration for this work. When the combination of stiffness it higher than the upper limit of this interval, the model presents numerical instabilities.

Figure 8.10 Natural frequencies of the model with elastic supports.

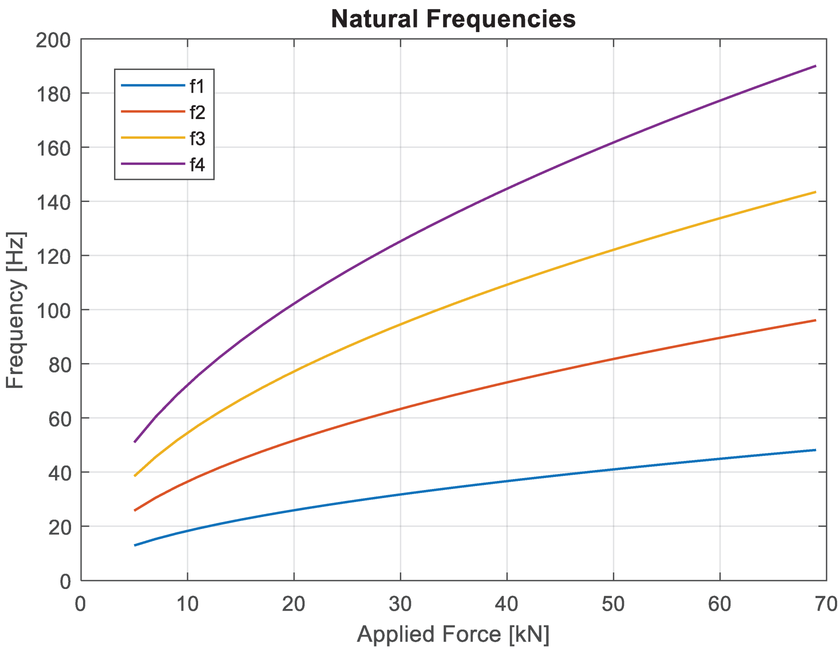

Source: Author.

Another important fact found in the analysis of the natural frequencies was that the values of the lowest frequencies do not change for any combination of stiffness defined within the interval $[1 \times 10^4, 1 \times 10^{14}]$k N/m. The introduction of elasticity in the supports affects only the values of the higher frequencies of the chain.

Comparing the values of the first four natural frequencies calculated with both models (Figure 8.11), it is noted that they are equal. Then, the consideration of flexibility in the supports does not affect the value of the lowest natural frequencies of the chain.

Figure 8.11 Natural frequencies calculated with the model with rigid supports and elastic supports.

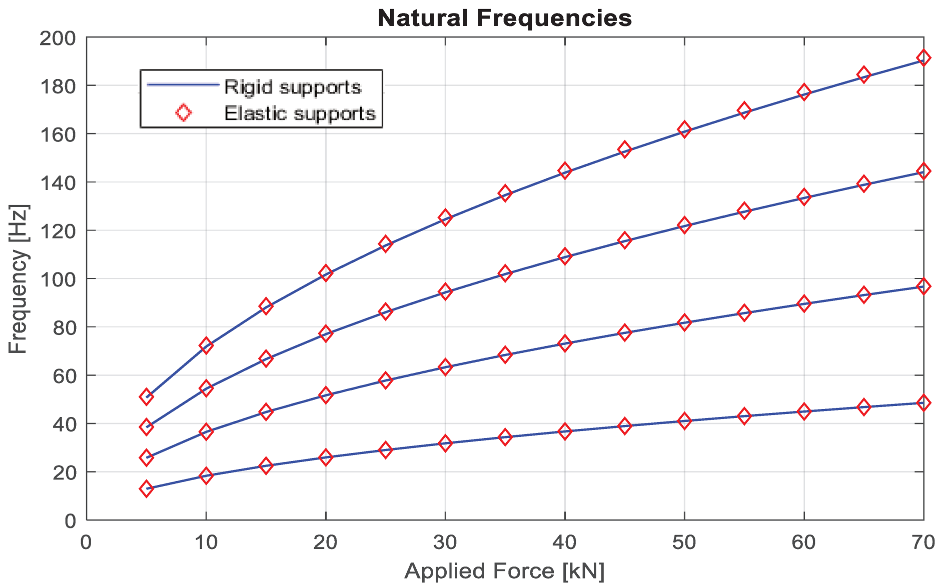

Source: Author.

After the analysis, it is possible to state that the discrepancies between the experimental and the simulated results are not due to the fact that the supports in the experimental procedure are flexible. It is necessary to continue searching the cause of these differences and this is precisely one of the studies proposed as future works.

The extensiometry analysis was performed in order to verify if there exist any variation of the axial force of the chain and the applied force. The force signal is obtained with the transformation described in the equation (4.2).

The measurements with strain gauges were carried out to check if there was any discrepancy between the axial load values measured by the load cell installed between the hydraulic actuator and the chain and that measured by the strain gauges. The force value was obtained with the transformation described in equation (4.2).

Figures 8.11 and 8.12 show the measured force signal in different points for applied load values equal to 30 kN and 50 kN, respectively.

Figure 8.12 Force signal of the strain gauge at 30 kN.

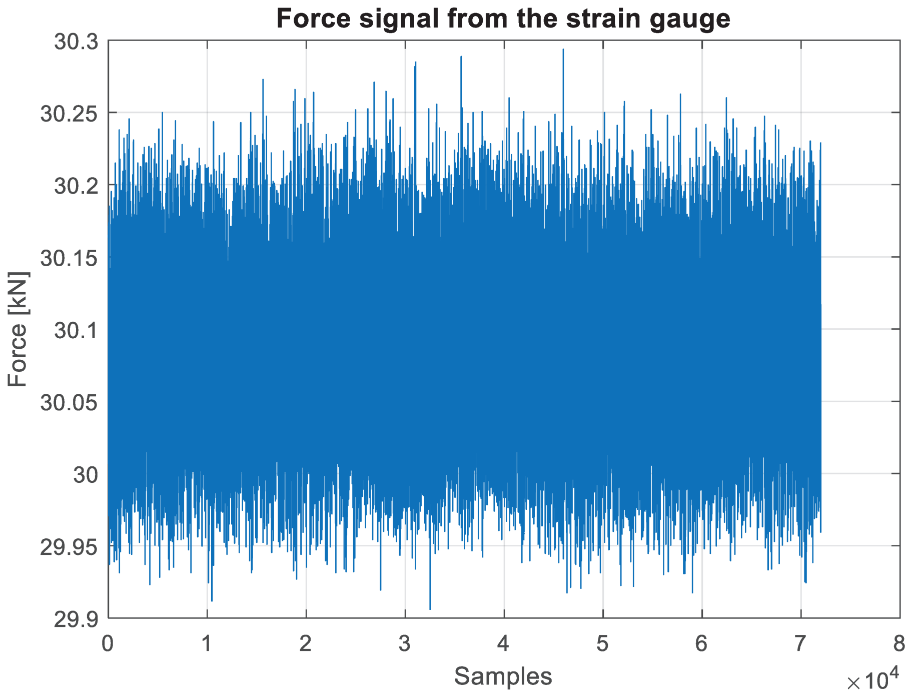

Source: Author.

Figure 8.13 Force signal of the strain gauge at 50 kN.

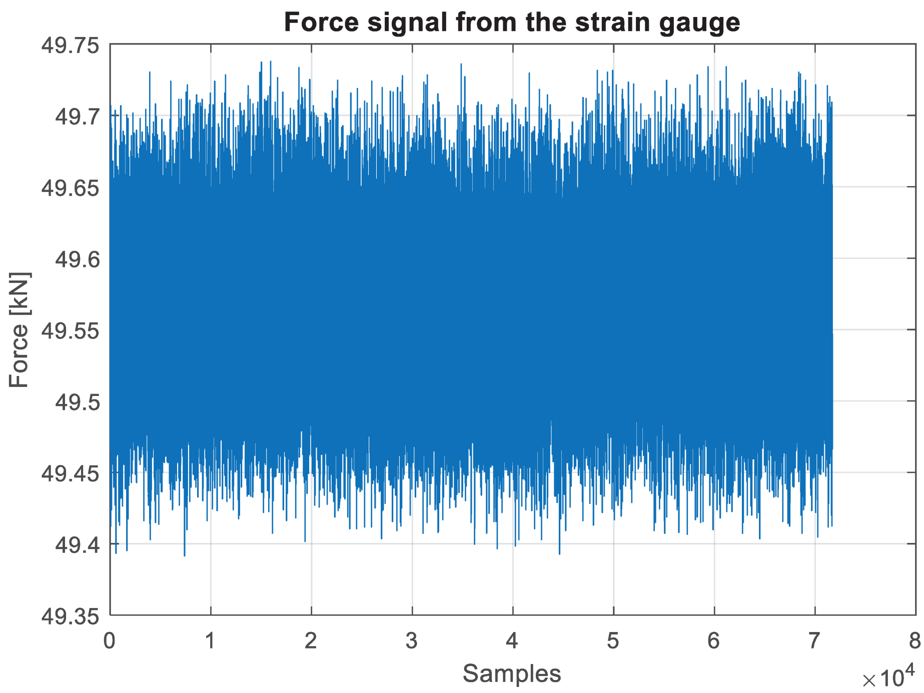

Source: Author.

The calculated forces show that the applied load and the one calculated with the signal from the strain gauges is practically equal. These results were the same for all six strain gauges installed on the chain.

8.3. Fuzzy inference system

Four fuzzy inference systems were built to estimate the force applied to the chain. Two of them used the Mamdani inference and two the Sugeno inference. Triangular and Gaussian membership functions (MF) were used to model the fuzzy sets of the antecedent parts, as well as the consequent one, in the case of Mamdani inference. The consequent part of the Sugeno system were defined as constants. All models were defined with 9 MF for each universe of discourse and used singleton fuzzification. The results of the fuzzy inference system without any optimization and using the computational model are shown in this section.

The parameter used to measure the performance of the fuzzy inference system was the root of squared mean error (RMSE) between the applied force and the value estimated by the fuzzy system.

Figure 8.14 presents the comparison of the force estimated by the Mamdani fuzzy inference system with triangular membership functions and the applied force of the mathematical model. This fuzzy system has a RMSE of 0.336 kN. Figure 8.15, on the other hand, shows the result for a Mamdani fuzzy inference system with 17 triangular membership functions. This model has a RMSE of 0.152 kN.

Observe that the number of membership functions influences in the estimation, since its increments makes the model more accurate reducing the root mean squared error. Usually, the higher the number of membership functions, the better the estimation. This implication has a counterpart, since it is necessary more rules to define the model, which means longer processing time.

Figure 8.14 Results of the Mamdani FIS with triangular MF.

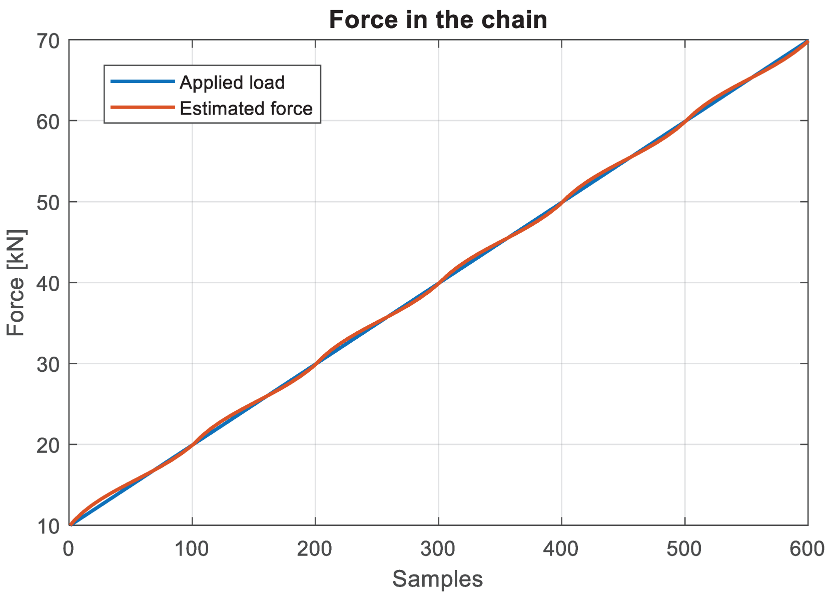

Source: Author.

Figure 8.15 Results of the Mamdani FIS with triangular MF.

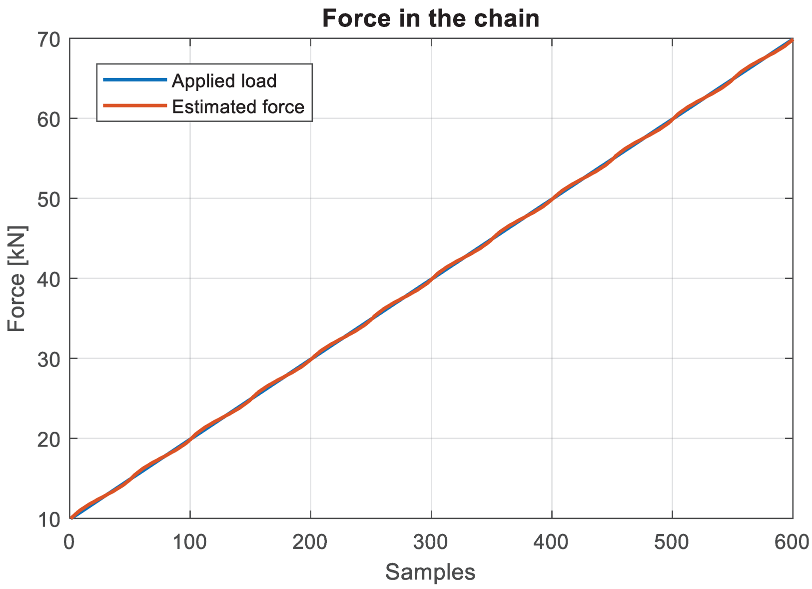

Source: Author.

Figure 8.16 presents the force estimated by a Mamdani fuzzy inference system with gaussian membership functions. The model has a RMSE of 1.564 kN. Observe that, in this type of fuzzy system, the root mean squared error increases significantly, when compared to the cases shown in Figures 8.14 and 8.15. The reason is the difficulty to set values for gaussian membership function parameters, mean and standard deviation, specially the last one, because of the complexity of its perception.

Figure 8.16 Results of the Mamdani FIS with gaussian MF.

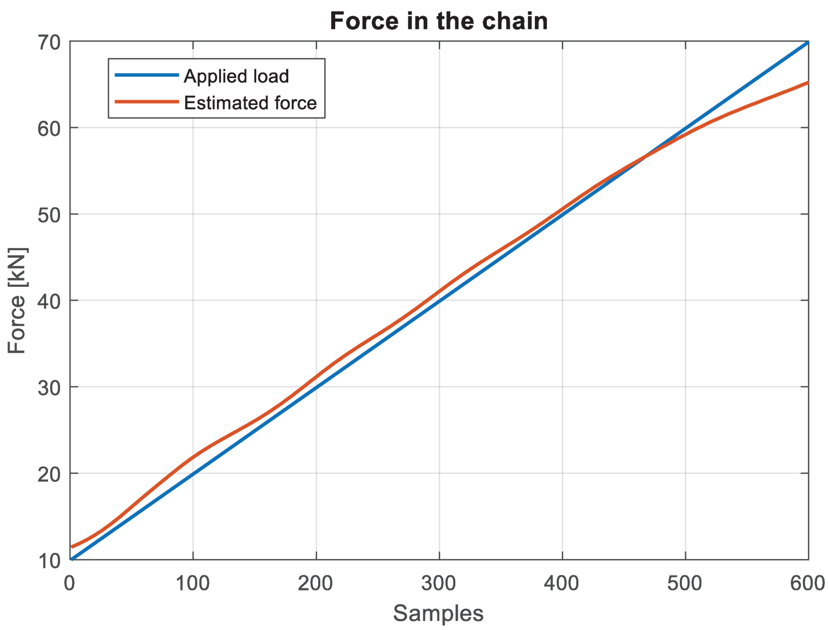

Source: Author.

The figure 8.17 shows the results for a Sugeno inference system with triangular membership functions. The model has a RMSE of 0.953 kN.

Figure 8.17 Results of the Sugeno FIS with triangular MF.

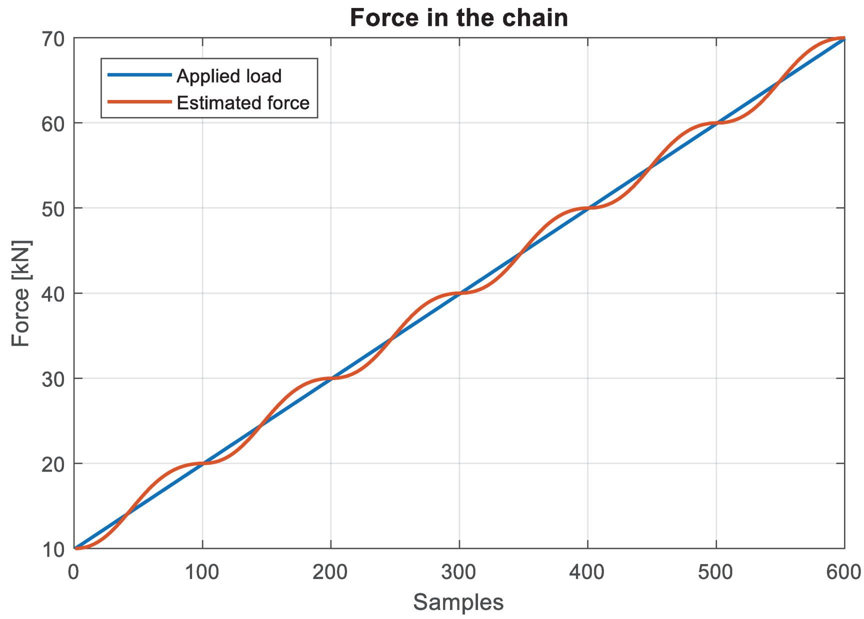

Source: Author.

Figure 8.18 shows the results for a Sugeno fuzzy inference system with gaussian membership functions. The model has a RMSE of 0.717 kN.

Figure 8.18 Results of the Sugeno FIS with gaussian MF.

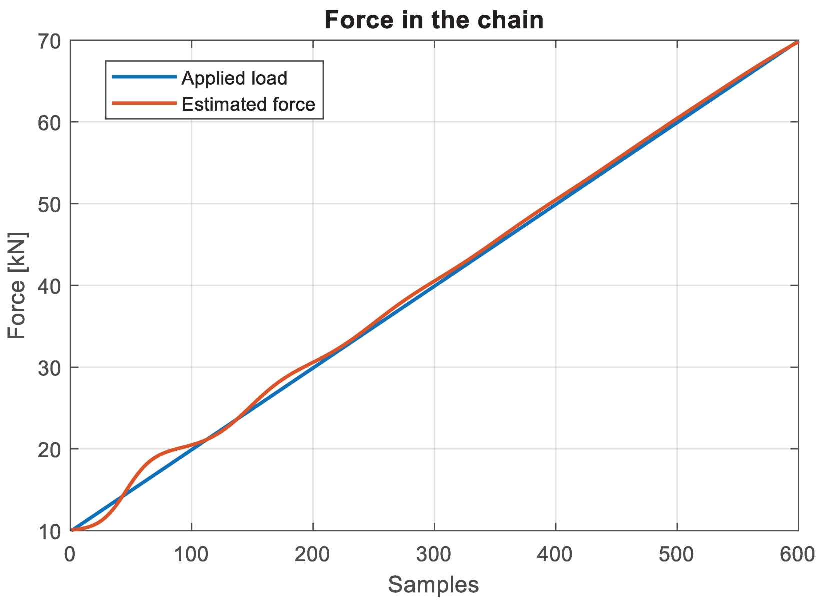

Source: Author.

The previous results correspond to fuzzy systems without any type of optimization. They all have the same rules and the same number of membership functions. The Mamdani fuzzy inference system with triangular membership functions was the one with the best performance.

It is important to emphasize that the parameters of the membership functions and the rules were selected based on the specialized knowledge acquired through the mathematical model and experimental data. The selection of the parameters of a fuzzy system is a complex process, because, in most cases, the number of parameters is high and, in addition, it can be difficult to define them, as is the case of the standard deviation.

Rules play an essential role in the fuzzy inference system. The correct definition of the rules directly affects the performance of the system. It is essential that the rules describe the system's behavior and characteristics accurately. It is important to pay close attention to the definition of all rules, as only one wrong rule can compromise the good performance of the fuzzy system.

8.4. Optimization of the fuzzy systems with genetic algorithm

The main objective of the optimization is to obtain the set of parameters of the membership functions of the antecedent parts that improve the ability of the fuzzy system to estimate the force accurately. Only the Sugeno inference system has been optimized. This section presents the changes that the genetic algorithm made to the parameters of the fuzzy system. The systems were trained with 600 samples from the training data and tested with another different 600 samples.

Figure 8.19 shows the membership functions for the first natural frequency that is one of the inputs of the fuzzy inference system. In this case, the membership functions here are not optimized. Figure 8.20, on the other hand, shows the membership functions of the first natural frequency of the fuzzy inference system optimized by the genetic algorithm.

Figure 8.19 Membership functions for the first natural frequency as defined by the author.

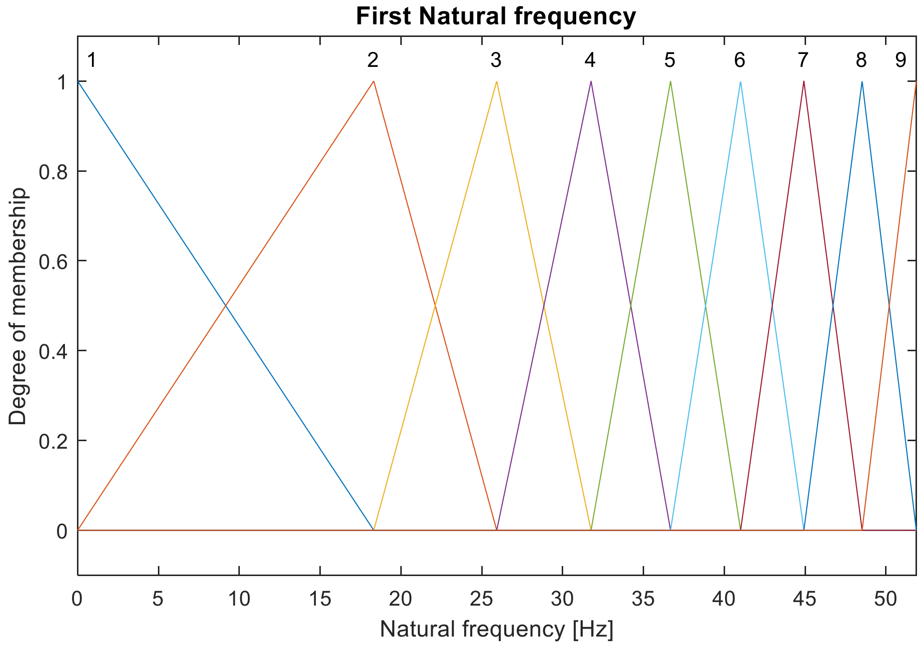

Source: Author.

Figure 8.20 Membership functions for the first natural frequency after the optimization process.

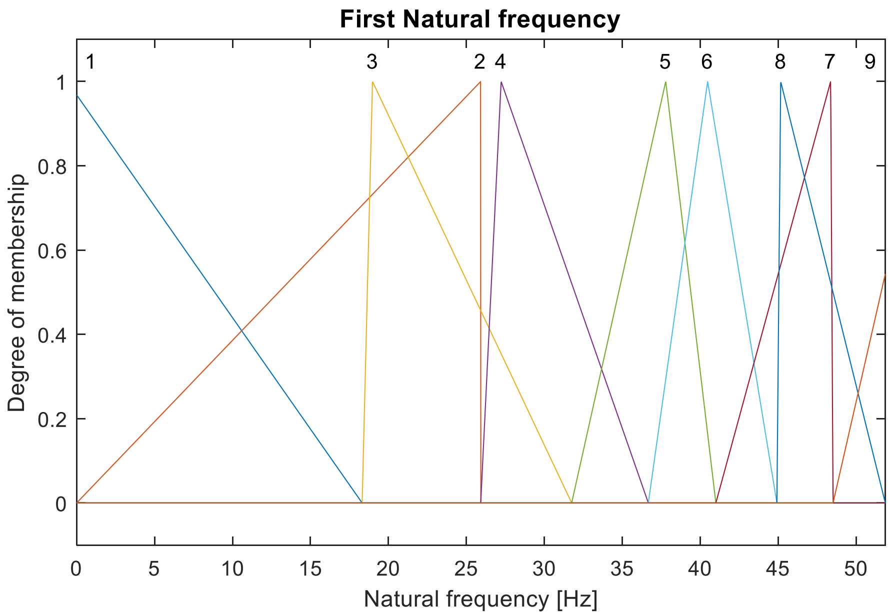

Source: Author.

Observe the changes that the algorithm made in the definition of the membership functions. All the membership functions of the antecedent parts were altered by the genetic algorithm. Only the first natural frequency is shown as an example.

Figure 8.21 presents the result for the Sugeno fuzzy system with triangular membership functions optimized by the genetic algorithm. The model has a RMSE of 0.075 kN. Observing this graphic, it is possible to perceive that the estimated and the simulated forces are practically the same.

Figure 8.21 Results of the optimized FIS with triangular MF.

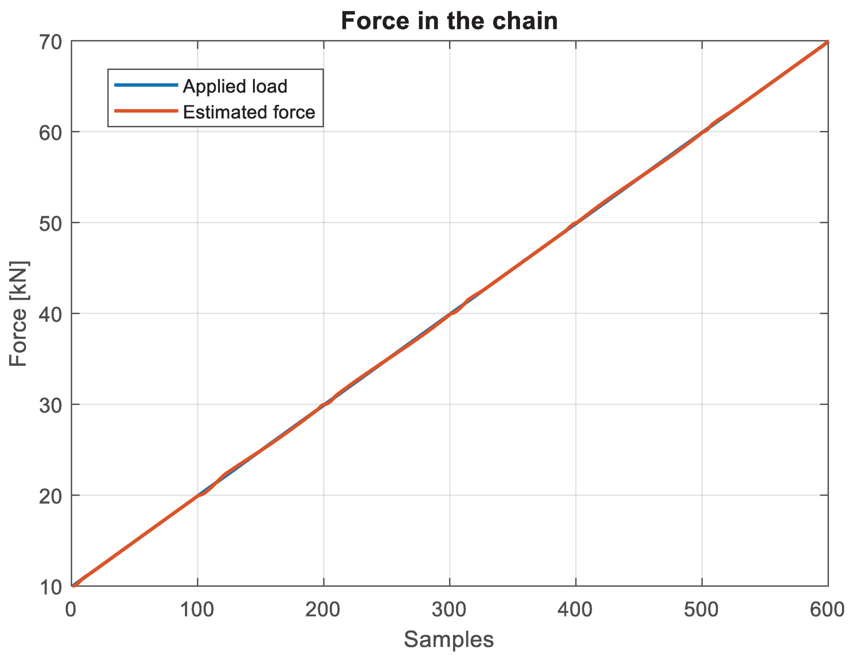

Source: Author.

The genetic algorithm was able to reduce the root mean square error from 0.953 kN to 0.075 kN for this model. It is important to note that fuzzy inference can be further optimized, but more computational time would be necessary.

Figure 8.22 shows the first antecedent part of the Sugeno fuzzy inference system with gaussian membership functions without optimization. After the process of optimization, the membership functions were changed as shows the Figure 8.23.

Figure 8.22 Membership functions for the first natural frequency as defined by the author.

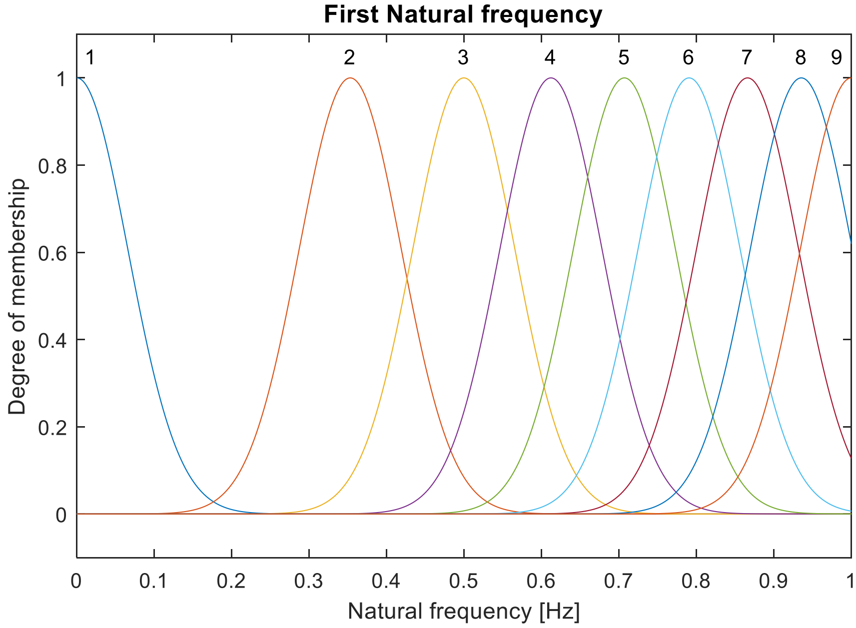

Source: Author.

Figure 8.23 Membership functions for the first natural frequency after the optimization process.

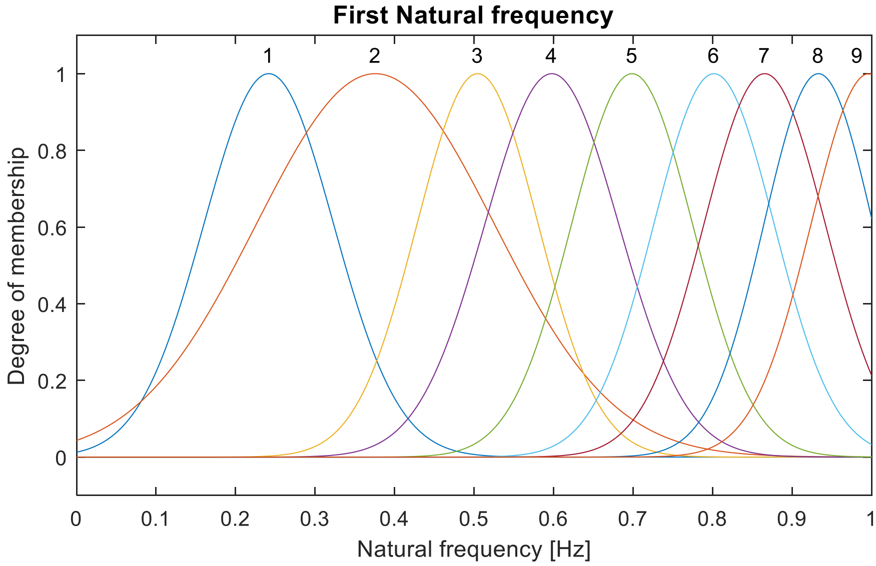

Source: Author.

Figure 8.24 shows the results obtained by the optimized Sugeno fuzzy inference system with gaussian membership functions. The model has RMSE of 0.031 kN. The genetic algorithm was able to reduce the RMSE from 0.717 kN to 0.031 kN.

Figure 8.24 Results of the optimized FIS.

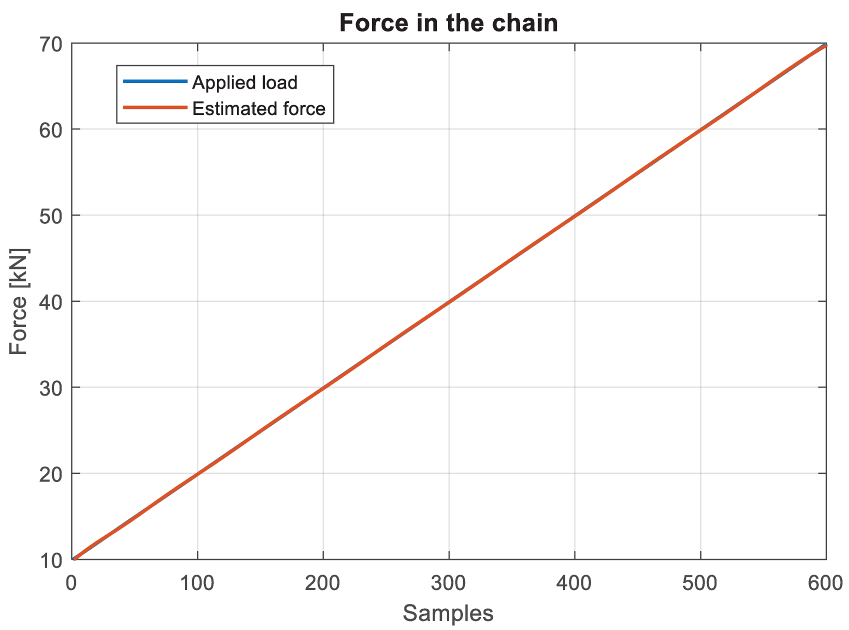

Source: Author.

The genetic algorithm modified the membership functions in order to improve the accuracy of the estimation. The fuzzy system with Gaussian membership functions performed better after optimization, possibly due to the fact that the Gaussian function models nonlinearities better than the triangular ones.

The process of optimization requires a considerable computational time. It is emphasized the fact that both optimized systems can still be improved, but it would be needed more computational time. The Mamdani fuzzy systems were not optimized because they have the procedure of defuzzification, which makes the iterative process very slow. In addition, for the optimization of this type of fuzzy inference, the computational investment is very high and the iterations can take a long time to achieve any enhancement.

In order to boost the iterations, some strategies can be done. The fuzzy system with gaussian membership functions was normalized in the interval [0, 1], which reduces the computational time. Another good thing to do is to define the population size not so high, but without endanger the variety of the chromosomes. The genetic algorithm does not require initial conditions to start the iterations, but, if it exists, it is vital that the initial conditions are selected carefully, as the incorrect initial condition can lead the algorithm to a non-optimal set of values.

The training data must truly represent the behavior of the system to be modeled, as these are the data that the algorithm uses to adjust the parameters, in addition to the fact that they strongly influence the convergence of the algorithm. Another parameter that affects convergence is the definition of boundary conditions. The genetic algorithm proved to be a good tool to improve the performance of fuzzy inference systems.

Figure 8.25 presents the results for a Sugeno fuzzy inference system with Gaussian membership functions, trained and tested with the experimental data. The system was trained with seven samples and tested with another different seven samples. The model has a RMSE of 0.022 kN.

Figure 8.25 Results of the FIS trained with experimental data.

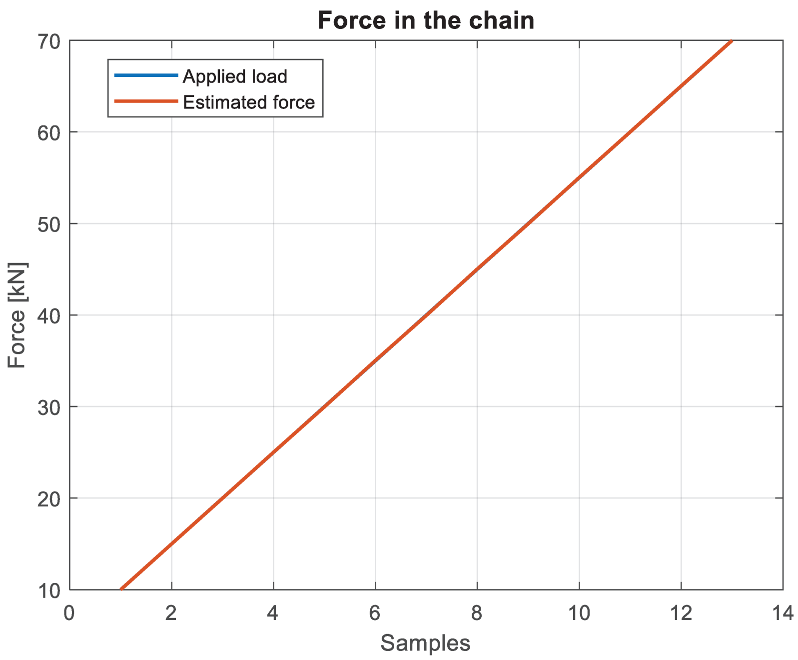

Source: Author.

Observe that the training of the fuzzy inference system worked even with few samples. Then, it is possible to apply the methodology when few training data is available.

8.5. The non-singleton fuzzification

In order to analyze the effects of the non-singleton fuzzification, some tests were performed. The natural frequencies were modified aiming to simulate a situation in which there is noise and their identification is impaired, thus obtaining values different from the real ones. The natural frequencies were changed by adding a random number from a normal distribution with a mean equal to the value of the original frequency and standard deviation of 2, 4, 6, for the first, second and third natural frequencies, respectively. Each frequency was modified with a different standard deviation value, trying to simulate a real situation, since each natural frequency varies differently. Table 8-3 shows the value of the noisy frequencies used to test the non-singleton fuzzification.

Table 8-3 Noisy inputs for the Fuzzy inference system.

Original frequencies			Noisy frequencies		
ω_1 [Hz]	ω_2 [Hz]	ω_3 [Hz]	ω_1 [Hz]	ω_2 [Hz]	ω_3 [Hz]
22.37	44.56	66.41	19.26	43.14	68.61
25.66	51.12	76.19	24.33	47.48	70.69
28.58	56.93	84.84	31.85	56.70	84.52
31.22	62.20	92.70	33.95	59.04	96.65
33.66	67.06	99.93	35.19	63.30	105.11
35.93	71.59	106.68	38.45	75.42	103.46
38.07	75.84	113.03	36.73	75.94	105.66
40.09	79.88	119.03	38.32	84.37	122.68
42.02	83.71	124.75	38.36	80.67	129.81
43.86	87.38	130.22	42.25	85.96	137.39
45.63	90.90	135.47	44.92	89.01	133.33
47.33	94.29	140.52	45.70	95.74	138.19
23.83	47.47	70.74	22.97	39.53	75.66
27.31	54.41	81.09	27.97	53.01	77.38
30.40	60.57	90.26	26.19	52.23	96.66
33.21	66.16	98.59	33.97	64.34	105.97
35.79	71.31	106.26	35.53	66.81	100.89
38.20	76.11	113.42	32.56	75.19	107.77
40.47	80.63	120.15	41.32	85.24	117.83
42.62	84.90	126.52	44.81	87.08	125.90
44.66	88.97	132.59	47.66	93.49	137.11
46.61	92.87	138.39	50.44	90.62	134.47
48.49	96.60	143.96	47.71	93.79	144.20

Source: Author.

The non-singleton fuzzification was implemented in a Mamdani fuzzy inference system with triangular membership functions. The input distribution was Gaussian with standard deviation 2, 4, 6, for the first, second and third frequency, respectively. These results are presented in Table 8-4.

Table 8-4 Comparison of the singleton and non-singleton fuzzification.

Expected force [kN]	Estimated force with singleton fuzzification [kN]	Percentual error %	Estimated force with non-singleton fuzzification [kN]	Percentual error %
14.9	13.81	**7.32**	13.77	**7.57**
19.6	17.17	**12.39**	17.14	**12.54**
24.3	25.02	**2.94**	25.76	**6.02**
29	32.47	**11.96**	31.30	**7.94**
33.7	35.04	**3.98**	35.22	**4.52**
38.4	42.52	**10.73**	41.83	**8.94**
43.1	40.20	**6.72**	40.52	**5.99**
47.8	50.00	**4.60**	49.56	**3.69**
52.5	40.00	**23.81**	49.32	**6.05**
57.2	56.00	**2.10**	56.85	**0.61**
61.9	59.95	**3.16**	59.93	**3.18**
66.6	63.95	**3.98**	65.04	**2.34**
16.9	16.41	**2.89**	15.97	**5.47**
22.2	21.40	**3.59**	21.56	**2.88**
27.5	25.17	**8.47**	22.20	**19.29**
32.8	33.77	**2.97**	34.26	**4.46**
38.1	33.95	**10.89**	35.15	**7.75**
43.4	38.37	**11.59**	38.30	**11.75**
48.7	51.44	**5.63**	50.96	**4.63**
54	56.97	**5.49**	56.95	**5.47**
59.3	65.82	**11.00**	65.69	**10.78**
64.6	40.00	**38.08**	65.77	**1.81**
69.9	67.67	**3.19**	67.91	**2.85**

Source: Author.

Table 8-4 shows the comparison of the estimated force when it is used singleton fuzzification and when it is not. When compared the percentual error of the estimation, it is possible to perceive that when the non-singleton fuzzification is implemented the error of the estimation is lower.

The non-singleton fuzzification can be a useful tool when the input values have considerable associated uncertainties. Observing Table 8-4, the non-singleton fuzzification reduces the percentual error significantly. For an application where the environment is not controlled, the non-singleton fuzzification can solve the problems of estimations, since the methodology considers the possible errors associated to the inputs. Figure 8.26 presents the performance of the fuzzy inference system with non-singleton fuzzification.

Figure 8.26 Performance of the non-singleton fuzzification.

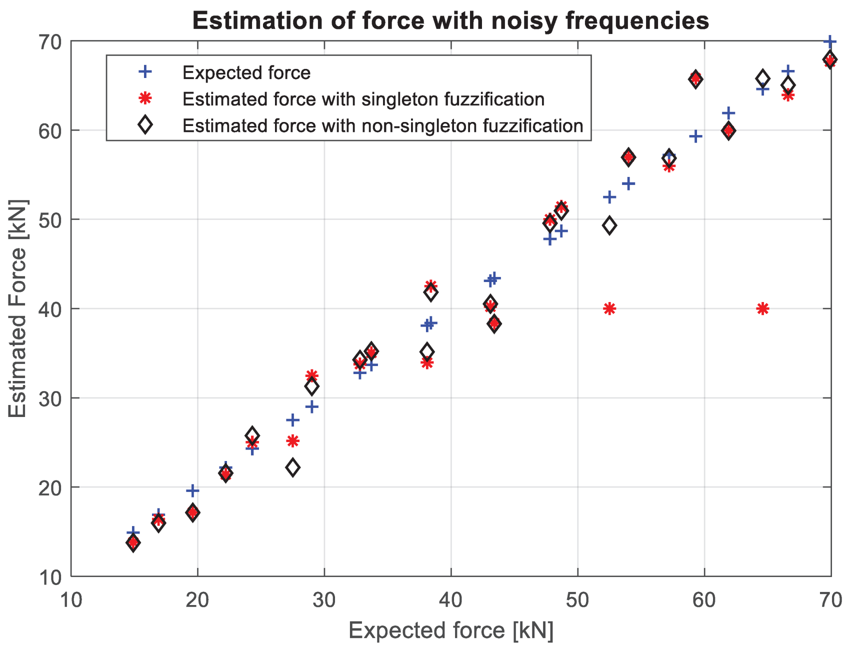

Source: Author.

9. CONCLUSIONS AND FURTHER WORKS.

The main goal of this work is to develop a methodology that allows the prediction of the external applied force on link chains through the measurement of its natural frequencies. In this context, a fuzzy inference system capable of performing such task was created. The fuzzy model was constructed using two methodologies: Mamdani and Sugeno. Both methodologies were implemented using triangular and Gaussian membership functions.

The Mamdani fuzzy inference system with triangular membership functions provided the best performance in estimating the force and was built using only specialized knowledge. In this case, the parameters of the membership functions and the rules were selected using only the author's sense and perception. On the other hand, the Mamdani fuzzy inference systems with Gaussian membership functions presented the worst results.

The results of applying these methodologies are due to two main factors: the first is that the handling of triangular association functions is easier than with Gaussian, since the control over linearities is greater than over non-linearities. The second factor is related to the defuzzification process. The centroid of a possible consequent diffuse set is best viewed when the figure is composed of straight lines instead of curved lines, as is the case with Gaussian functions.

The fuzzy systems with Sugeno inference depend on the output level which is calculated as the product of the membership degrees and the definition of the consequent functions.

The rules are the soul of the fuzzy inference systems. The definition of the rules must be objective, and they need to describe the behavior of the modeled system accurately. The lack of a rule could compromise the capability of the fuzzy system since it is a stage of the modeled system not considered. In addition, the over-definition of the system can introduce errors.

The genetic algorithm significantly improves the performance of the fuzzy inference system. The algorithm is able to adjust the parameters of the membership functions, improving the estimation capacity, providing the force value with minimal errors.

The fuzzy system with Sugeno inference and Gaussian association functions provides the best performance after optimization. This proves that Gaussian functions are better suited to the treatment of nonlinearities than triangular ones. In addition, the importance of a system improvement method is shown, since, although Gaussian functions are difficult to define, a correct combination of parameters can significantly improve the system. And this applies to any type of membership function.

The genetic algorithm uses the training data to tune the parameters. The training data play a fundamental role in the optimization, since the algorithm adjust the model aiming to reproduce the cases of the training data with the fuzzy inference system. The training data must contain at least one example of all possible behavior of the modeled system.

It is important to note that the genetic algorithm or any other optimization procedure can improve fuzzy systems, but the correct convergence depends on the designer's knowledge of the system's behavior. The adjustable parameters of fuzzy systems can range from membership functions to rules. It is advisable to provide a path for optimization, that is, the smaller the number of parameters to optimize, the better the convergence. In this case, the tuning of the parameters of the antecedent parts is sufficient to obtain good results.

Regarding the mathematical model of the chain, it presented reliable qualitative results, but it differs in the quantitative results, when compared to the values obtained experimentally. Considerations such as the deformation of the links and the stiffness of the contact between the links can make the model represent the real behavior of a link chain. For this work, the proposed model was sufficient, as it was proposed in order to obtain the training data to apply the technique. The dynamic behavior of the chain requires further study and more experiments, which is outside the scope of this dissertation.

As a final conclusion, it can be said that fuzzy inference systems have demonstrated that they are powerful tools for modeling systems. They are versatile and adaptable, allowing their use in a wide variety of problems. For the case of this study, the diffuse inference system met the expectations and was able to accurately estimate the force of the link chain.

9.1. Further works

The author suggests the following topics for future research works:

1. To model the chain considering the deformation of the links as well as studying the influence of the contact conditions between the links.
2. To model different configurations of the chain, taking into account the slope of the chain or the effect of gravity (catenary).

3. To perform more experiments with different chains, to validate the model and discover the relationship between natural frequencies.
4. To optimize the Mamdani fuzzy system by implementing some computational strategies, as well as using advanced computational resources.
5. To implement non-singleton fuzzification with the Sugeno fuzzy system, in order to evaluate its performance.
6. To model the fuzzy inference system using type 2 fuzzy logic, which considers an uncertainty footprint in the membership functions, improving the estimation capacity when the data is noisy.
7. To introduce some machine learning tool to automate the fuzzy inference system, making it adaptable to varying environmental conditions.

References

ABDOUN, O.; ABOUCHABAKA, J.; TAJANI, C. Analyzing the Performance of Mutation Operators to Solve the Travelling Salesman Problem. **International Journal of Emerging Sciences**, v. 2, n. 1, p. 61–77, 2012.

ANGUS JAMIESON. **METHOD OF DETERMINING THE TENSION IN A MOORING LINE.** United States, 2013.

CASTILLO, O.; MELIN, P. Type-1 fuzzy logic. **Studies in Fuzziness and Soft Computing**, 2008.

CHAI, Y. T.; VARYANI, K. S.; BARLTROP, N. D. P. Three-dimensional Lump-Mass formulation of a catenary riser with bending, torsion and irregular seabed interaction effect. **Ocean Engineering**, v. 29, n. 12, p. 1503–1525, set. 2002.

DU, Y. et al. A novel underwater measurement method for mooring system using self-contained technique. **Advances in Mechanical Engineering**, v. 7, n. 5, p. 1–12, 19 maio 2015.

EIBEN, A. E.; MARCHIORI, E.; VALKÓ, V. A. **Evolutionary Algorithms with On-the-Fly Population Size Adjustment**. Lecture Notes in Computer Science. **Anais**...2004Disponível em: <http://link.springer.com/10.1007/978-3-540-30217-9_5>

FILIPICH, C. P.; ROSALES, M. B. Dynamic Analysis of Plane Mooring Chains of Inextensible Links. **Mecánica Computacional**, v. 26, p. 2479–2495, 2007.

FRITZKOWSKI, P.; KAMINSKI, H. Dynamics of a rope as a rigid multibody system. **Journal of Mechanics of Materials and Structures**, v. 3, n. 6, p. 1059–1075, jun. 2008.

GARCÍA-CERDAÑA, À.; ARMENGOL, E.; ESTEVA, F. Fuzzy Description Logics and t-norm based fuzzy logics. **International Journal of Approximate Reasoning**, v. 51, n. 6, p. 632–655, 2010.

GOTSHALL, S.; RYLANDER, B. Optimal population size and the genetic algorithm. **Proceedings On Genetic And Evolutionary Computation Conference**, p. 1–5, 2000.

HUANG, S. Dynamic analysis of three-dimensional marine cables. **Ocean Engineering**, v. 21, n. 6, p. 587–605, ago. 1994.

JADAAN, O. AL; RAJAMANI, L.; RAO, C. R. Non-Dominated Ranked Genetic Algorithm for Solving Constrained Multi-Objective Optimization Problems. **Journal of Theoritical and Applied Information Technology**, n. October 2014, p. 640–651, 2009.

JEBARI, K.; MADIAFI, M. Selection Methods for Genetic Algorithms. **International Journal of Emerging Sciences**, v. 3, n. 4, p. 333–344, 2013.

KIM, B. W. et al. Comparison of linear spring and nonlinear FEM methods in dynamic coupled analysis of floating structure and mooring system. **Journal of Fluids and Structures**, v. 42, p. 205–227, out. 2013.

KORA, P.; YADLAPALLI, P. Crossover Operators in Genetic Algorithms: A Review. **International Journal of Computer Applications**, v. 162, n. 10, p. 34–36, 2017.

KURIAN, V. J. et al. Nonlinear Dynamic Analysis of Multi-component Mooring Lines Incorporating Line-seabed Interaction. **Research Journal of Applied Sciences, Engineering and Technology**, v. 6, n. 8, p. 1428–1445, 10 jul. 2013.

LEVINSON, D. A. Natural frequencies of a hanging chain. **American Journal of Physics**, v. 45, n. 7, p. 680–681, jul. 1977.

LI, J. et al. Transversal vibration analysis of resonance condition and frequency for orchard chain ropeway system. **Nongye Gongcheng Xuebao/Transactions of the Chinese Society of Agricultural Engineering**, v. 30, n. 23, p. 50–57, 2014.

LI, S. et al. Study on interaction between soil and anchor chain with finite element method. **China Ocean Engineering**, v. 30, n. 6, p. 942–953, 25 dez. 2016.

LIMA, J. A. et al. **Fitness function design for genetic algorithms in cost evaluation based problems**. Proceedings of the IEEE Conference on Evolutionary Computation. **Anais**...IEEE, 1996Disponível em: <http://ieeexplore.ieee.org/document/542362/>

LOW, Y. M.; LANGLEY, R. S. Time and frequency domain coupled analysis of deepwater floating production systems. **Applied Ocean Research**, v. 28, n. 6, p. 371–385, dez. 2006.

MAHALINGAM, S. Transverse vibrations of power transmission chains. **British Journal of Applied Physics**, v. 8, n. 4, p. 145–148, abr. 1957.

MAMDANI, E. H.; ASSILIAN, S. An experiment in linguistic synthesis with a fuzzy logic controller. **International Journal of Man-Machine Studies**, v. 7, n. 1, p. 1–13, 1975.

MENDEL, J. M. Uncertainty, fuzzy logic, and signal processing. **Signal Processing**, v. 80, n. 6, p. 913–933, 2000.

MIZUMOTO, M.; TANAKA, K. Fuzzy sets and their operations. **Information and Control**, v. 48, n. 1, p. 30–48, 1981.

MOUZOURIS, G. C.; MENDEL, J. M. Nonsingleton fuzzy logic systems: Theory and application. **IEEE Transactions on Fuzzy Systems**, 1997.

NOËL, J. M. et al. Natural configurations and normal frequencies of a vertically suspended, spinning, loaded cable with both extremities pinned. **European Journal of Physics**, 2008.

PRIOUR, D.; DEGRES, Y. A tension-recording sensor for mooring lines. **Aquaculture International**, v. 3, n. 2, p. 134–142, jun. 1995.

PUGSLEY, A. G. ON THE NATURAL FREQUENCIES OF SUSPENSION CHAINS. **The Quarterly Journal of Mechanics and Applied Mathematics**, v. 2, n. 4, p. 412–418, 1949.

RAZALI, N. M.; GERAGHTY, J. **Genetic algorithm performance with different selection strategiesin solving TSP**. Proceedings of the World Congress on Engineering 2011, WCE 2011. **Anais**...2011

ROBERT, I. et al. **LOAD INDICATOR FOR MOORING LINE**United States, 1973.

ROEVA, O.; FIDANOVA, S.; PAPRZYCKI, M. Population size influence on the genetic and ant algorithms performance in case of cultivation process modeling. **Studies in Computational Intelligence**, v. 580, n. October 2014, p. 107–120, 2015.

ROGER JANG, J.-S. **Neuro-Fuzzy and Soft Computing**. New York: Prentice Hall, 2000.

SUGENO, M.; KANG, G. . Structure identification of fuzzy model. **Fuzzy Sets and Systems**, v. 28, n. 1, p. 15–33, out. 1988.

TAKAGI, T.; SUGENO, M. Fuzzy Identification of Systems and Its Applications to Modeling and Control. **IEEE Transactions on Systems, Man and Cybernetics**, v. SMC-15, n. 1, p. 116–132, 1985.

TOMASZEWSKI, W.; PIERANSKI, P. Dynamics of ropes and chains: I. The fall of the folded chain. **New Journal of Physics**, v. 7, 2005.

VERBIN, Y. Boundary conditions and modes of the vertically hanging chain. **European Journal of Physics**, v. 36, n. 1, p. 015005, 1 jan. 2015.

VULLINGS, L. A. E. et al. Dealing with the Uncertainty of Having Incomplete Sources of Geo-Information in Spatial Planning. **Applied Spatial Analysis and Policy**, 2013.

WAGNER, C.; PIERFITT, M.; MCCULLOCH, J. **Juzzy online: An online toolkit for the design, implementation, execution and sharing of Type-1 and Type-2 fuzzy logic systems**. IEEE International Conference on Fuzzy Systems. **Anais**...2014

WANG, C. Y. Vibration of a vertical axially moving string or chain under the influence of gravity. **Acta Mechanica**, v. 228, n. 1, p. 357–362, 2017.

XIONG, L.; YANG, J.; ZHAO, W. Dynamics of a taut mooring line accounting for the embedded anchor chains. **Ocean Engineering**, v. 121, p. 403–413, jul. 2016.

YANG, M.-D. et al. An Efficient Fitness Function in Genetic Algorithm Classifier for Landuse Recognition on Satellite Images. **The Scientific World Journal**, v. 2014, p. 1–12, 2014.

YANG, M. D.; TENG, B. Static and dynamic analysis of mooring lines by nonlinear finite element method. **China Ocean Engineering**, v. 24, n. 3, p. 417–430, 2010.

YANG, Z. et al. Transversal Vibration of Chain Ropeway System Having Support Boundary Conditions with Polygonal Action. **Shock and Vibration**, v. 2015, p. 1–9, 2015.

ZADEH, L. A. A computational approach to fuzzy quantifiers in natural languages. **Computers and Mathematics with Applications**, 1983.

ZADEH, L. A. Fuzzy logic = computing with words. **IEEE Transactions on Fuzzy Systems**, v. 4, n. 2, p. 103–111, 1996.

APPENDIX. CATALOG CHAINS GRADE 8.

Correntes de Elos
Conforme Norma EN 818-2 | Grau 8

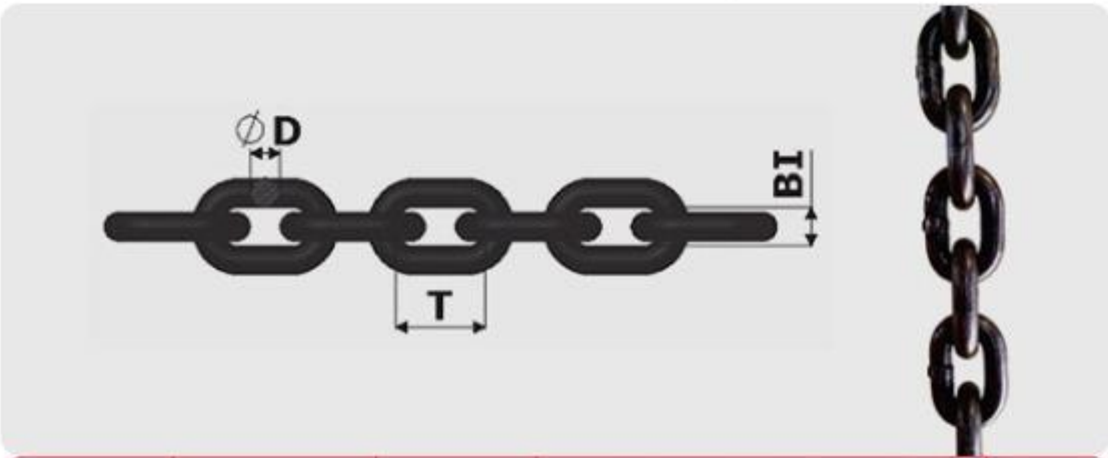

REF.	DESCRIÇÃO D x T (mm)	CARGA DE TRABALHO (ton.)	DIMENSÕES (mm)			PESO KG/M
			D	T	BI MÍN	
CR-06/G8	6 X 18	1,12	6	18	7,8	0,80
CR-07/G8	7 X 21	1,50	7	21	9,1	1,10
CR-08/G8	8 X 24	2,00	8	24	10,4	1,40
CR-10/G8	10 X 30	3,20	10	30	13,0	2,20
CR-13/G8	13 X 39	5,30	13	39	17,0	3,70
CR-16/G8	16 X 48	8,00	16	48	20,8	5,70
CR-19/G8	19 X 57	11,20	19	57	24,7	8,10
CR-22/G8	22 X 66	15,00	22	66	28,6	10,90
CR-26/G8	26 X 78	21,20	26	78	33,8	15,20
CR-32/G8	32 X 96	31,50	32	96	41,6	23,00
CR-36/G8	36 X 126*	40,00	36	126*	46,8	28,00

Source: Coforja.